

Science Camp #170802.8

02-04 August 2016 @ the Condo, the Nelson Cabin, and surrounding area



Advisors

H. Roice Nelson, Jr., Andrea S. Nelson,
Paul F. Nelson, Benjamin B. Nelson



Attendees

Ethan E. Nelson, Grant M. Nelson, Colby C. Wright,
Taylor R. Wright, Ella D. Nelson, Halle N. Wright,
Bobbie Sophia Waldron, Dallin Spencer Nelson,
Avalyn Joyce Wright, Rachel Lee, & Ian Lee

7. Geophysics

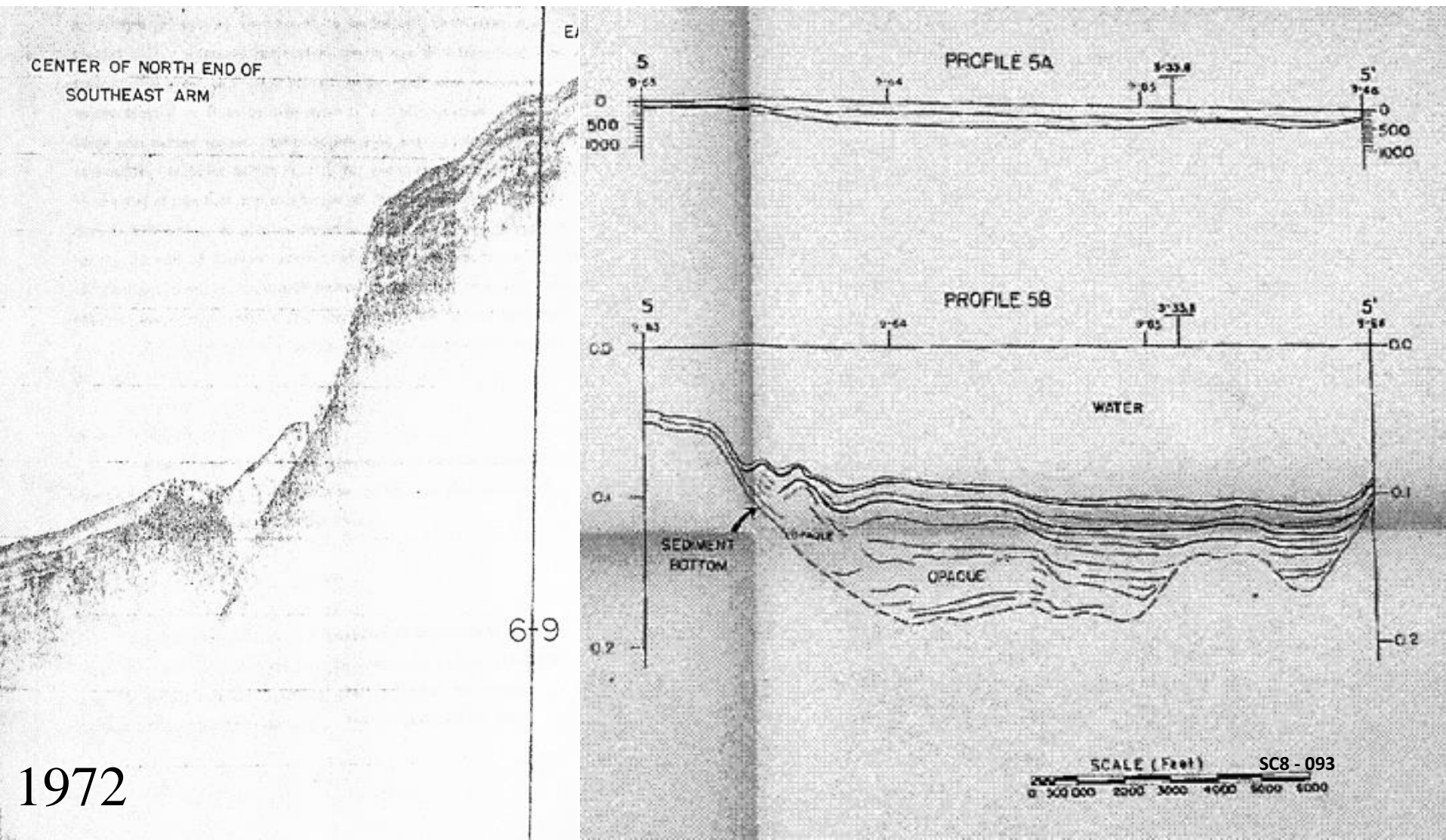


The study of the Earth by quantitative physical methods, especially by seismic reflection and refraction, gravity, magnetic, electrical, electromagnetic, and radioactivity methods.



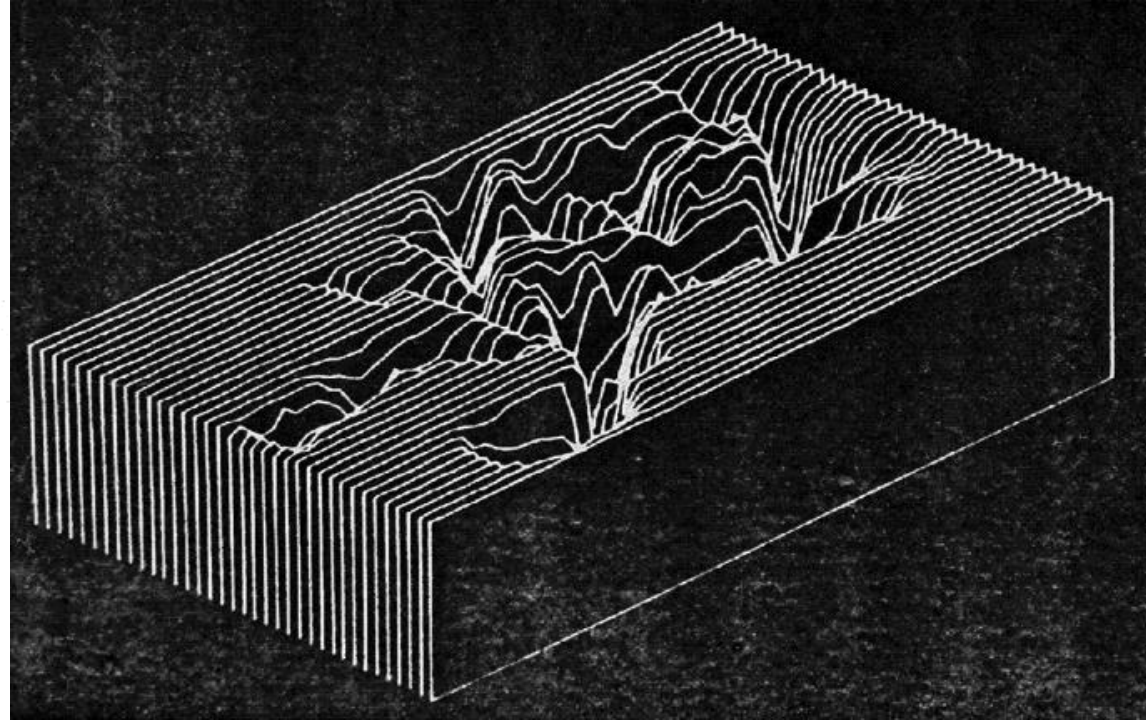
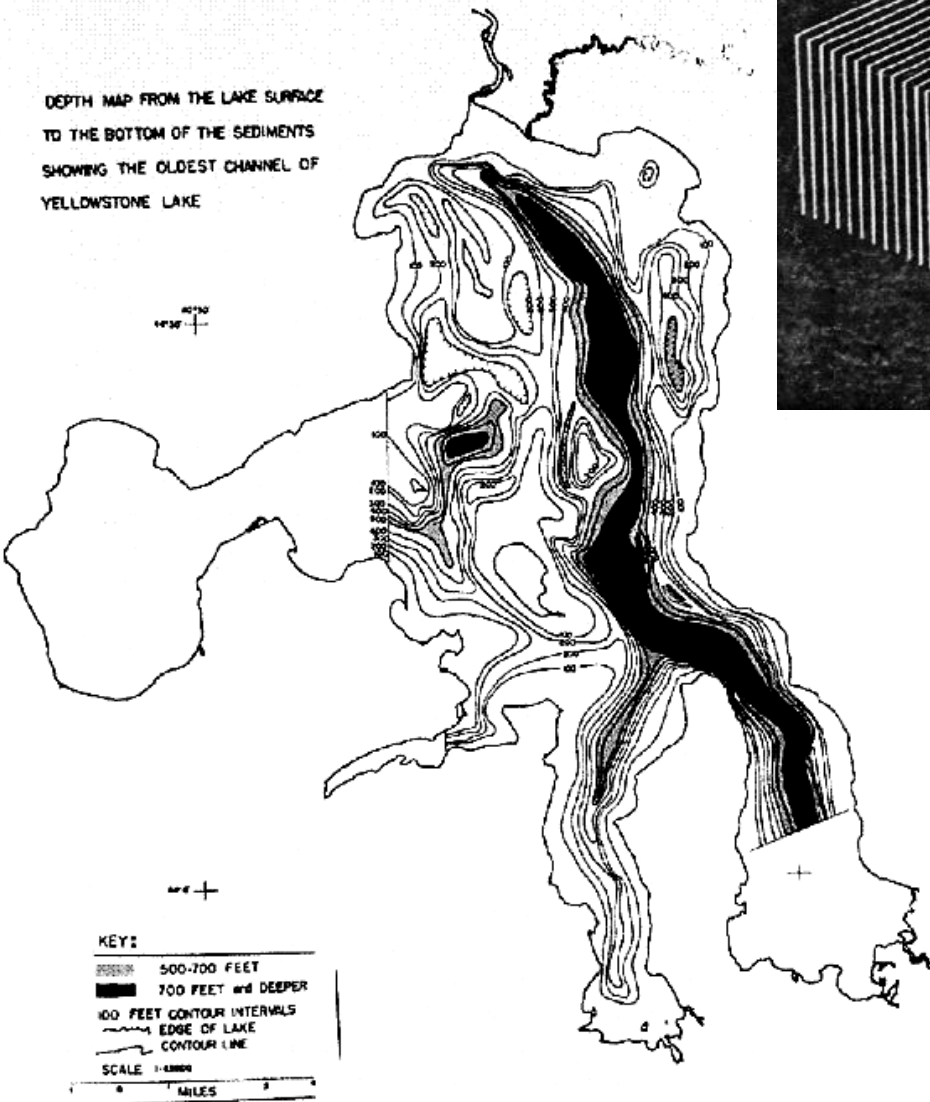
SC8 - 092

Yellowstone Lake Sparker Survey



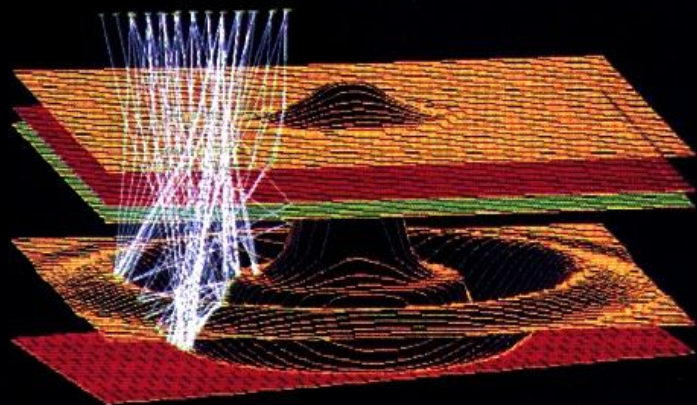
1972

Base Quaternary Sediments Yellowstone Lake



Grandpa's
Senior Thesis

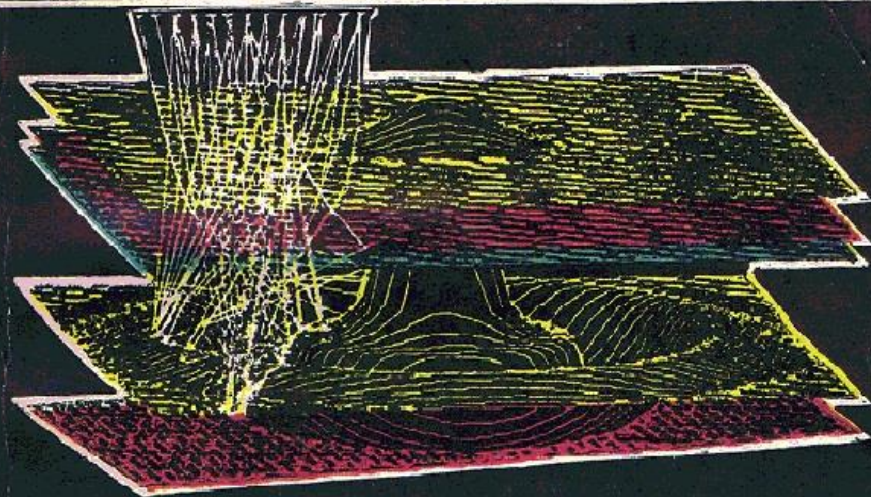
New Technologies in Exploration Geophysics



Trends and new developments in exploration
methods using reflection seismology

H. Roice Nelson, Jr.

〔美〕H. R. 纳尔逊 著

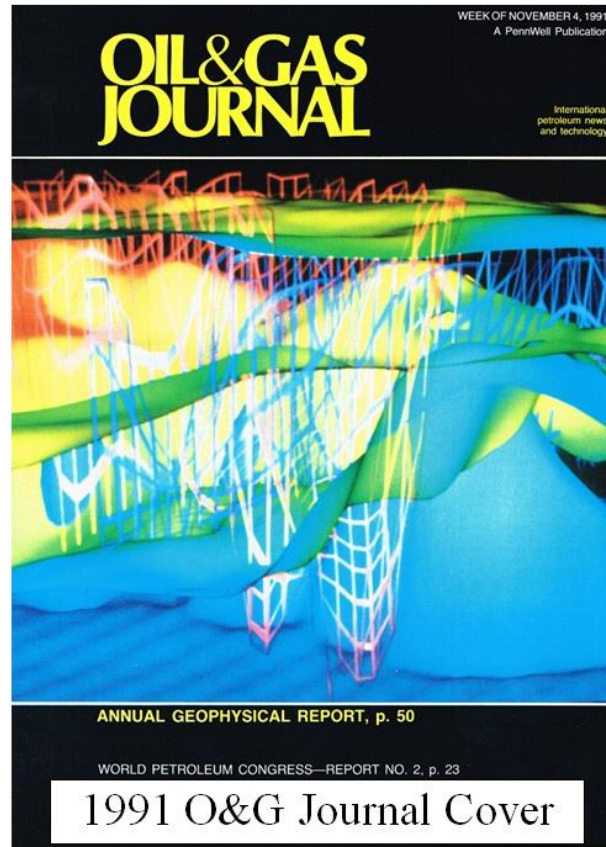
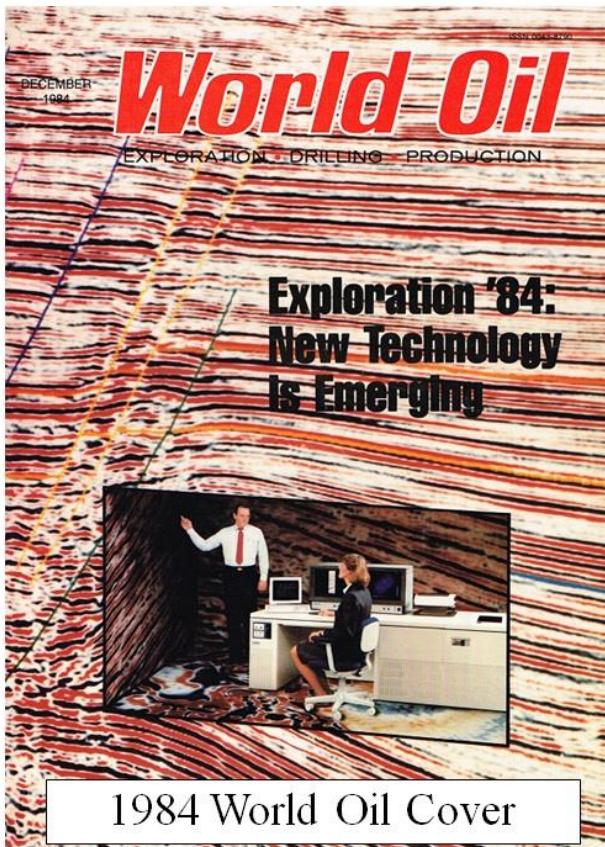


勘探地球物理新技术

石油工业出版社

SC8 - 095

4 of over 200 Publications



H. Roice Nelson Jr.: Quixotic geophysics

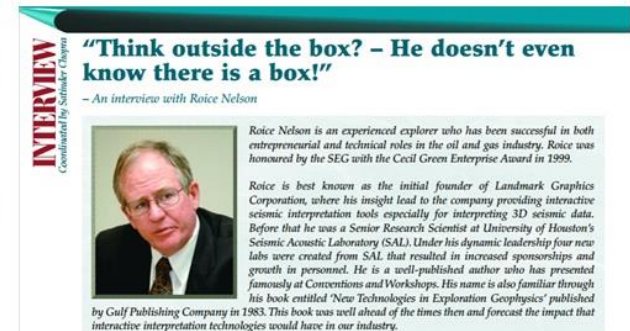
Dolores Proulx, associate editor, TLE



"When it comes down to what wisdom is all about, it is about the stories and the transfer of experiences. We are not capturing these stories, and they will dissipate. We've got this great big bubble of experience that's moving into retirement, we are not replacing it, and what we're going to end up with is horrendous gaps of knowledge because we are not taking advantage of the previous generation's vast experience."

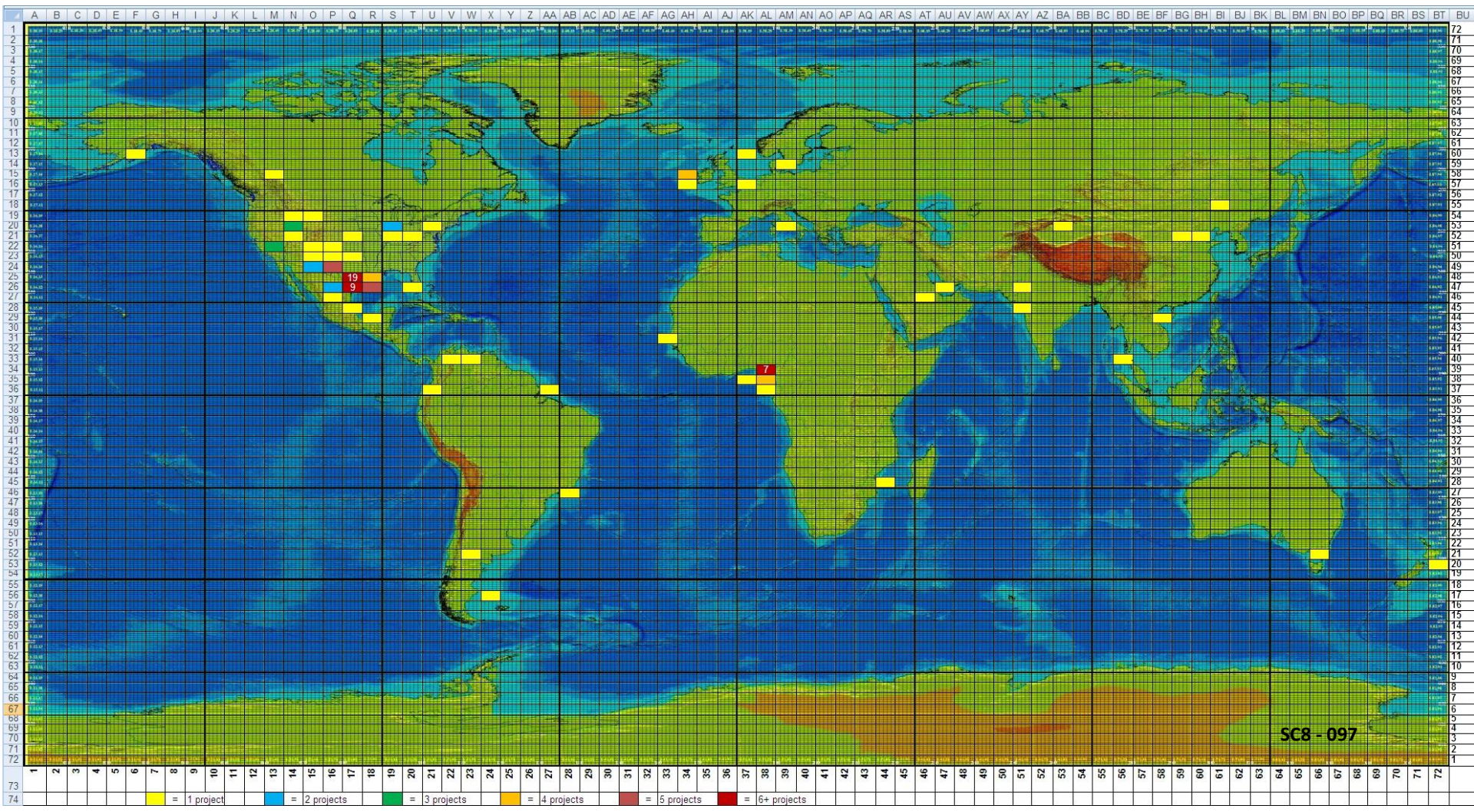
Howard Roice Nelson Jr. grew up on a farm flanked by stratigraphic and metamorphic geology in southern Utah. After school and chores, rather than play he would explore the land on horseback or build things. Music provided a social outlet for the shy youngster. On 24 February 1964, inspired by The Beatles' debut on American television, Roice and four other junior high schoolers gathered in that hotbed of rock 'n' roll, a garage, from which they emerged as "The KeyNotes," with Roice the lead and rhythm guitarist.

2003 The Leading Edge

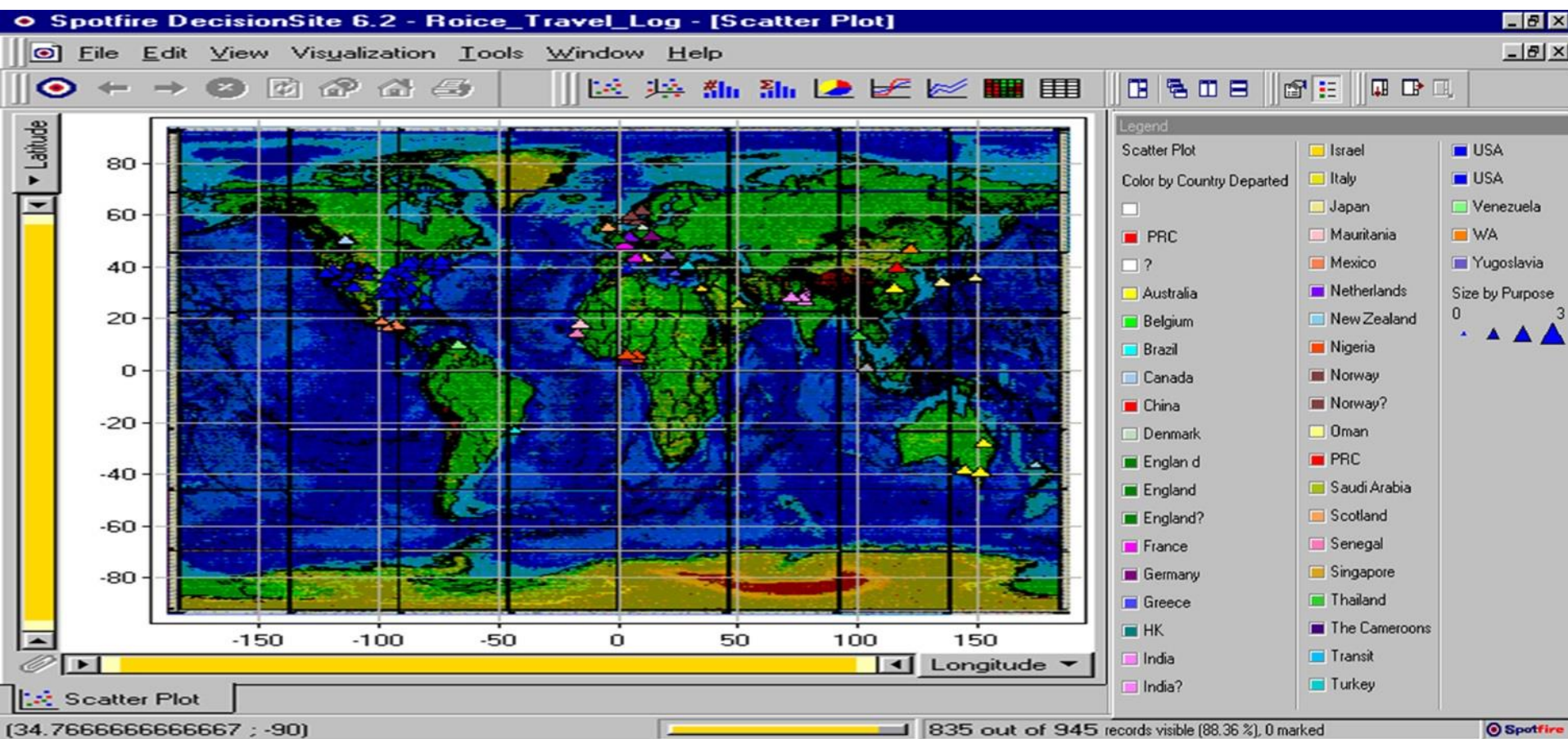


2008 CSEG Recorder

Where Grandpa Worked



Where Grandpa Travelled for Work



Notes



A



B



C

Figure 1-5. Typical land crew operations in southwestern Utah. (A) Surface shooting using ten 5-lb sacks of explosives on a primachord string. The environmental damage is temporary, but overshooting, like overgrazing, can cause long-term problems. (B) Shallow hole shooting of, say, 10 lbs of dynamite per shotpoint is better in agricultural areas. (C) The most common land seismic source is Vibroseis.TM Normally, four of these trucks vibrate in synchronization.



Seismic Acquisition

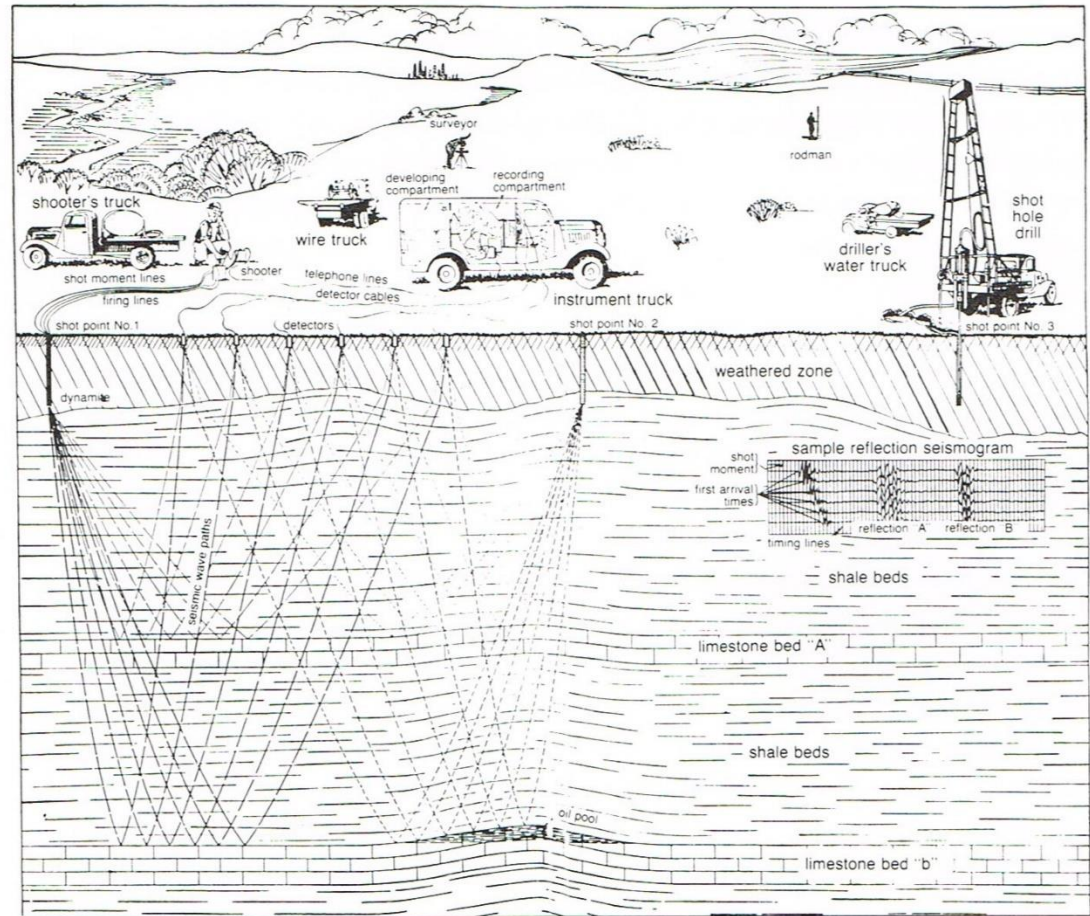


Figure 1-7. This diagram of a 1940s seismic shothole crew reflects the same basic configuration used today, except crews now use many more channels, various seismic sources, and sophisticated instrumentation. (After Nettleton.²)

SC8 - 100

Reflection Seismology

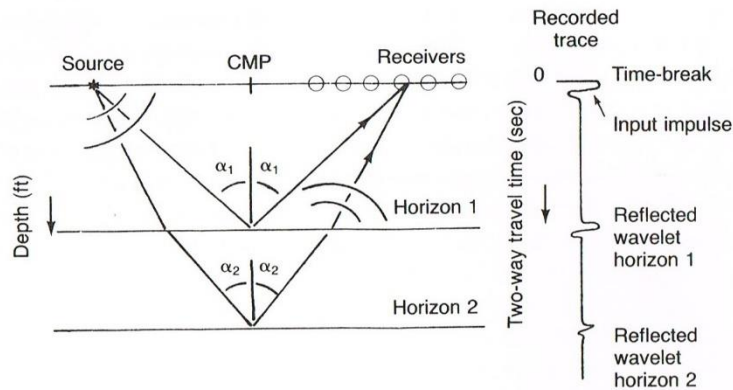


Figure 1-1A. This diagram shows the concept of common mid-point (CMP). Note that boundaries act as sources for new wavefront paths and that the angle of incidence equals the angle of reflection.

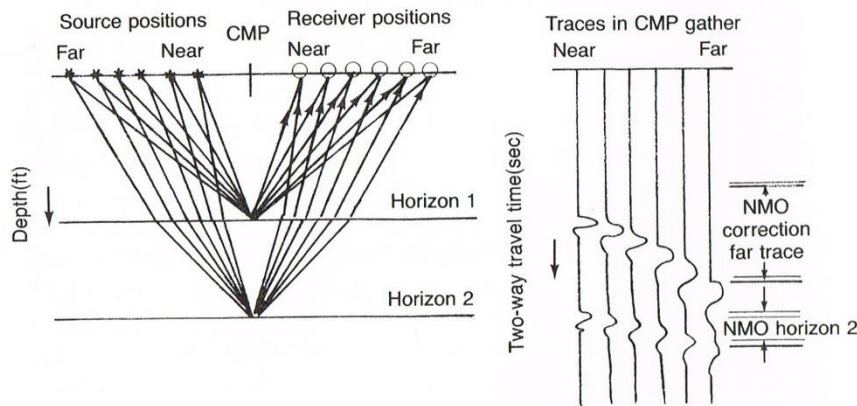


Figure 1-1B. In this CMP gather, reflections are recorded by six different sets of source/receiver locations. The data is sorted into a CMP gather during processing. Dispersion, or the widening of the wavelet with offset, is exaggerated in the traces drawn on the right.

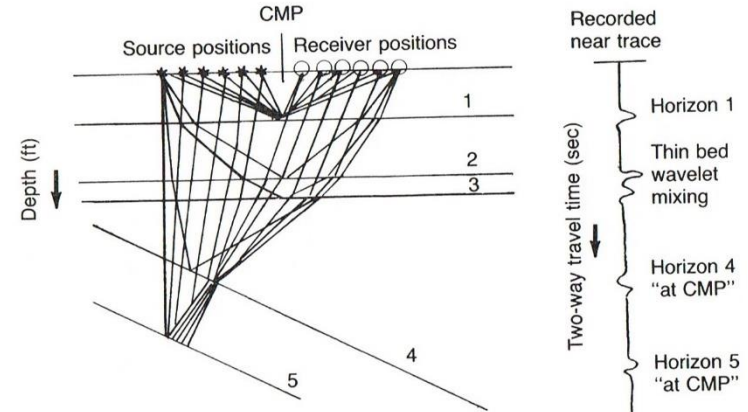


Figure 1-1C. A CMP gather over dipping beds shows one of the problems with the CMP method. Not only are the ray-traced reflection points at horizons 4 and 5 not located spatially at the CMP, but also note how the spatial locations of different source/receiver combinations move as a function of offset on horizon 5.

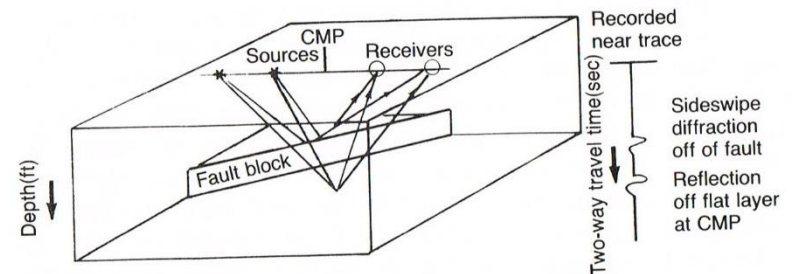


Figure 1-1D. Sideswipe reflections can come from steeply dipping layers. This example shows how diffractions from a fault block put out-of-plane events on a CMP trace.

Processing

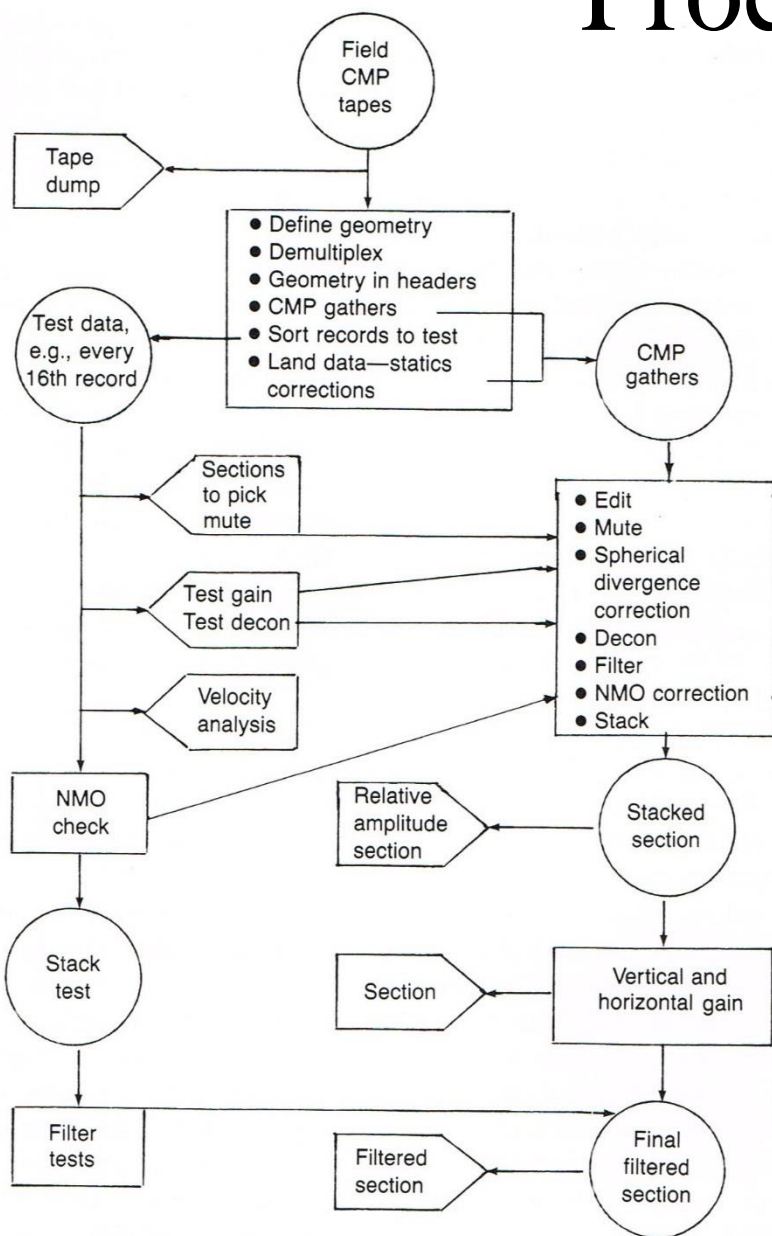


Figure 1-8. Flow chart of the processing steps involved in compositing CMP gathers into a stacked seismic section.

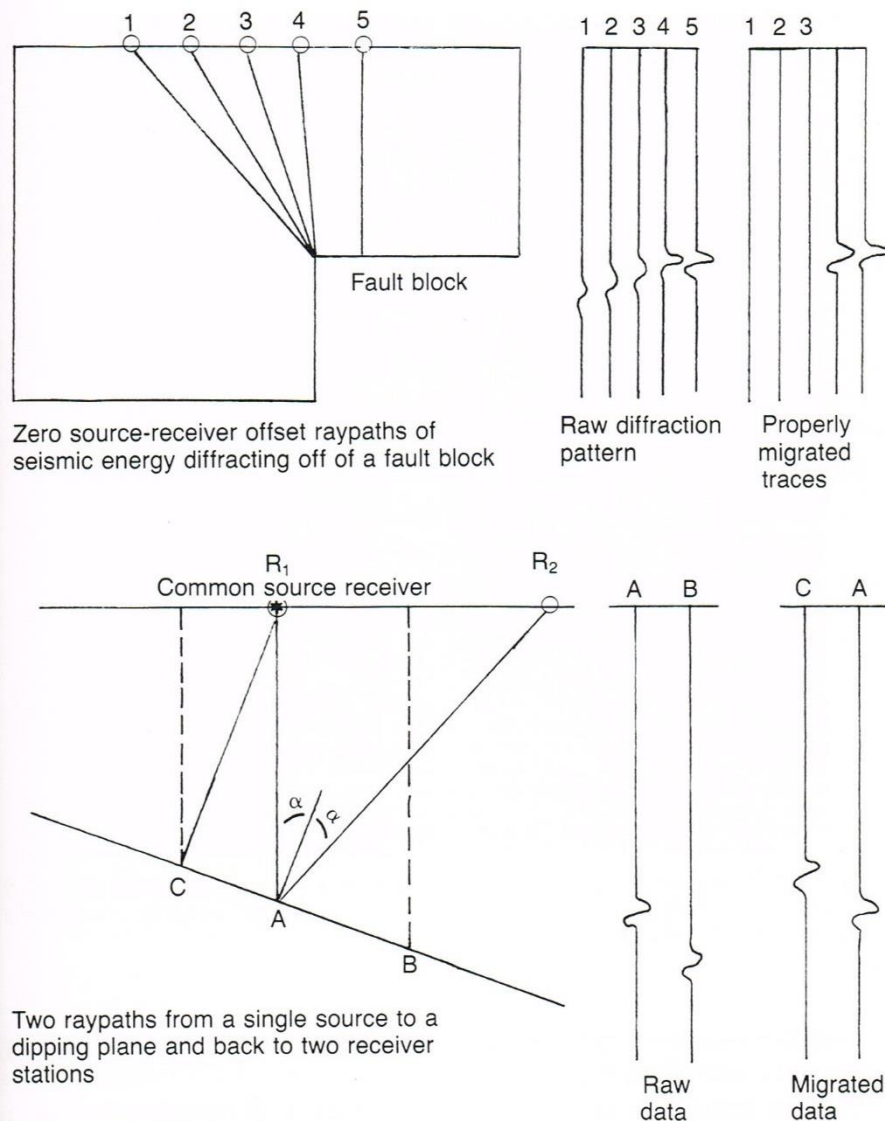


Figure 1-11. Migration is a mathematical, computer focusing procedure that collapses diffractions (top) and plots reflections from dipping layers in their actual spatial location instead of at the CMP (bottom).

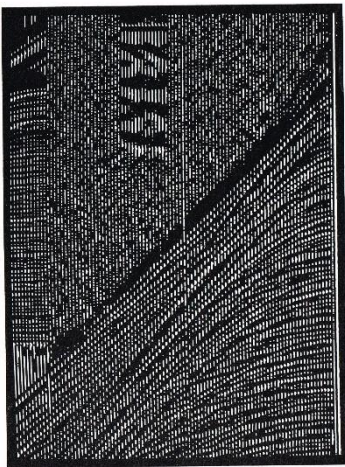
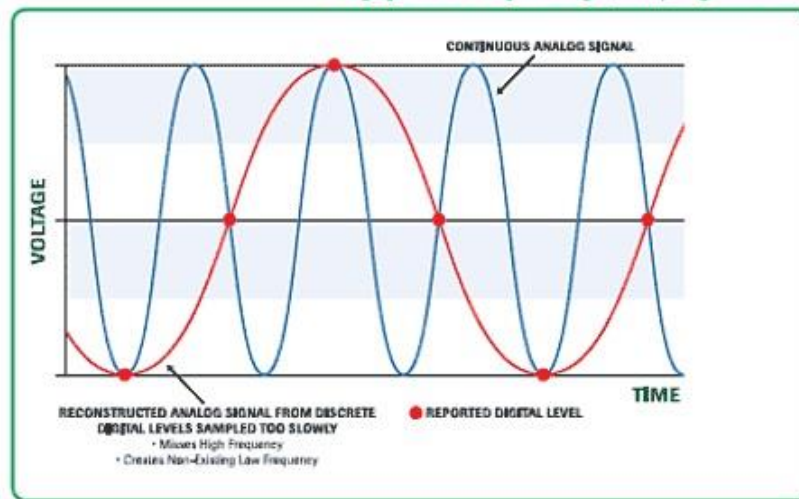


Figure 2-3. The seismic field record is displayed on a vector refresh graphics terminal. Seismic data displays require large amounts of trace data to be stored simultaneously so that correlation between traces can be analyzed. (Courtesy Adage, Inc.)

Nyquist Frequency (sampling too slow)



Seismic Shot Gathers

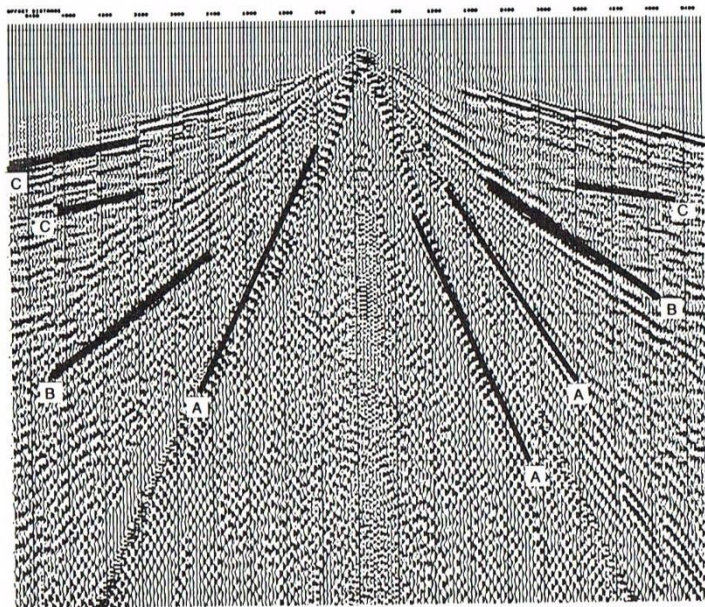


Figure 1-6A. A noise survey showing example air waves (A), ground roll (B), and reflections (C). The receivers were grouped at each of 12 receiver stations and the vibrators moved out to 8 source positions in each direction.

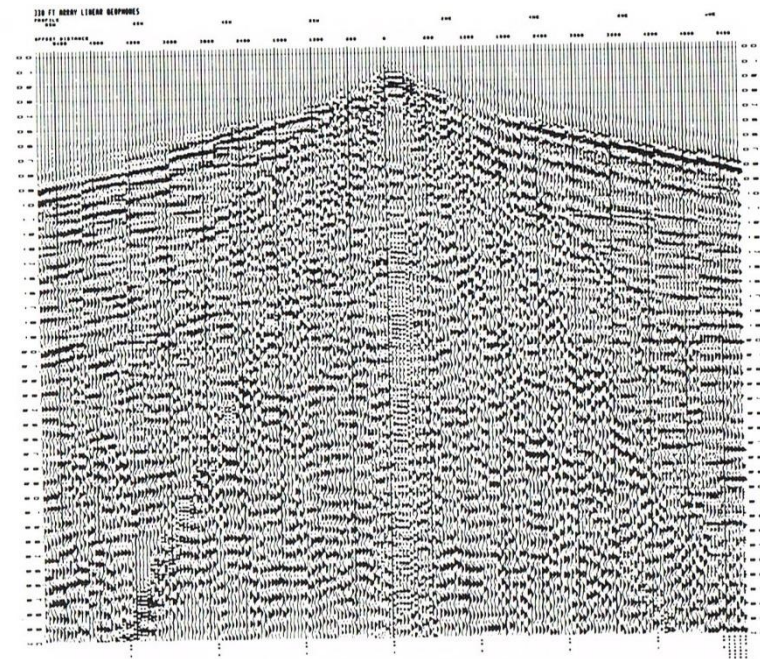


Figure 1-6B. A noise survey showing how a 330-ft linear receiver array cancels the strong air wave and ground roll. This same procedure can be done in processing if receiver stations are close enough together.

Seismic Interpretation

48 New Technologies in Exploration Geophysics

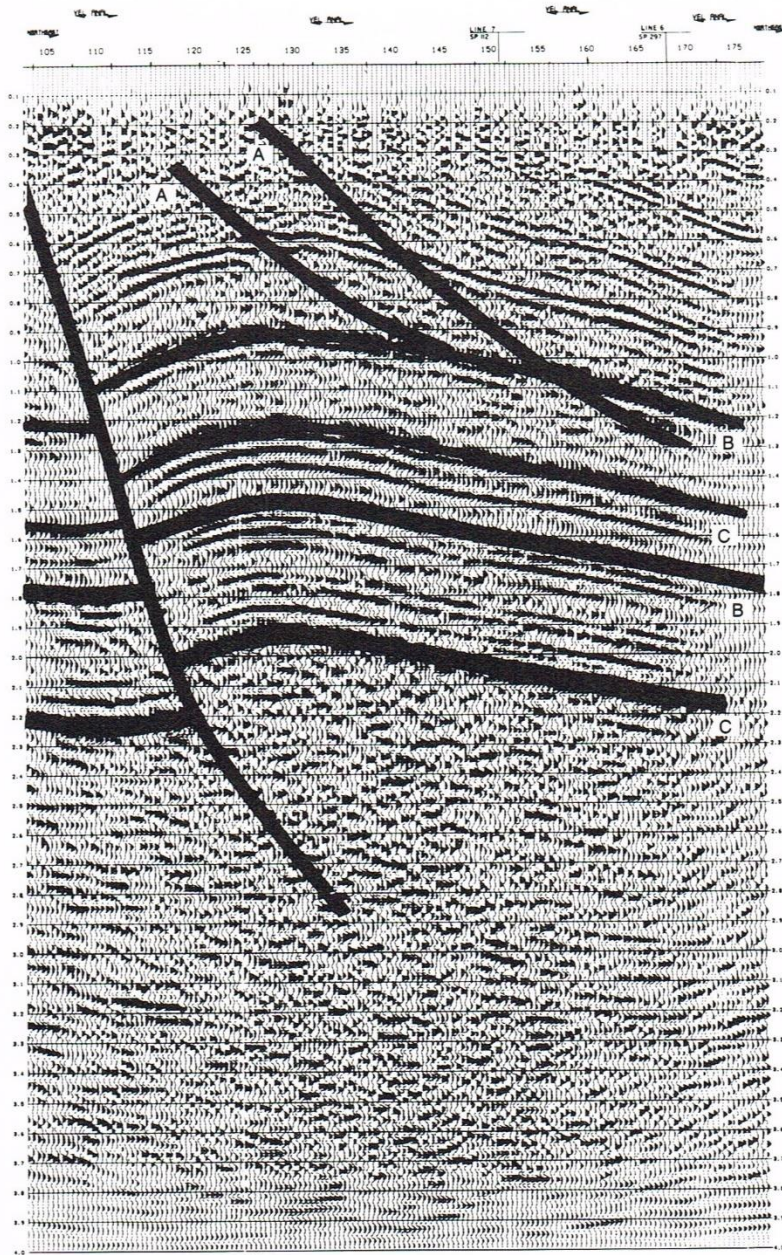


Figure 1-17. An interpreted seismic section across the Wind River Overthrust. (After Steiner.³⁶)

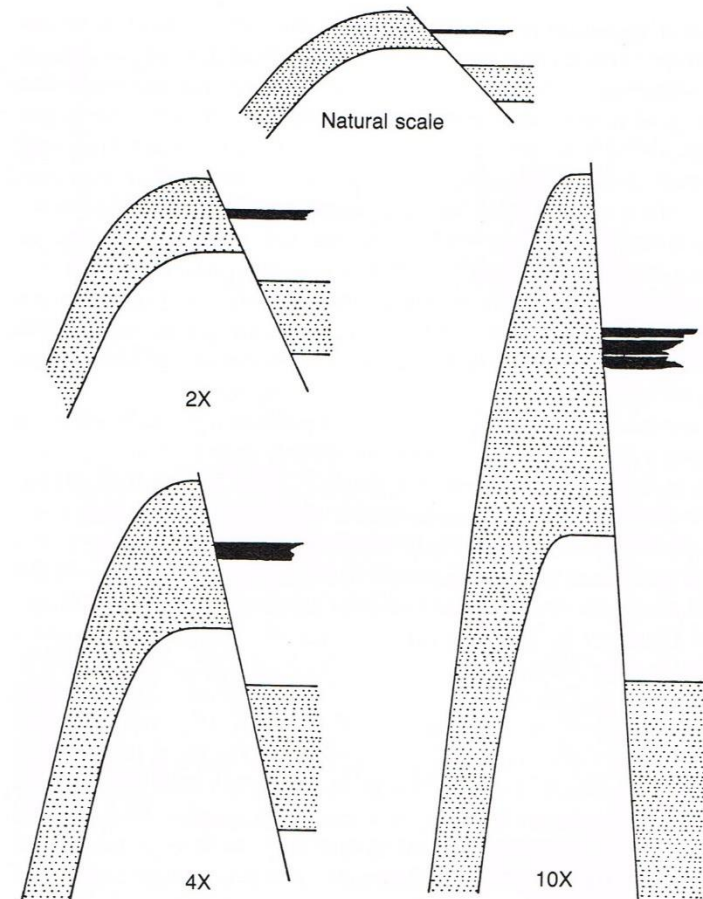


Figure 1-15. Vertical exaggeration allows one to see vertical and horizontal context, but severely distorts bed thickness, structural relationship, fault dip, etc. The vertical exaggeration on a seismic section varies as a function of the velocity of the rocks, but is typically within this range. (After Sheriff.¹⁷)

Contouring and Seismic Attributes

54 New Technologies in Exploration Geophysics

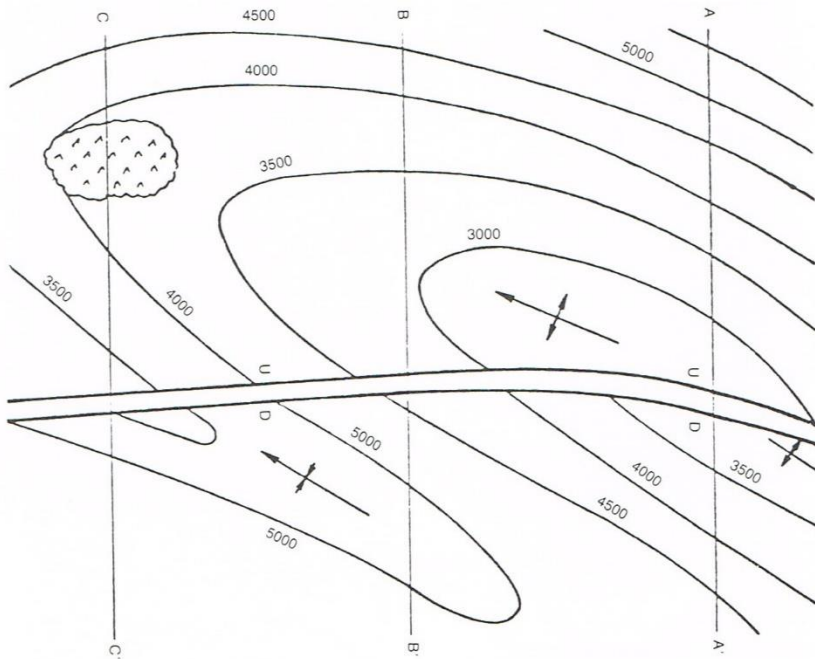
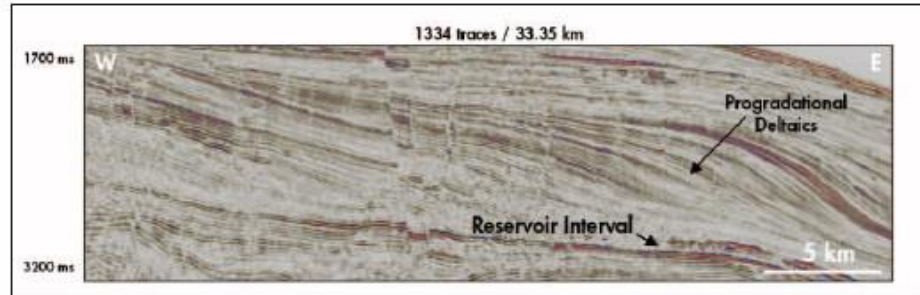
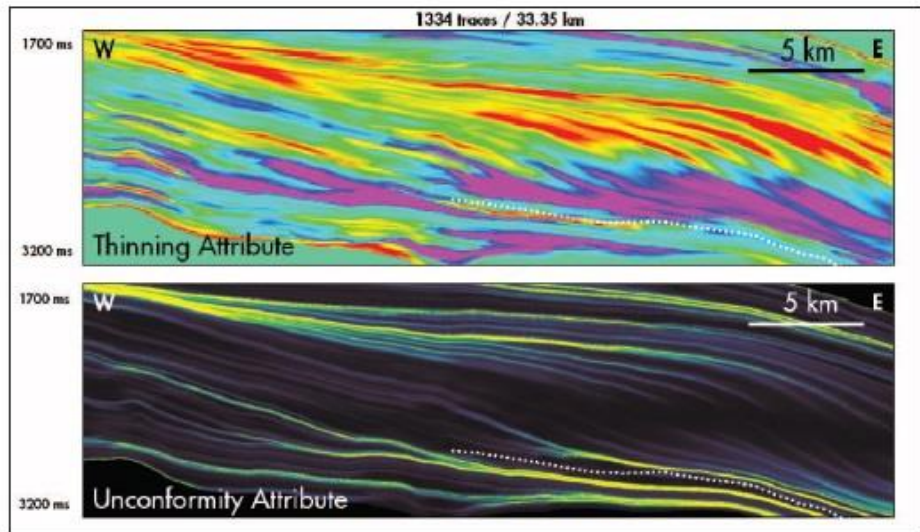


Figure 1-18. Contour map showing a fault, a salt piercement, and a basin. (After Sheriff.¹⁷)



Barnacuda Field seismic expression. Reservoir has single-cycle expression with relatively high negative amplitudes. Progradational deltaic packages, overlying reservoir interval, provide top seal. Faults offset feeder systems.



Barnacuda geometric attribute expression. Thinning attribute demonstrates thinning to left in red and thinning to right in purple. Unconformity attribute: dark grey to black = areas of relatively parallel layers; yellow = areas of convergence. Reservoir interval is highlighted by dotted line in both images.

Notes

This image shows a single sheet of white paper with horizontal blue ruling lines. The lines are evenly spaced and run across the width of the page. There are no margins, text, or other markings on the paper.



3-D Acquisition Design

3D Seismic Techniques 97

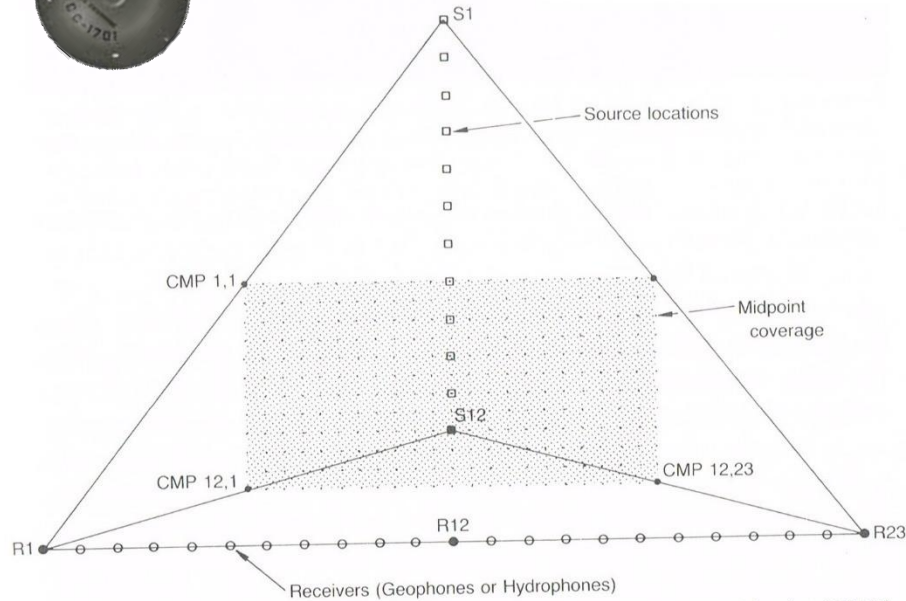


Figure 4-2. Cross-spread or T-spread data collection provides common mid-point (CMP) traces that cover an area. The T-spread is the simplest reduction of a 3D collection scheme, and can be expanded by running the receivers or sources in any arbitrary direction.

logies in Exploration Geophysics

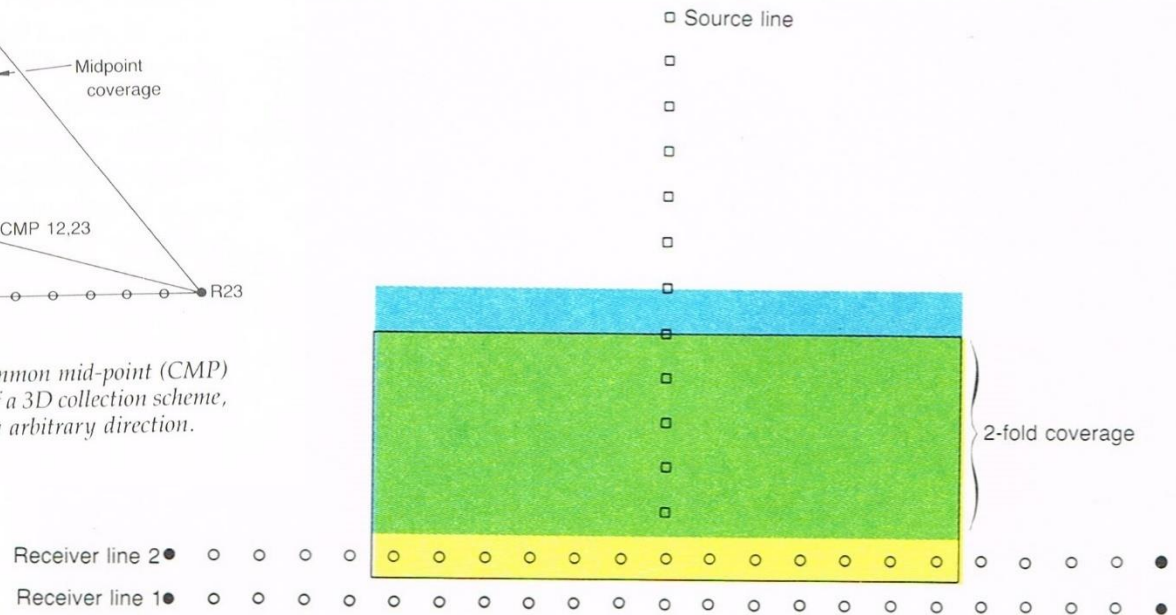


Figure 4-5. By shooting multiple source lines into the same receiver array, any desired CMP redundancy can be achieved. In the example above there is 2-fold coverage in the overlapped area and single fold coverage elsewhere. When there are two traces with different offsets at the same CMP, the data is referred to as 2-fold. Most 2D data collected today is 24, 48 or 96-fold, and by adding this redundant data together it improves the

SC8 - 107

3D Acquisition Design & CMP Display

98 New Technologies in Exploration Geophysics

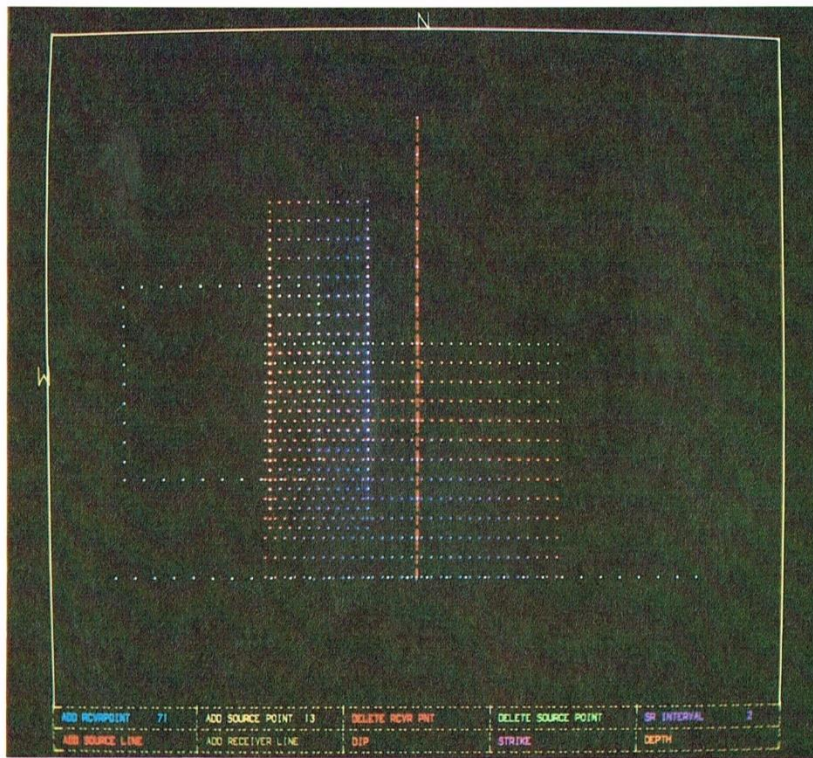


Figure 4-3. A map or aerial view of shot and receiver positions for a typical 3D survey shows the spatial relationship to generated CMP's. The shot points are marked in red along the vertical part of the X-spread. Receiver locations are marked in white, and are along both arms of the X-spread, as well as on the perimeter of a small square off to the north-west. The CMP's fall in between and are color coded by offset. (Courtesy Geosource, Petty-Ray Geophysical Division.)

3D Seismic Techniques 99

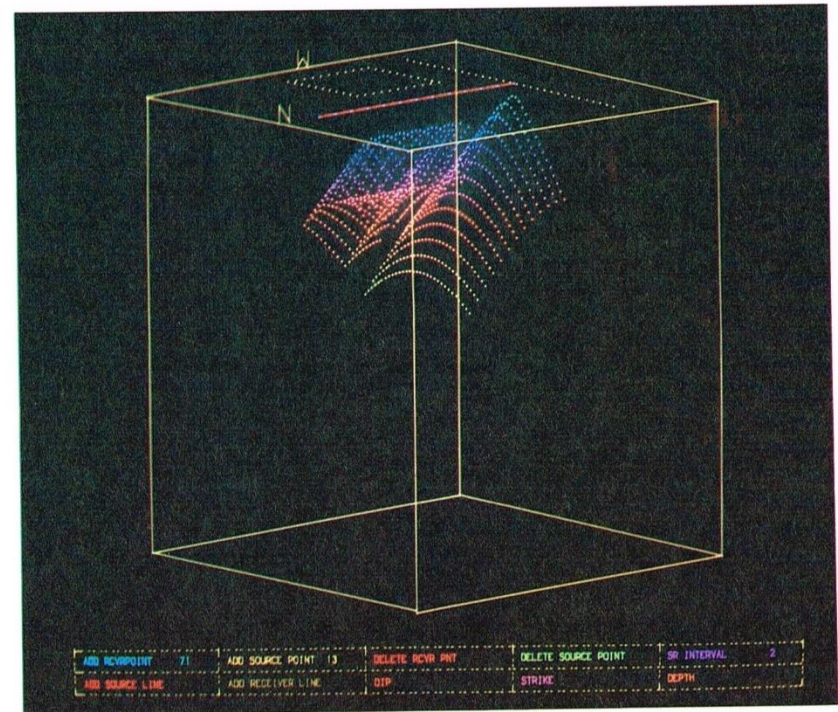


Figure 4-4. The offset differences for different CMP's are visually enhanced when the same information is displayed with offset shown as a function of required NMO correction along the z-axis. With an interactive display device, it is easy to rotate, translate, or scale this display to any desired orientation. (Courtesy Geosource, Petty-Ray Geophysical Division.)

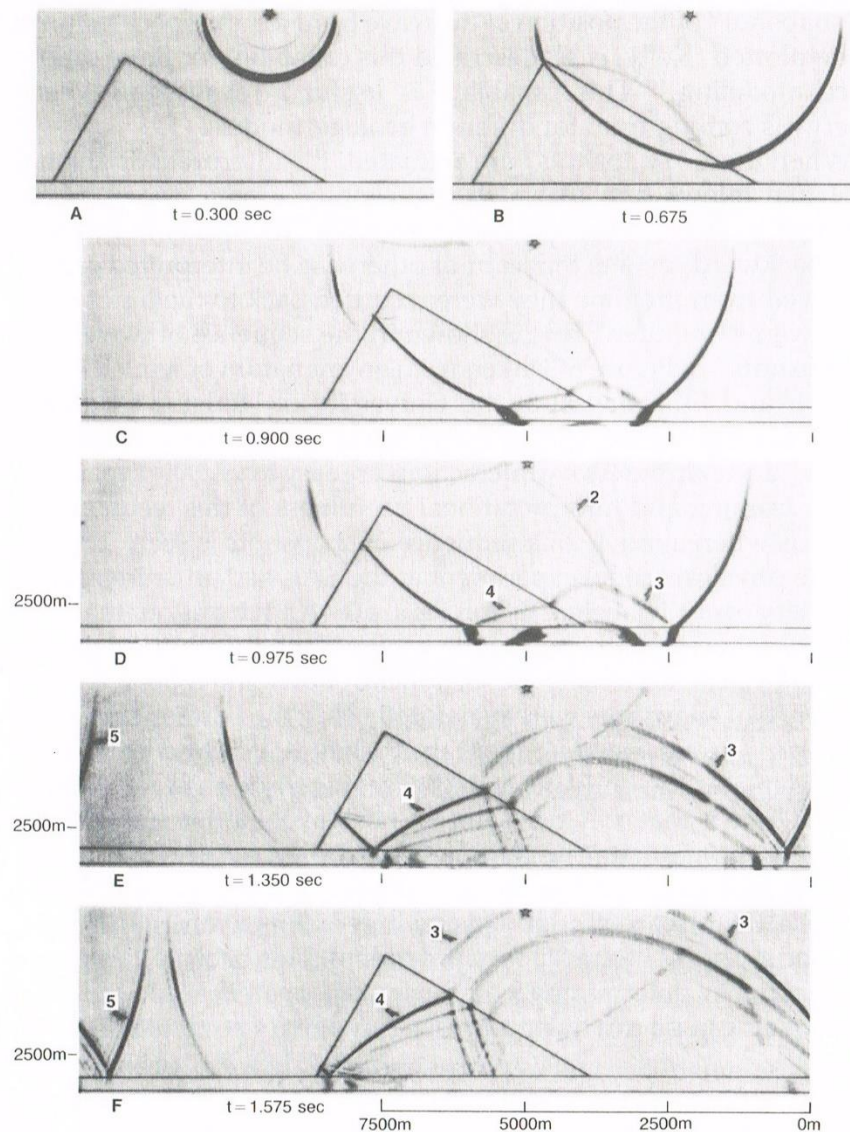


Figure 6-3. A sequence of wavefront "snapshots" calculated using the Kosloff, Baysal Fourier modeling technique. The pressure response is calculated at specific time steps and then the snapshots are "animated" to help interpret specific events. Event 2 is reflected energy off of the low-velocity wedge. Events 3 and 4 are reflected energy off of the high-velocity flat base. Event 5 is wrap-around due to the Fourier transforms used in this method. (After Kosloff and Baysal.)

Wedge Numerical and Physical Model

Numerical and Physical Modeling 135

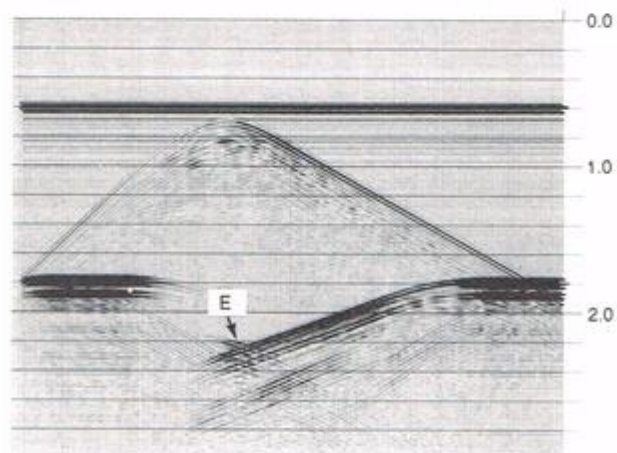


Figure 6-4. A 2D wedge physical model is shown accompanied by a seismic section across the model. Event E, the "mystery event on the physical model section, is the diffraction energy from the top of the wedge.

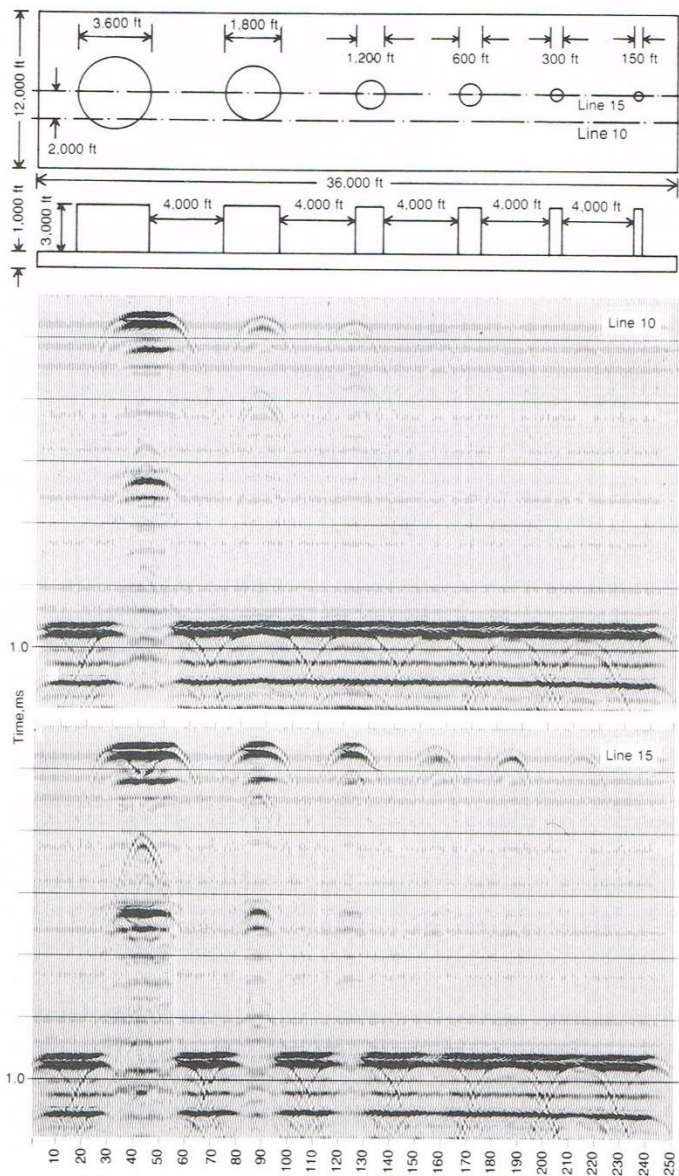


Figure 6-9. A map view (including section locations) and side view of physical model SALFRS is shown. Note the expected response on the seismic section for Line 15 as the cylinders get smaller. The 2,000-ft separation between the sections shows the importance of proper spatial sampling in order to see events that can indicate significant hydrocarbon prospects.²²

Fresnel & HCI Models

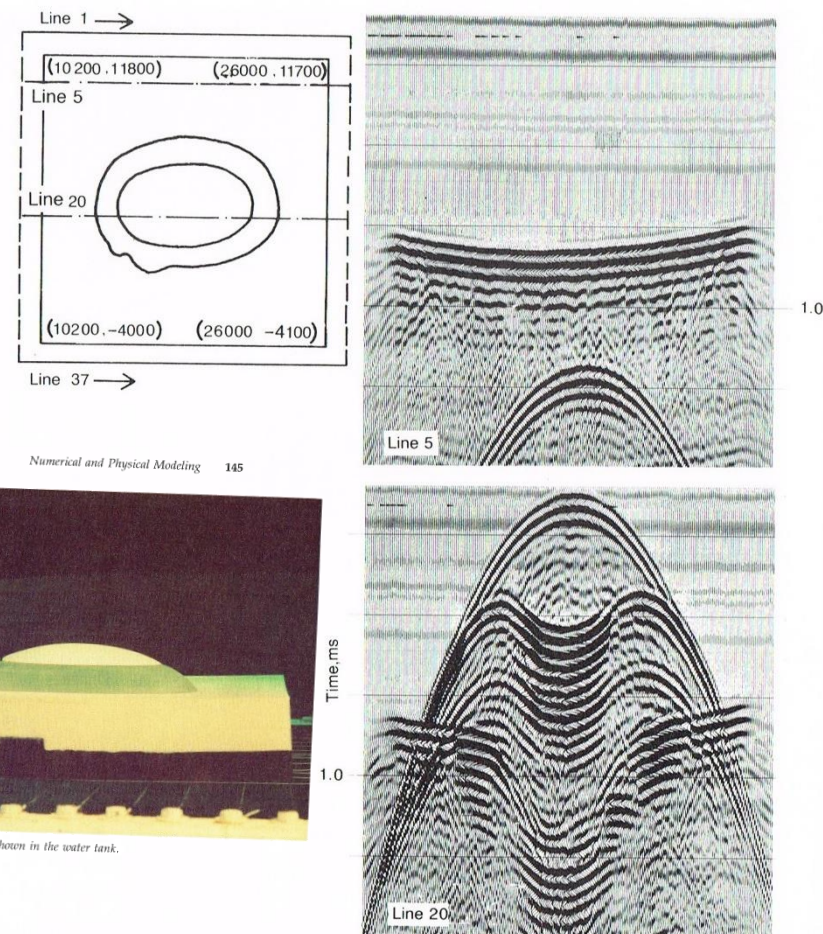


Figure 6-10. The 3D model SALHCI is shown in the water tank.

Figure 6-11. A map view of the SALHCI model is shown with two seismic lines referenced. Seismic sections for each of the lines are illustrated. Note the sideswipe from the model edge as indicated in the section for Line 5. The velocity push-down from the low velocity (gas) cap is shown in the section from Line 20.²³

SALNEL

Alluvial Stream Model

Numerical and Physical Modeling 147

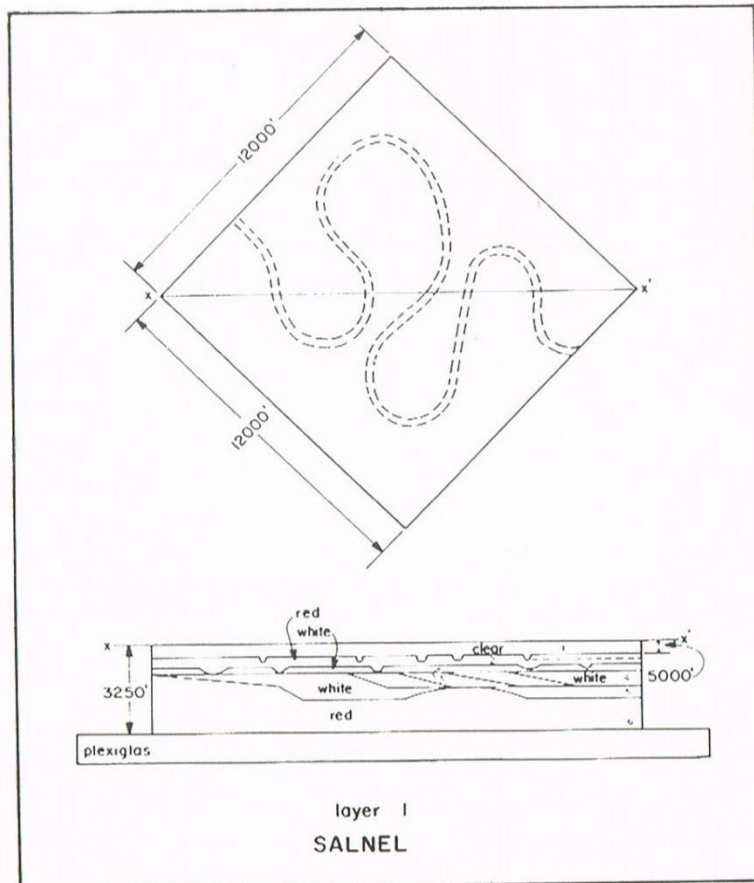


Figure 6-12A. Line drawing of SALNEL showing the six different layers represented by the model.²⁵

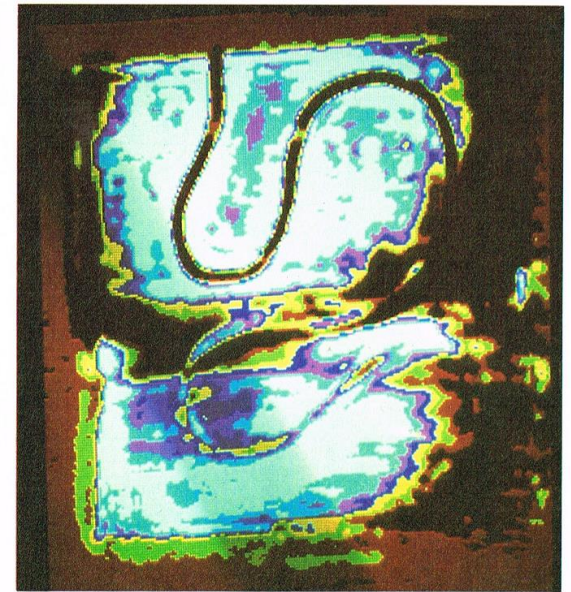


Figure 6-12B. Time-slice or horizontal section through the SALNEL meandering stream.

Numerical and Physical Modeling 149

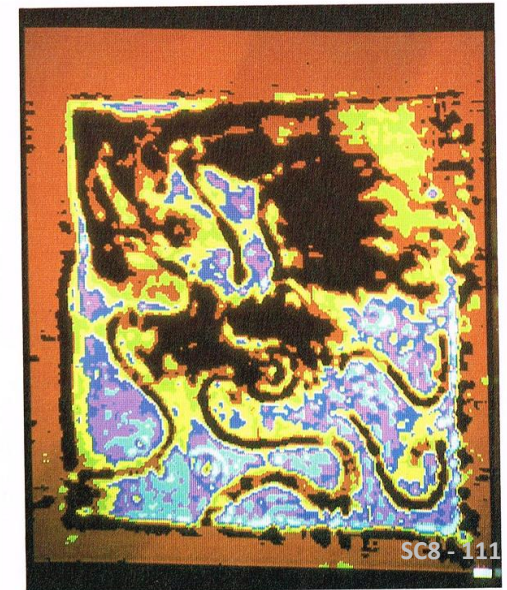


Figure 6-12C. Time-slice or horizontal section through the SALNEL braided streams.

3D Display & Migration Lens Model

True 3D Display Types 193

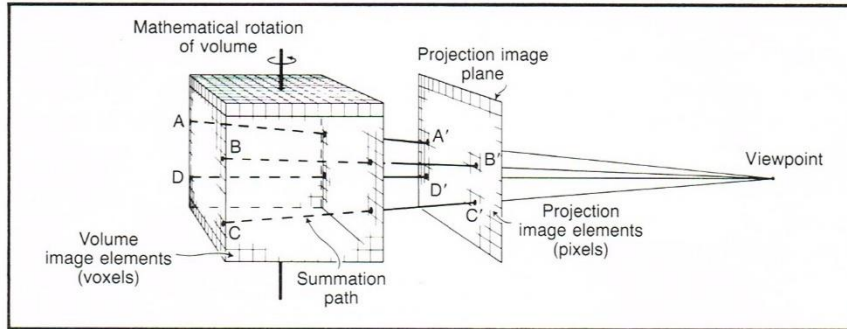


Figure 8-4. Picture elements (voxels) of the volume on the left are numerically summed along projection paths (four representative paths shown) to form the picture elements (pixels) of the two-dimensional projection image in the center. When the resulting digital image is displayed, it is as though the observer views the volume image from the viewpoint on the right. (Reproduced from SEG Reprint,²² Courtesy L.D. Harris, "Identification of the Optimal Orientation of Oblique Sections Through Multiple Parallel CT Images," *Journal of Computer Assisted Tomography*)

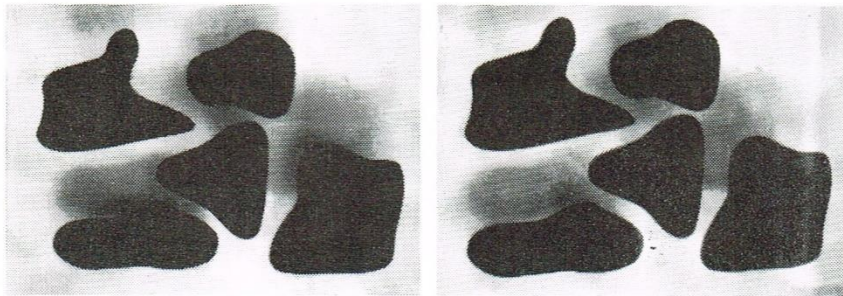


Figure 8-5. Stereoscopic photograph of a physical model with five plexiglass lenses raised above a plexiglass base. The highest lens is in the bottom right corner, they staircase down to the top left corner lens, and the bottom left and top right lenses are lowest and are at the same elevation.²³

True 3D Display Types 195

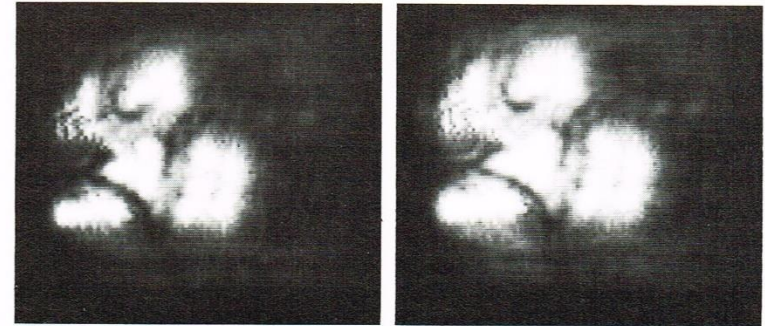


Figure 8-6. A stereoscopic projection of a volume of unprocessed seismic data over the physical model from Figure 8-5. Note the unfocused appearance caused by the diffractions.²³

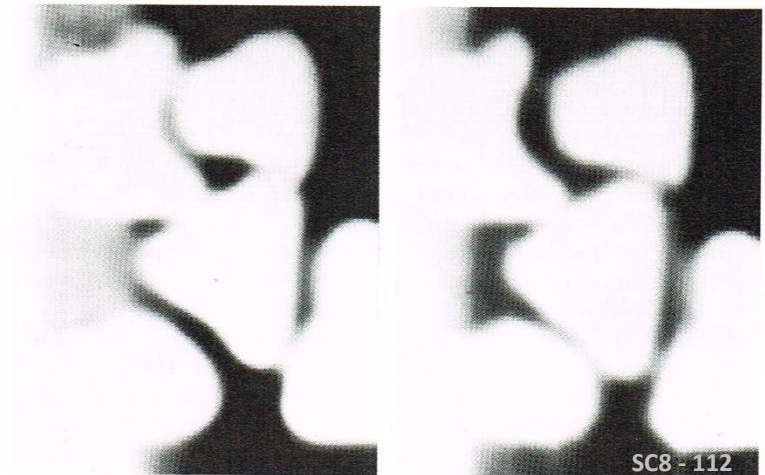


Figure 8-7. A stereoscopic projection of a volume of Hilbert Transformed 3D migrated data from the physical model in Figure 8-5. Note the focusing effect of migration compared to Figure 8-6.²⁴

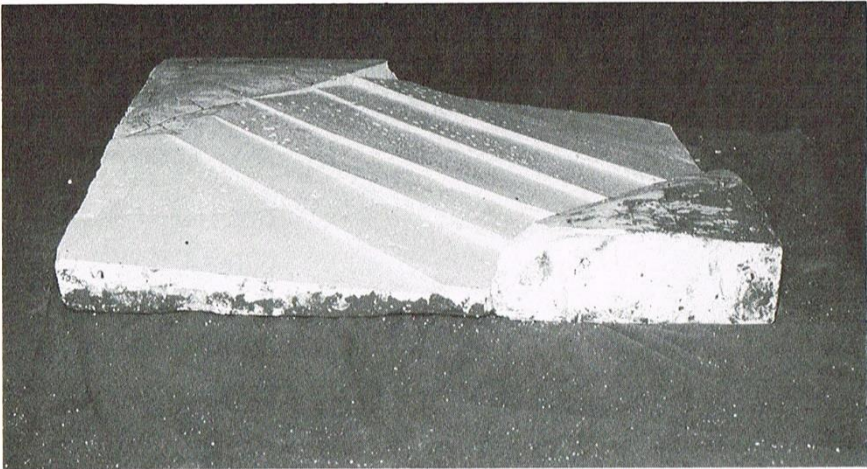


Figure 6-13B. A view of the SALNOR J-Unconformity plaster cast after it was shaved off to the Base Statfjord horizon.

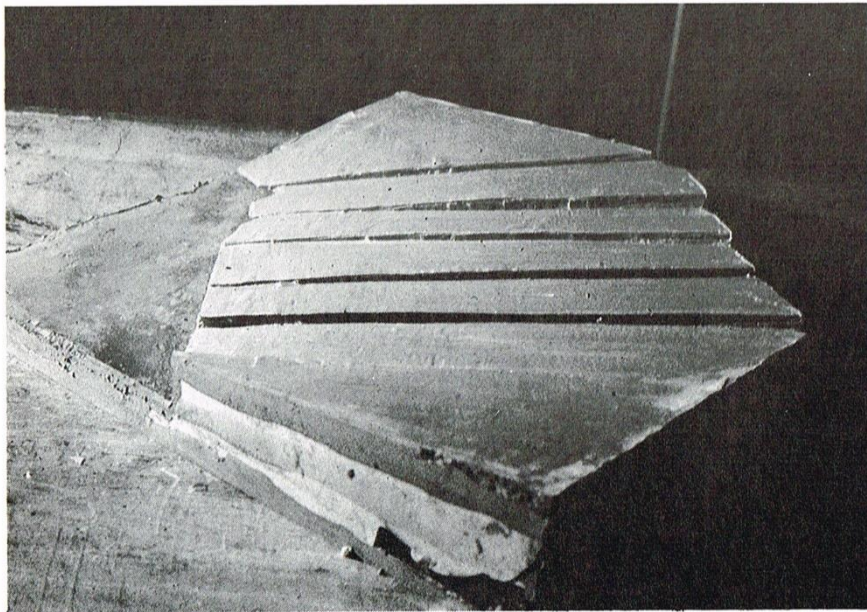


Figure 6-13C. The silicon rubber for deeper layers was added by pouring between the model and the plaster cast. This shows the SALNOR model after the Statfjord horizon had been poured.

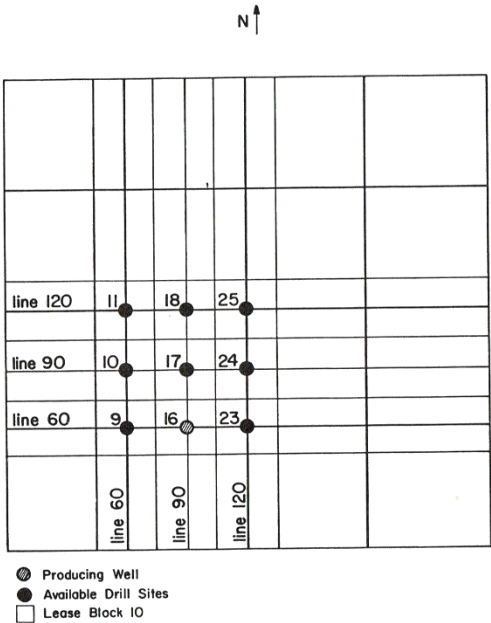


Figure 6-13F. A map showing the relationship of 7 north-south, 7 east-west, and 9 possible drilling locations. This is part of an interpretation training exercise.

SALNOR Model of Norwegian North Sea Geology

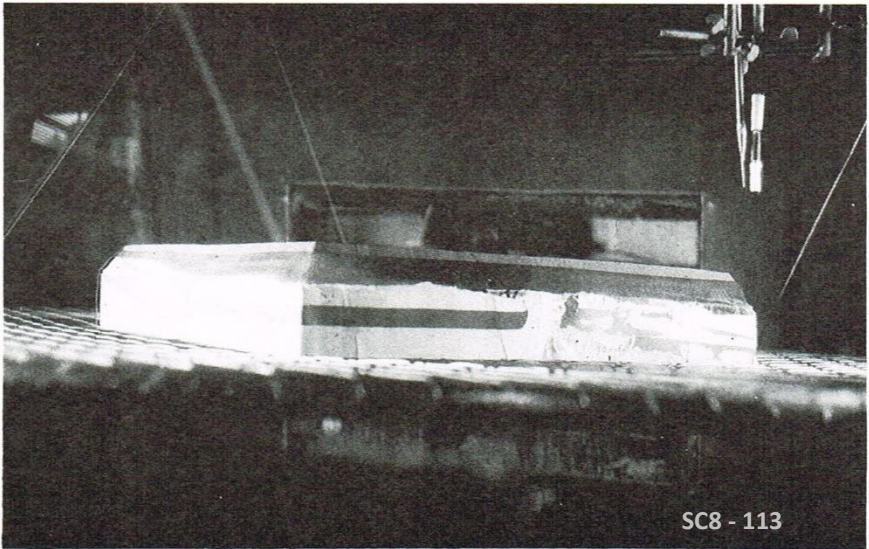


Figure 6-13A. The completed SALNOR physical model in the modeling tank.

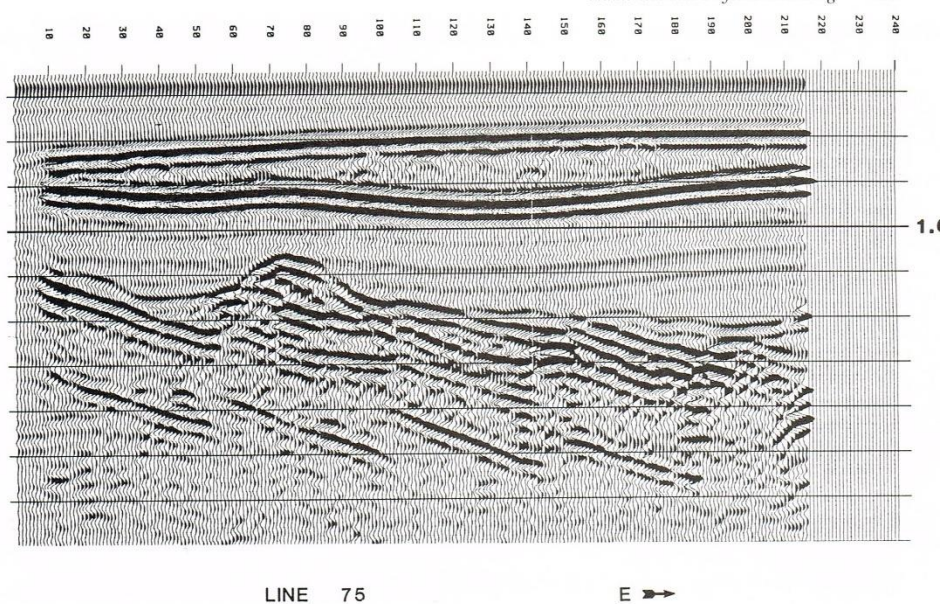


Figure 6-13D. An east-west vertical seismic section across the SALNOR model. The top three horizons represent the Top Paleocene, Top Cretaceous, and J-Unconformity. The other horizon easily recognized, which has four faults, is the Base Statfjord horizon.

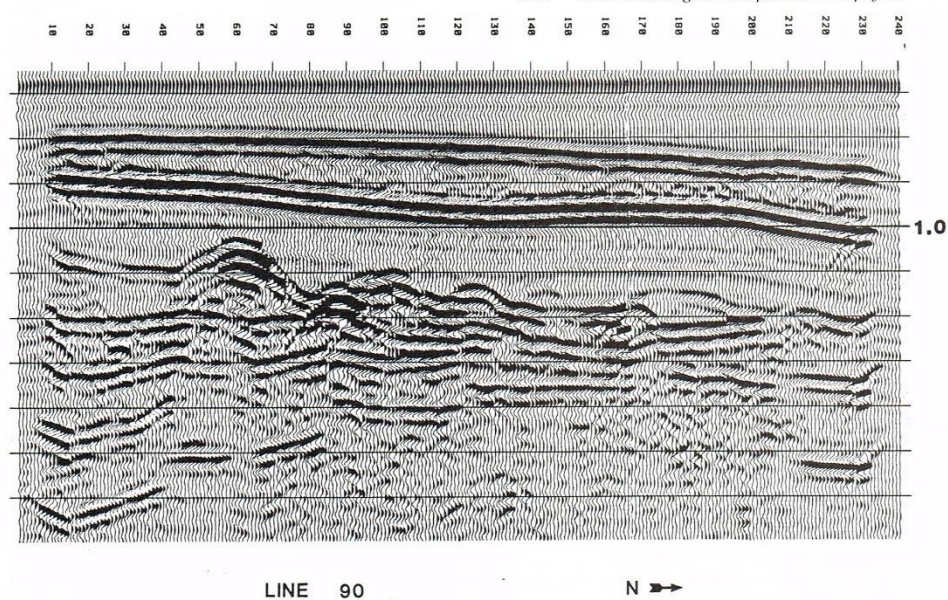


Figure 6-13E. A north-south vertical seismic section across the SALNOR model. The same horizons noted in Figure 6-13D can be recognized. On the left side, the Top and Base Brent and Top and Base Statfjord are also easily seen.

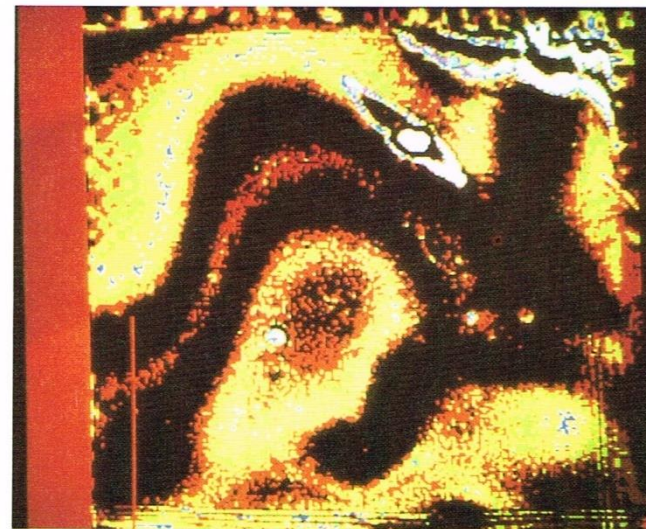


Figure 6-13G. A horizontal seismic section from a 3D survey collected across the North Sea physical model. The time-slice section is at 1.06 seconds and cuts the J-Unconformity structural highs.



Figure 6-13H. A time-slice section from the same SALNOR 3D survey at time 1.22 seconds. At this depth the section cuts through the two dipping, producing Brent and Statfjord sandstones. The fault cuts are easily identified, especially when a sequence of time-slices are animated like a movie.

Notes

This image shows a single sheet of white paper with horizontal blue ruling lines. The lines are evenly spaced and run across the width of the page. There are no margins, text, or other markings on the paper.



Volumetric Data Allowed Study of 3-Dimensional Geology

96 *New Technologies in Exploration Geophysics*

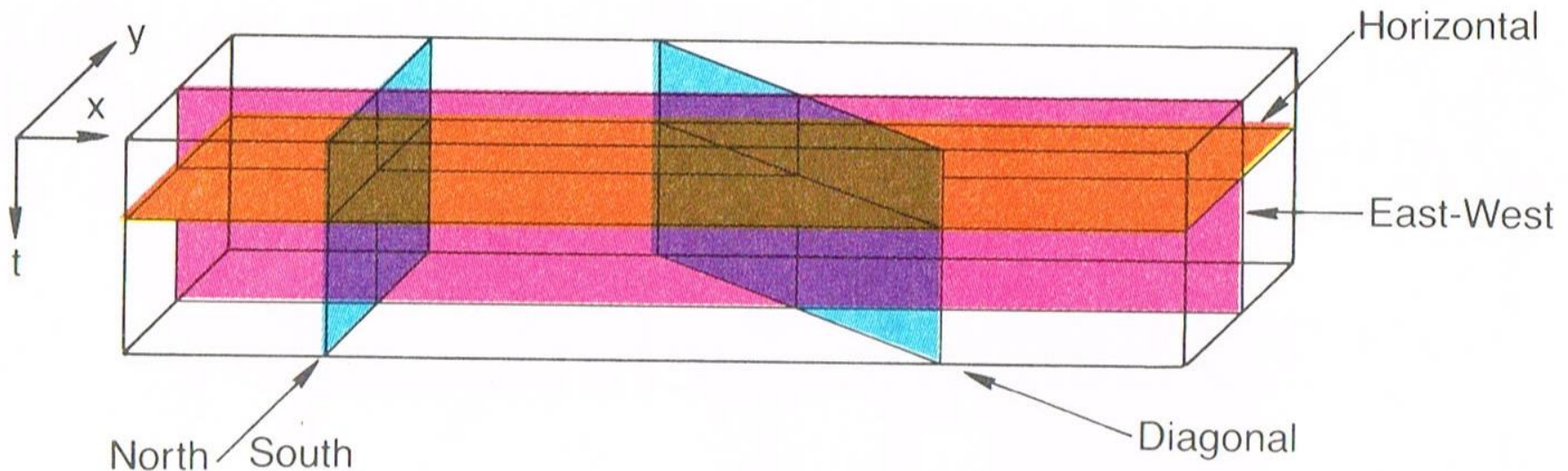


Figure 4-1. A 3D data volume allows for a much more complete evaluation of the subsurface. The data can be vertically sliced in any arbitrary direction to allow interpretation along the lines critical to an accurate evaluation. Horizontal sections can also be generated from a data volume.

GSI & E&S

3-D Displays

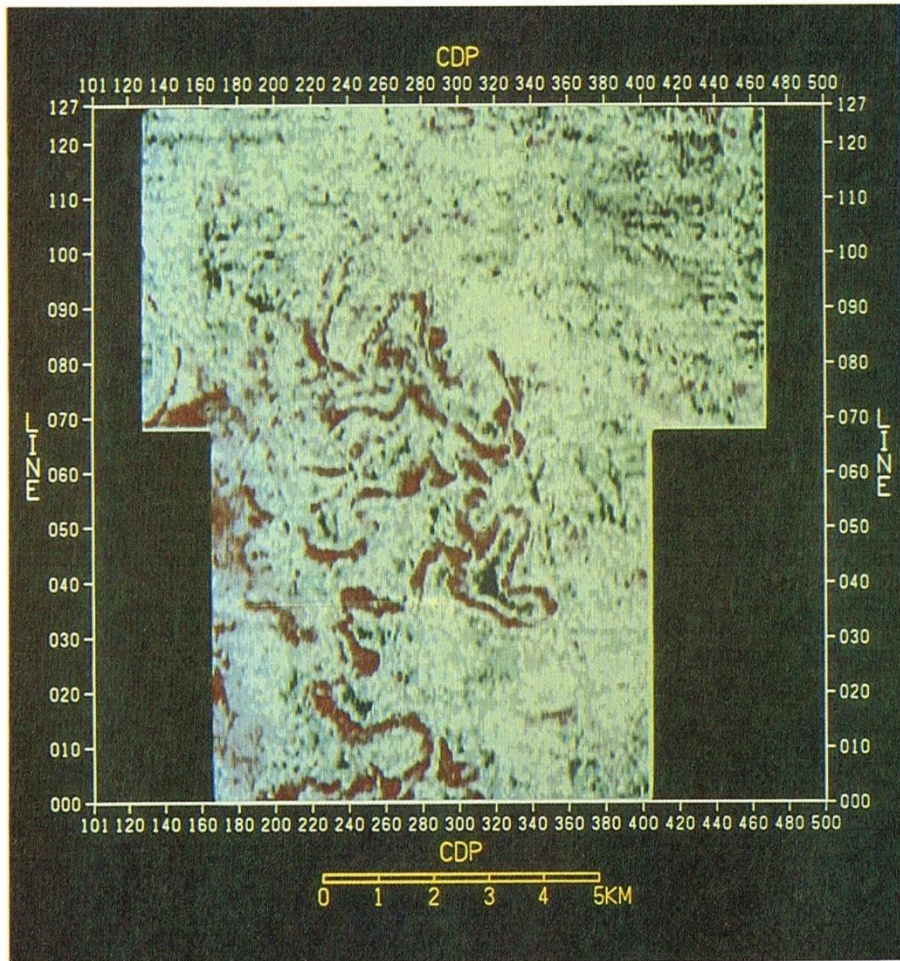
106 *New Technologies in Exploration Geophysics*

Figure 4-7. The unique capabilities to interpret a subsurface geologic sequence with 3D data volumes is shown by this horizontal (SEISCROP) seismic section slicing a meandering stream channel in the Gulf of Thailand. (Courtesy Geophysical Service, Inc.)

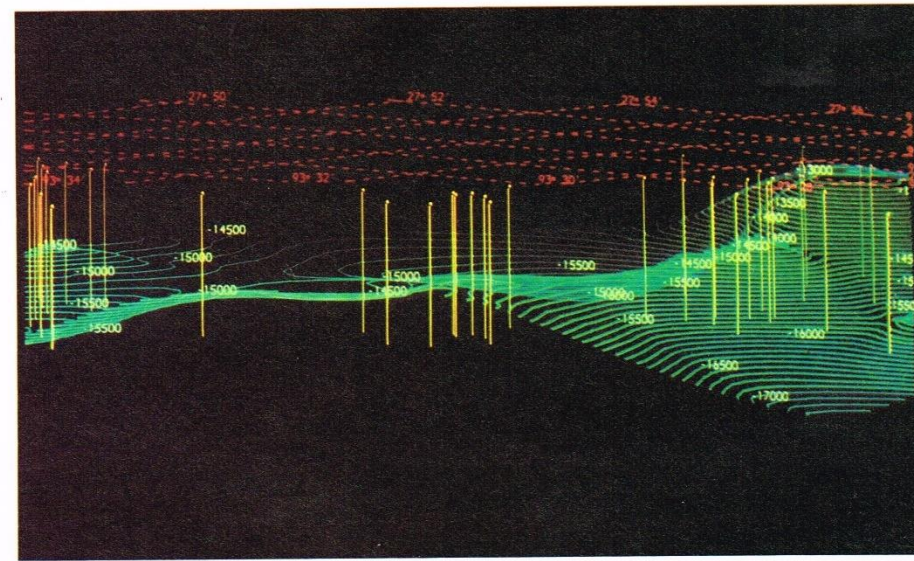
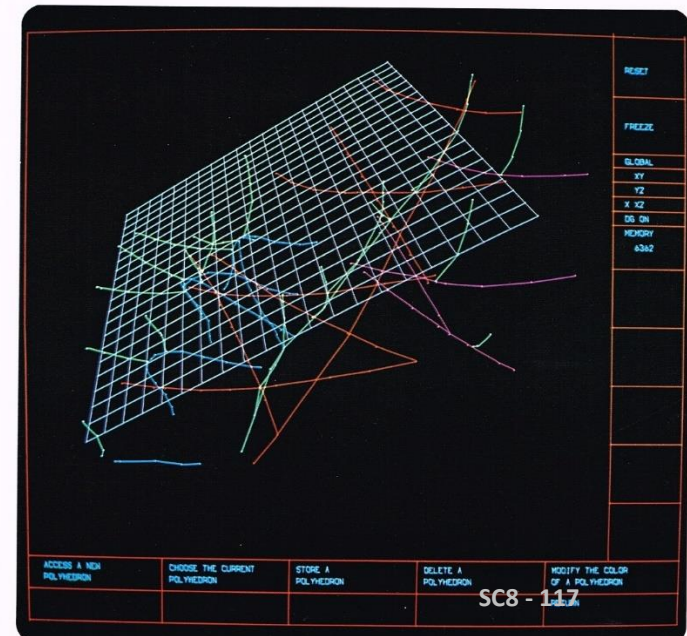


Figure 2-2. Example of a full-color, 3D display that is rotatable around an axis. Such capability enhances seismic data interpretation in a world with 3D relationships. (Courtesy Evans and Sutherland.)

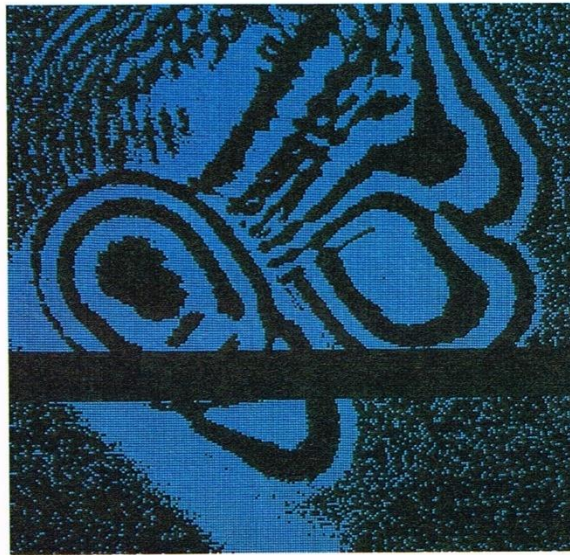
EVANS & SUTHERLAND



Seismic Data Analysis—The Picture System can be a powerful tool for interpreting seismic data. Here fault lines are displayed beneath a grid representative of the earth's surface. Color is used to identify lines belonging to a common fault plane.



A

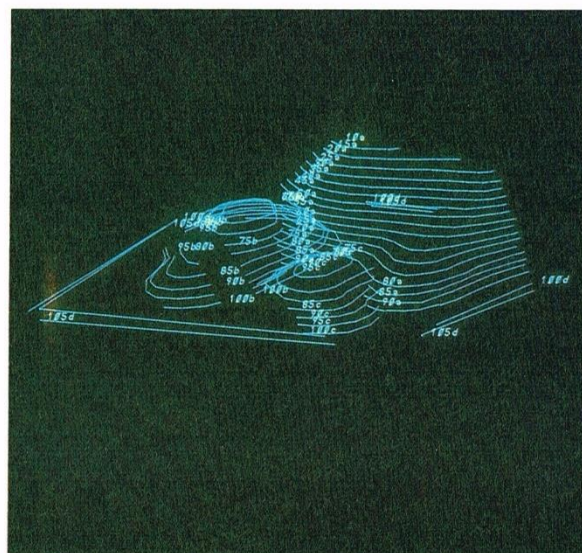
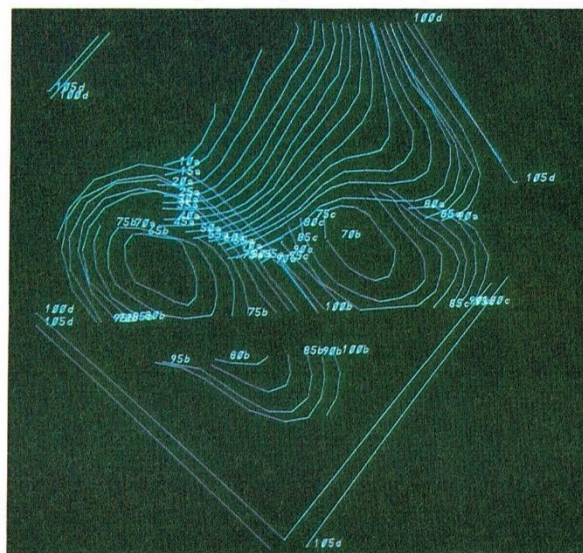


B

Figure 4-8. Interactive 3D interpretation techniques are becoming much more common. Here two horizontal sections across the SALGLF model are shown (A and B). There is no data in the black strip because of a data collection error.

First Interactive 3-D Displays on the Adage Raster Segment Generator and Vector Display

108 New Technologies in Exploration Geophysics



D

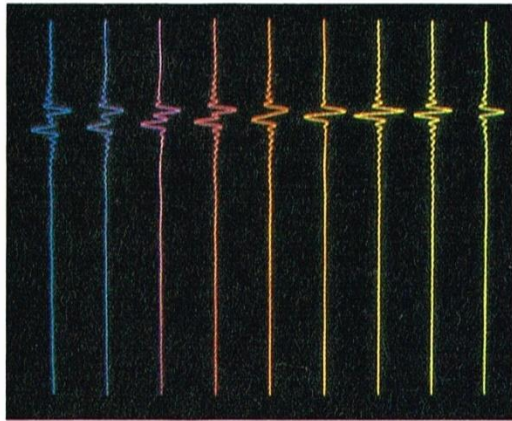
Figure 4-8 (continued). As horizontal sections are stepped through, they can be interactively interpreted as a 3D contour map that can be rotated in 3D space in real time (C and D).

Complex Seismic Traces

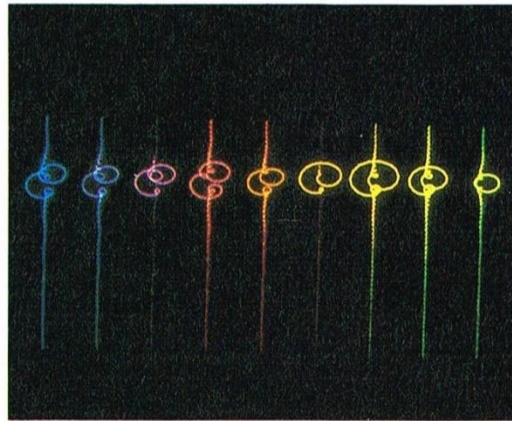
3-D Rotating Phase at NASA on E&S

Interactive Interpretation

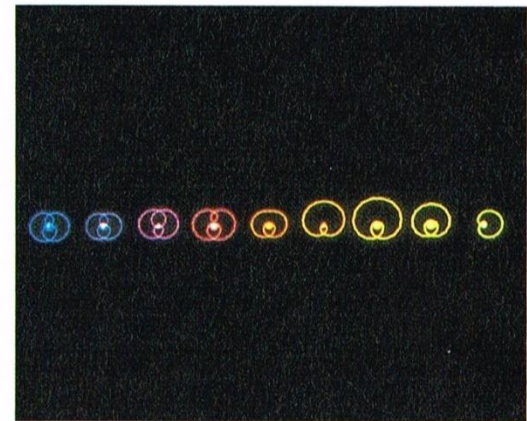
227



A



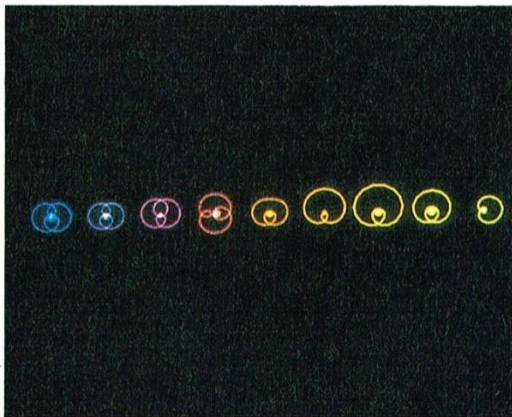
B



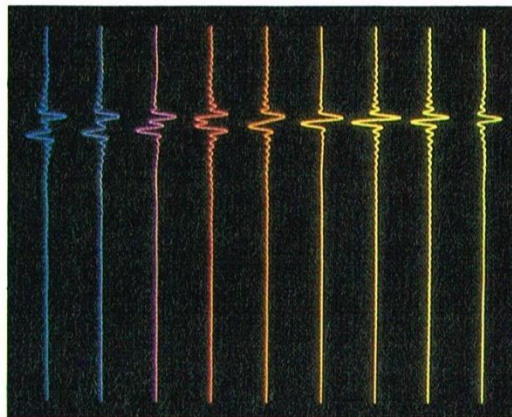
C

Figure 9-11. This sequence of photos displays a 90° phase shift of one synthetic complex seismic trace across a formation pinchout. From A to B the complex traces are rotated, until a top down view is reached in C. At this point, all of the traces are in phase. In D, the fourth trace from the left is rotated to an out-of-phase position. It remains in this out-of-phase position when the entire group of traces is then rotated back to their original vertical position (E). It now appears that the fourth trace no longer fits into the pinchout. Such phase discrepancies are commonly found when trying to tie seismic sections together from different surveys. This is only one example of the subtle characteristics of and problems with seismic data interpretation. (Courtesy Geosource, Petty-Ray Geophysical Division.)

SC8 - 119



D



E

Vibrating Mirrors & Holograms

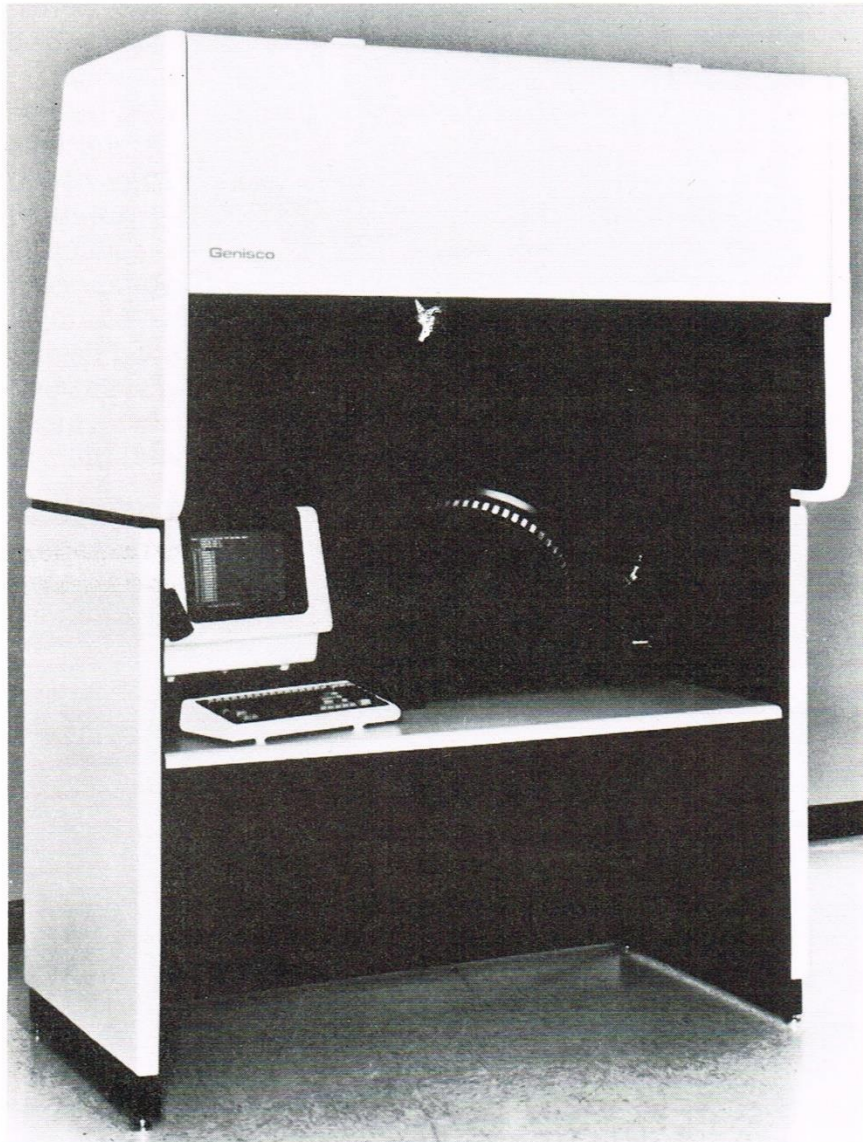
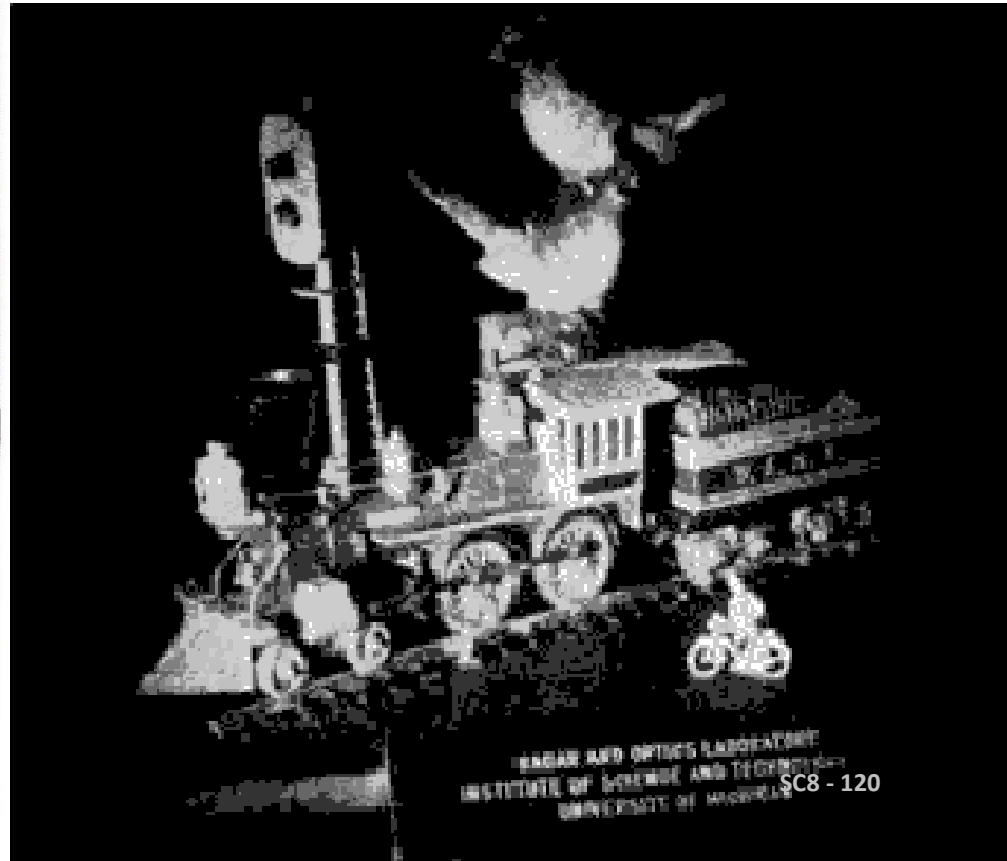
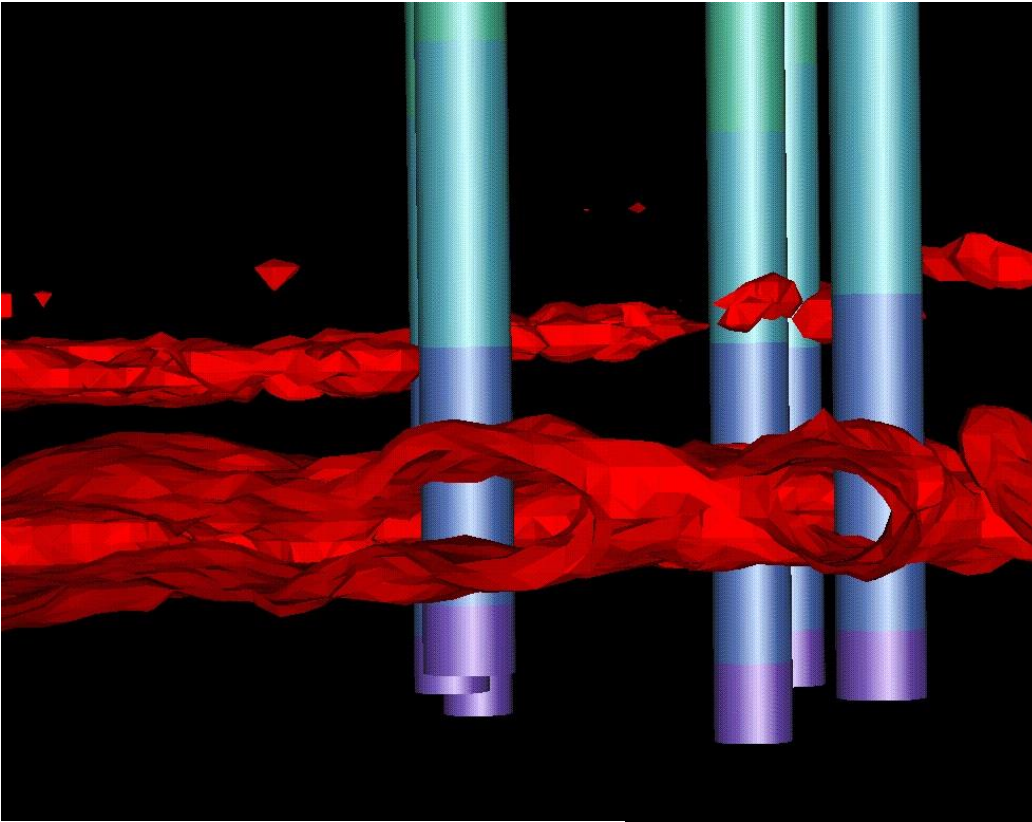


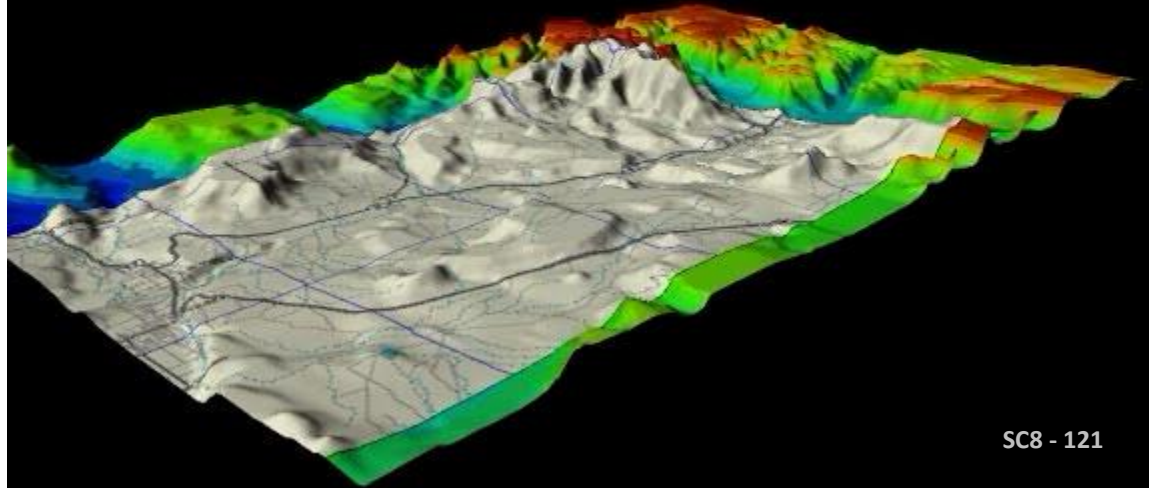
Figure 8-10. The Genisco SpaceGraph vibrating mirror 3D display device. A 40-cm vibrating mirror is partially shown at the center of the display. A high-resolution CRT is housed within the overhead casing. (Courtesy Hand Stover, Genisco Computer Corp.)



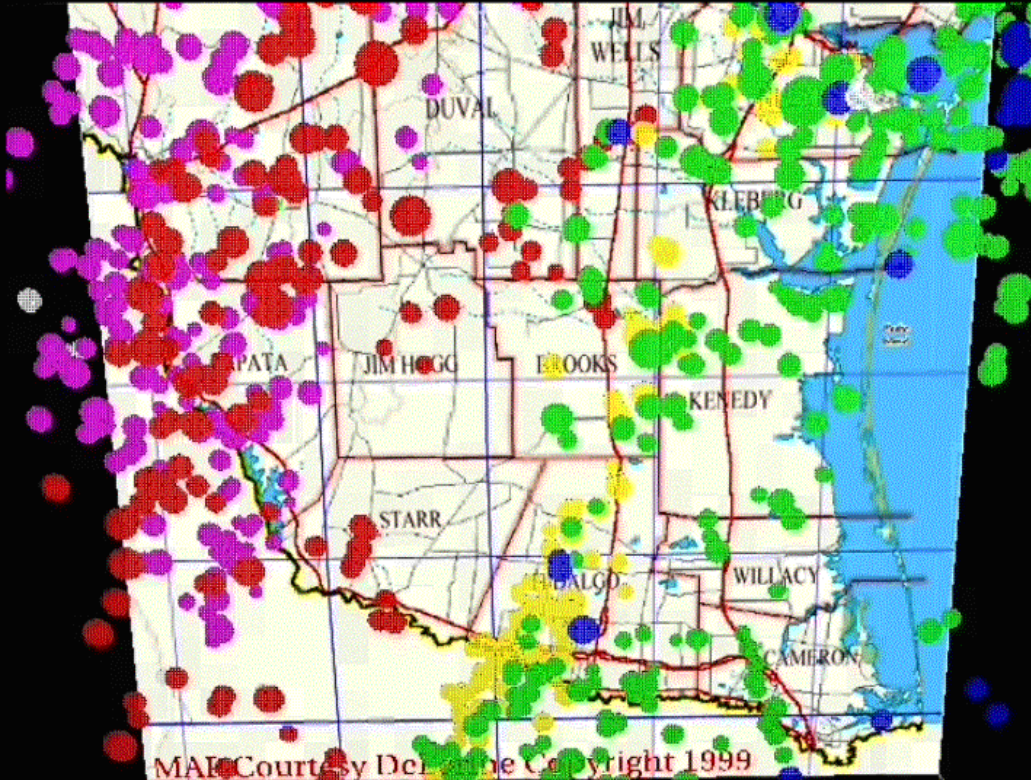
U of U 3D & Continuum Resources



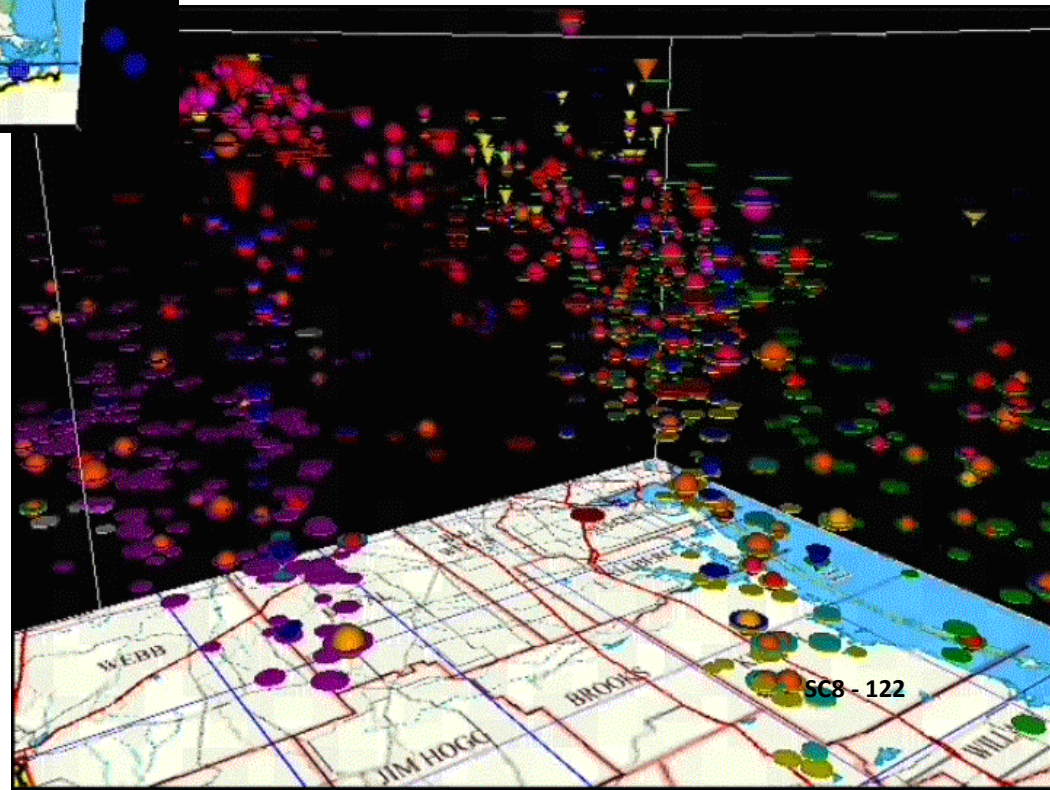
Zion and the
Road to Hurricane



South Texas Horizon Tops in 3-D at Continuum

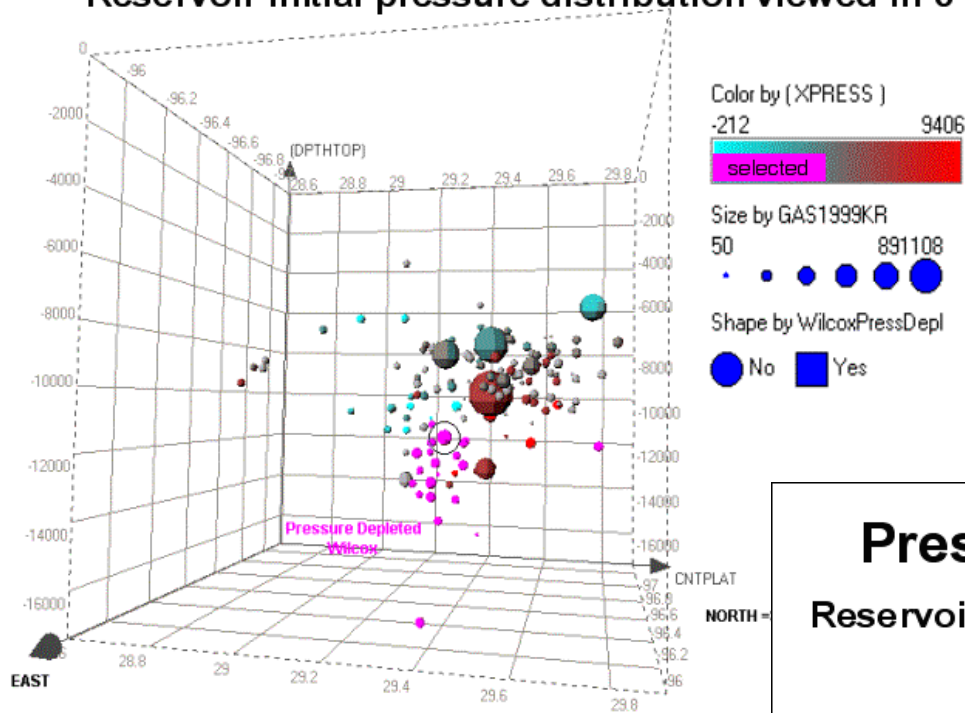


South Texas Example
of Visualizing an Entirely
New Exploration Play:
Wilcox Turbidite Channels



Data Mining and Search Strategies

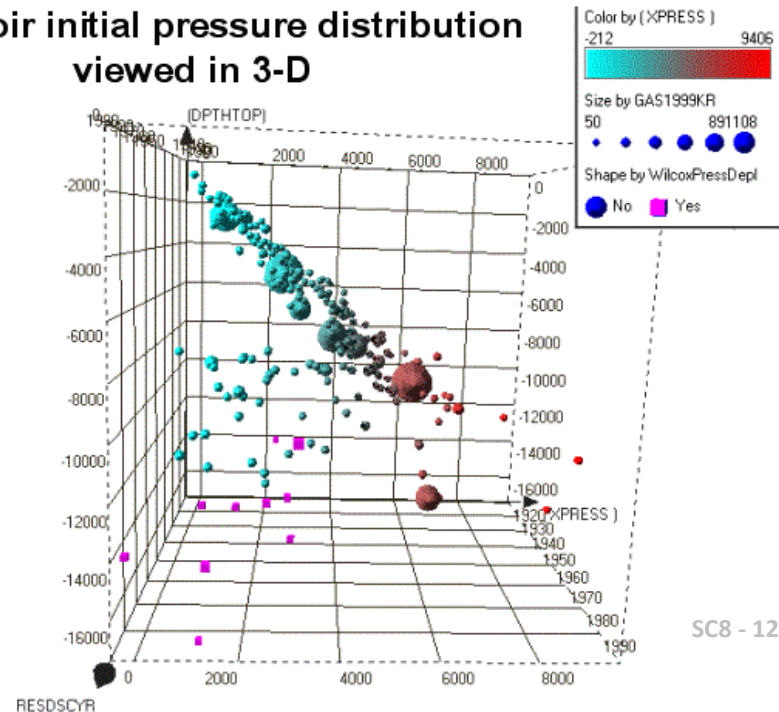
Reservoir initial pressure distribution viewed in 3-D



Depth of Gas & Geopressure

Pressure/Depth Exploration History

Reservoir initial pressure distribution
viewed in 3-D



Colorado County
Gas Wells and
New Trends

Notes

This image shows a single sheet of white paper with horizontal blue ruling lines. The lines are evenly spaced and run across the width of the page. There are no margins, text, or other markings on the paper.

LAND MARK



Landmark Graphics Corporation will meet the needs of the seismic data interpretation market by introducing a stand-alone color raster computer graphics workstation with proprietary software. It will be used by explorationists in display, manipulation and interpretation of one-dimensional (1D) logs with synthetic traces, two-dimensional (2D) seismic and geologic sections, and three-dimensional (3D) seismic volumes.

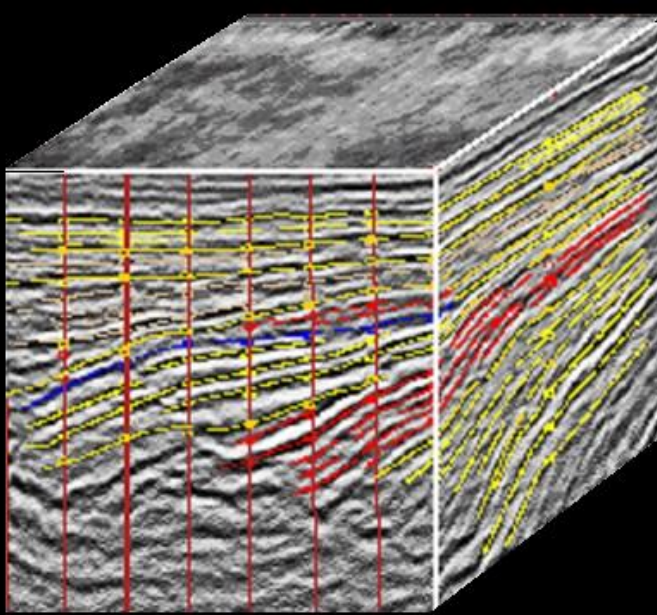
Landmark Graphics Corporation has assembled the best talent in the seismic industry to define, develop, assemble and market a computer graphics seismic interpretation system.

August 1, 1982

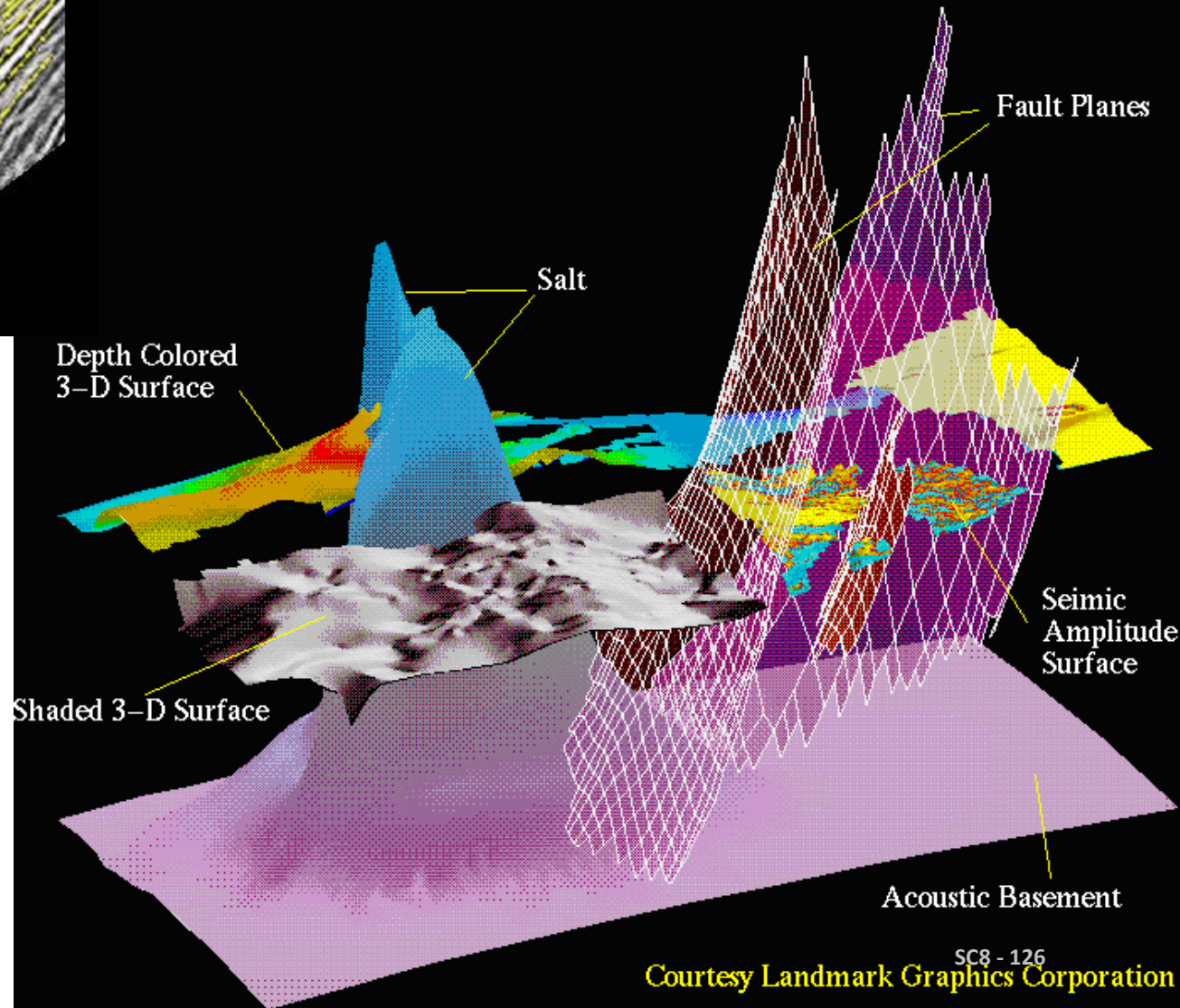
Landmark Graphics Corporation Business Plan

Founded by: Roice Nelson, John Mouton, Andy Hildebrand, Bob Limbaugh

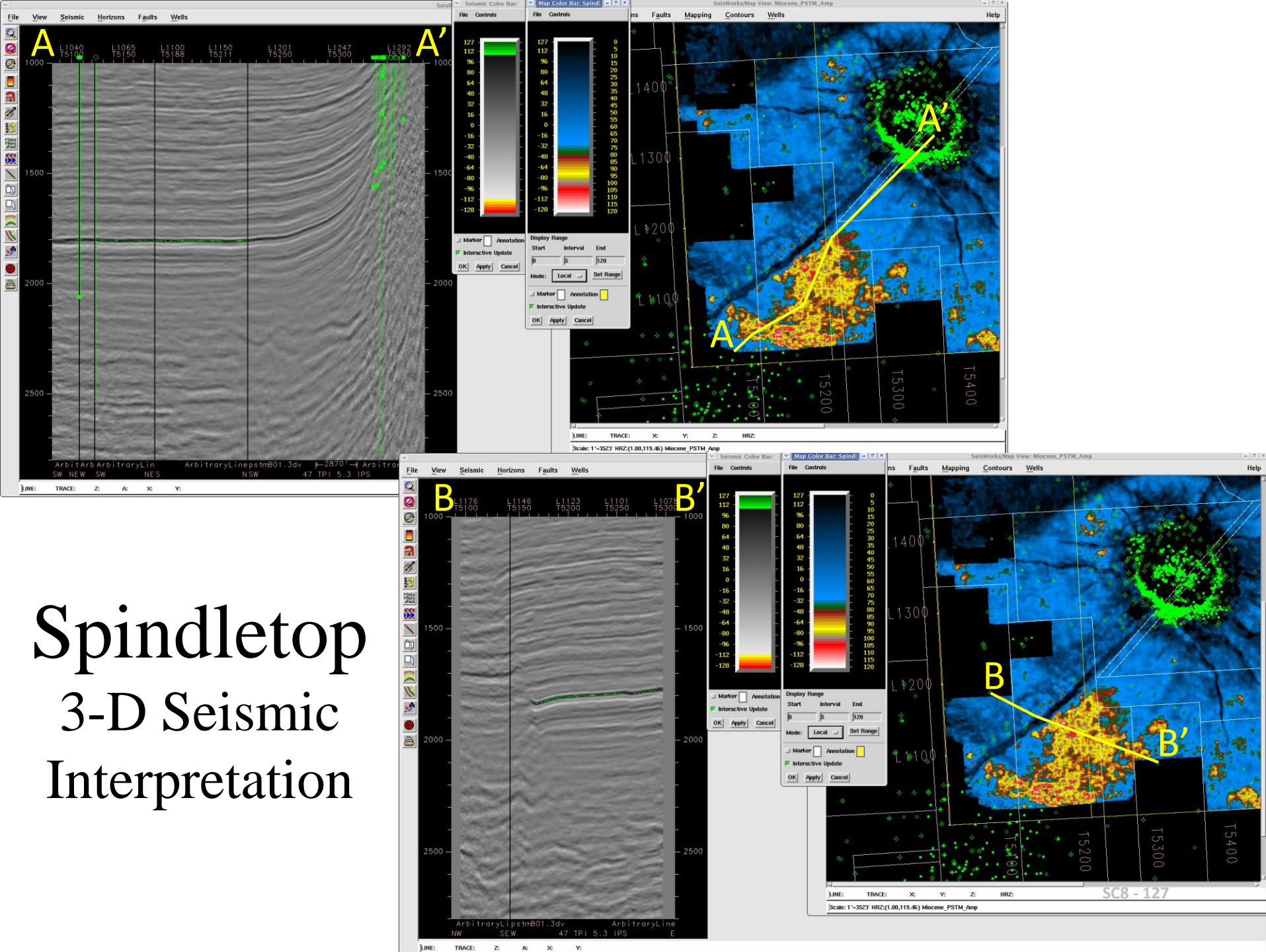
3-D Landmark Displays



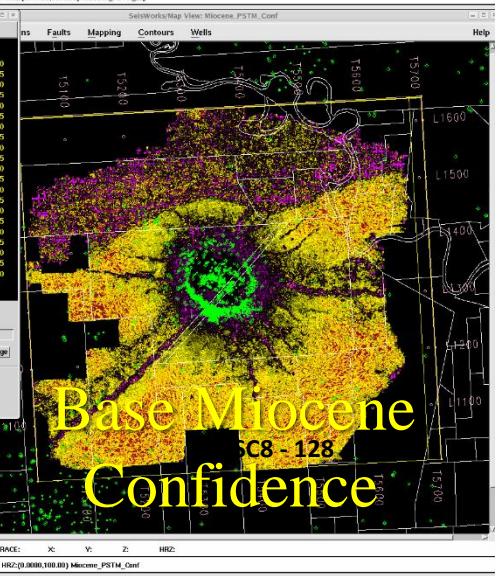
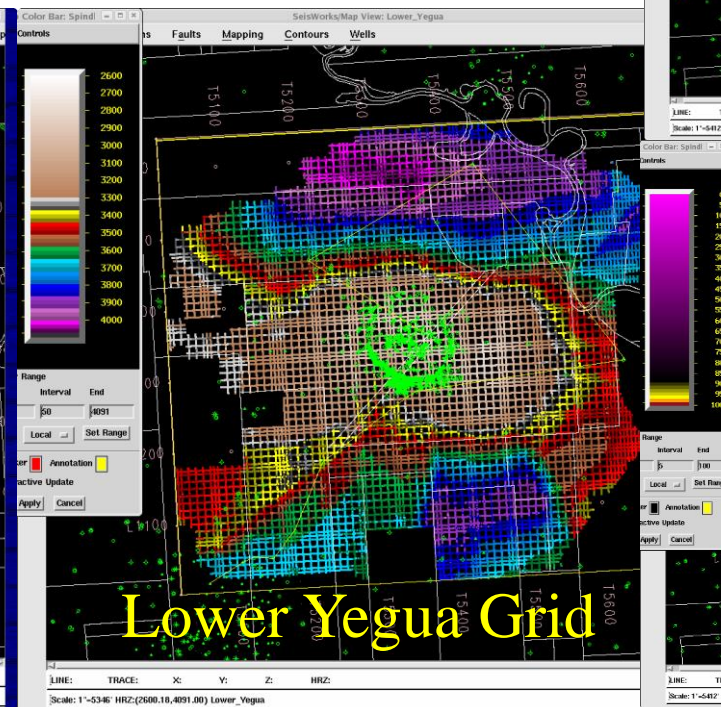
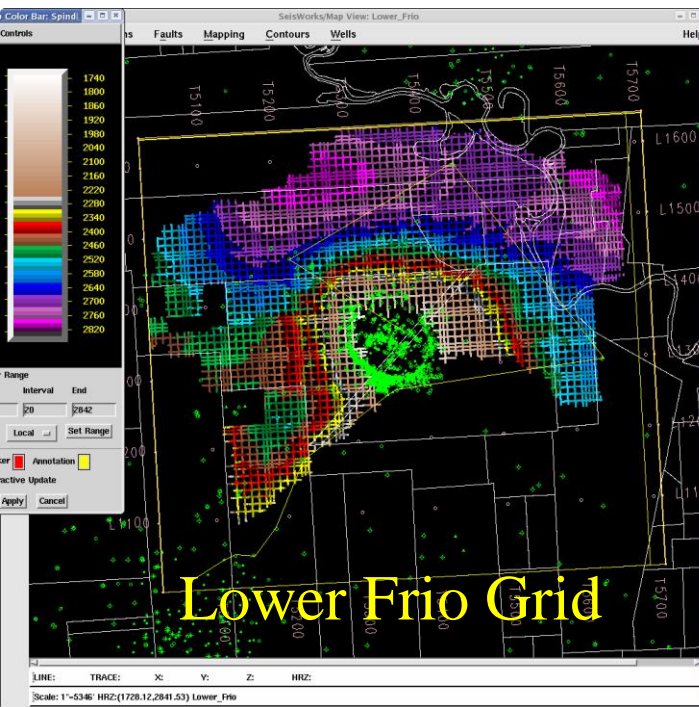
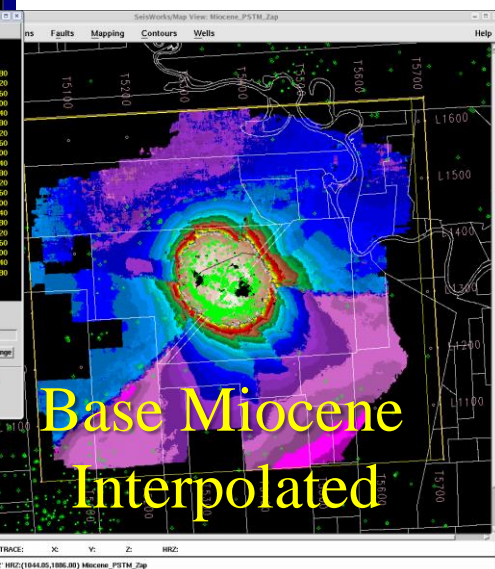
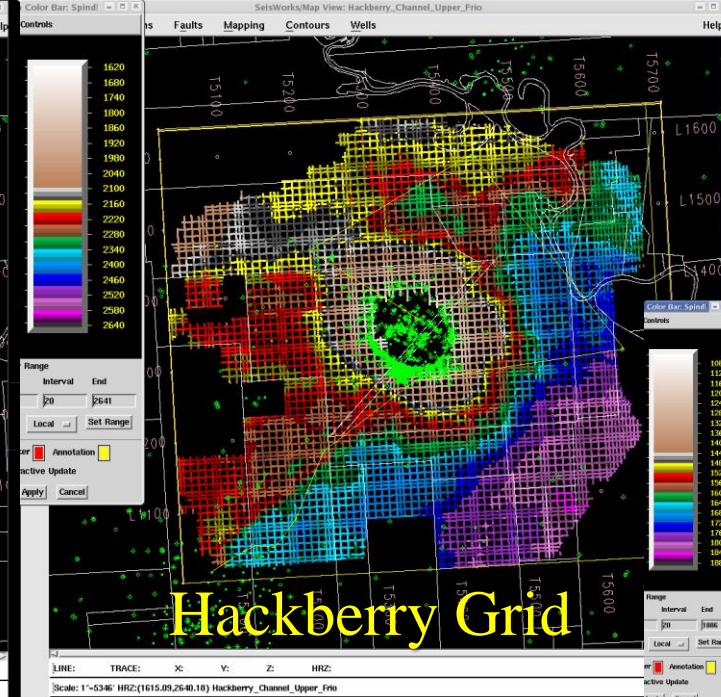
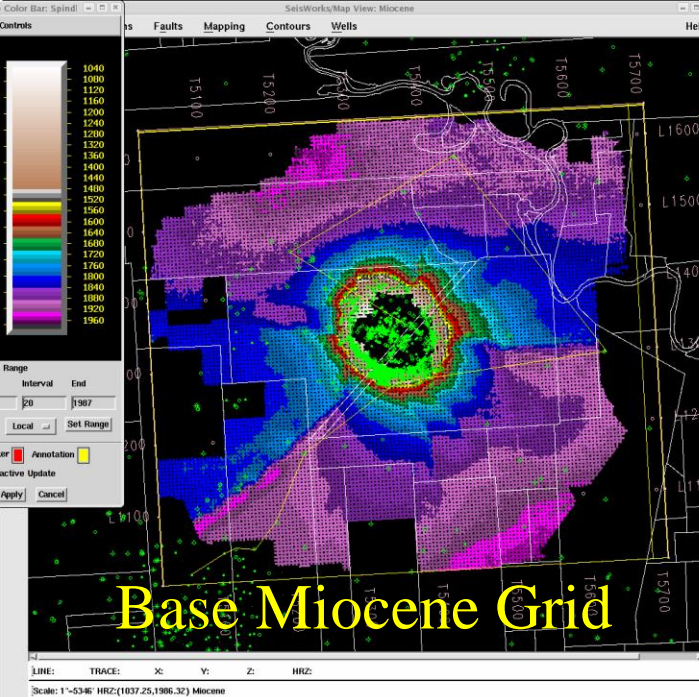
1994, Still Doing
Jimmy-Rig
3-D Displays
(Stratton Above)

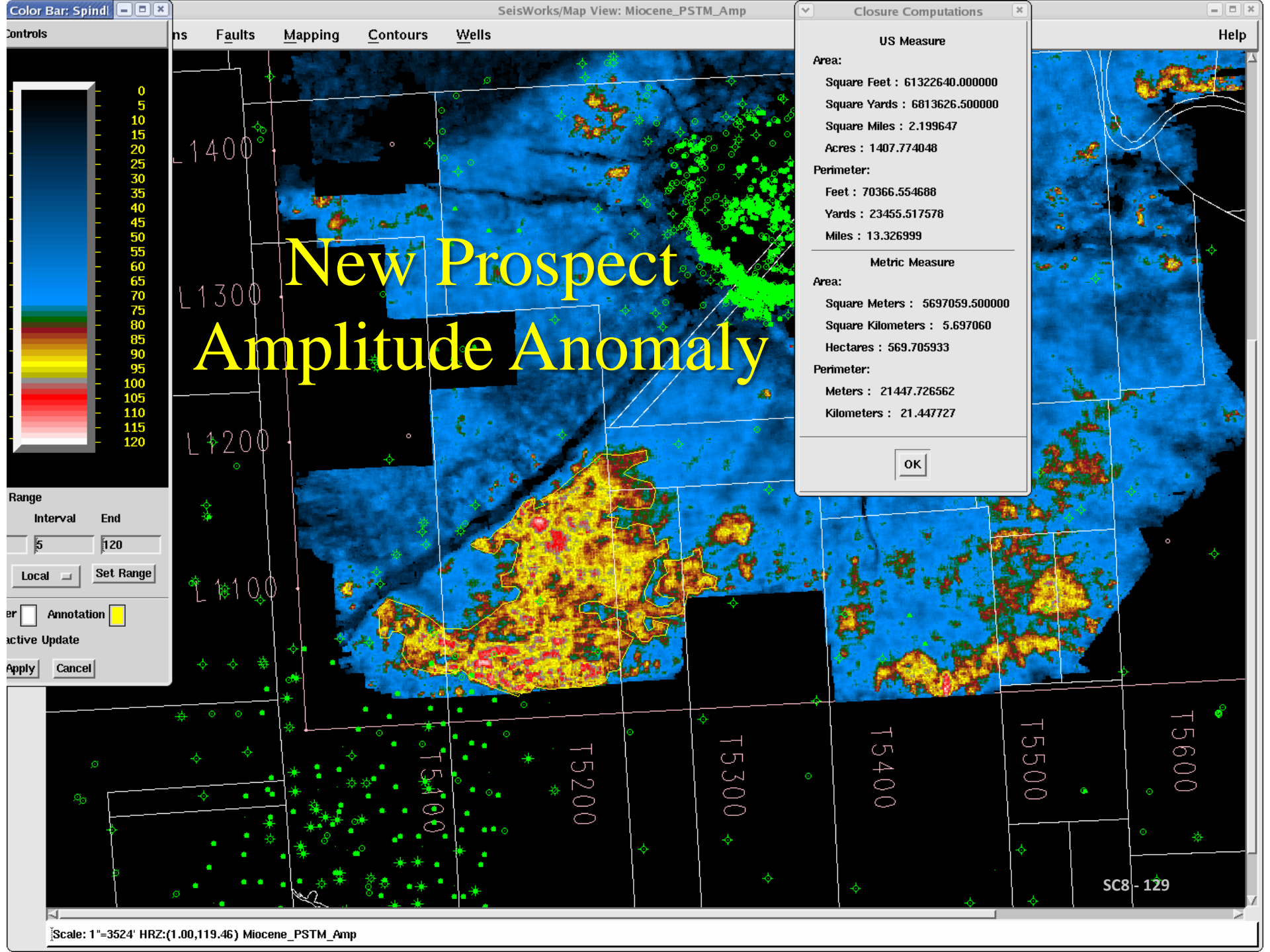


Spindletop 3-D Seismic Interpretation



3-D Interpretation

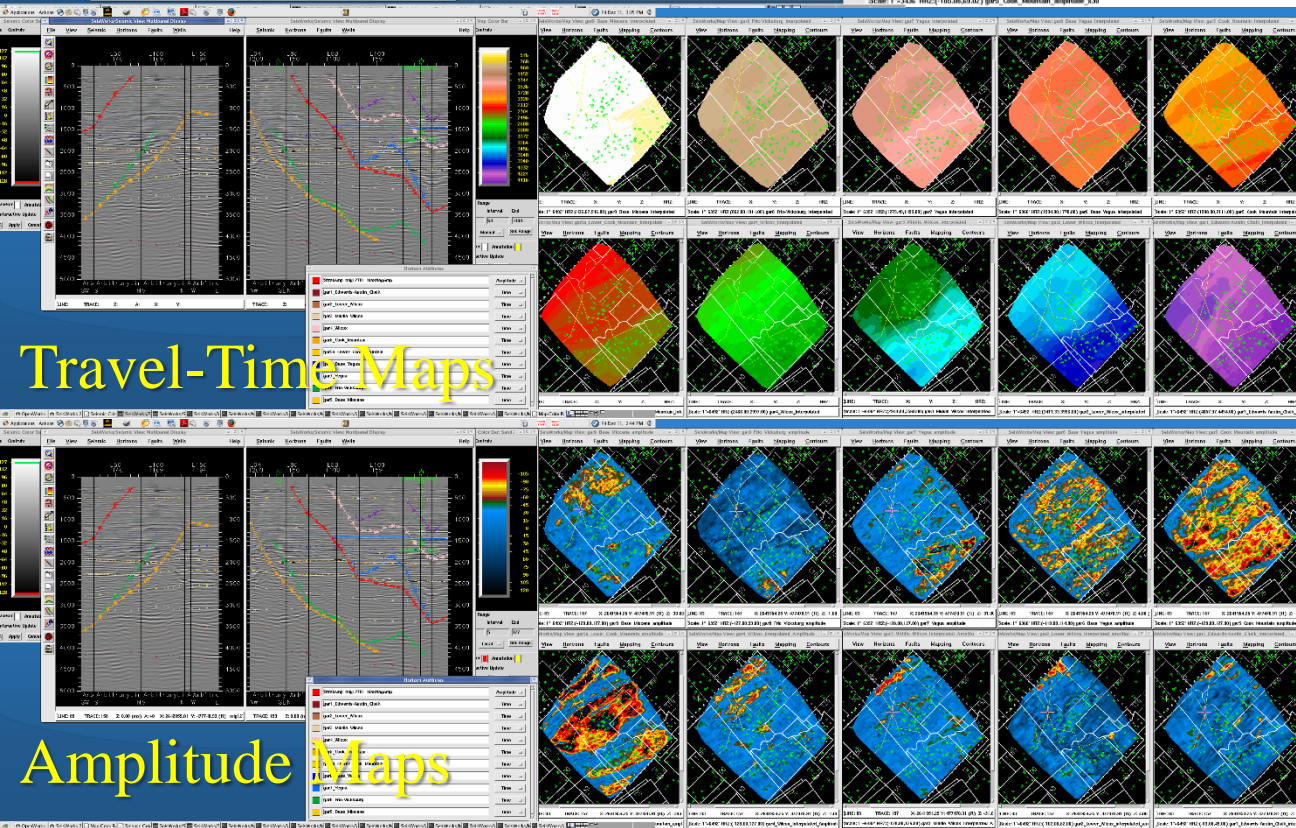
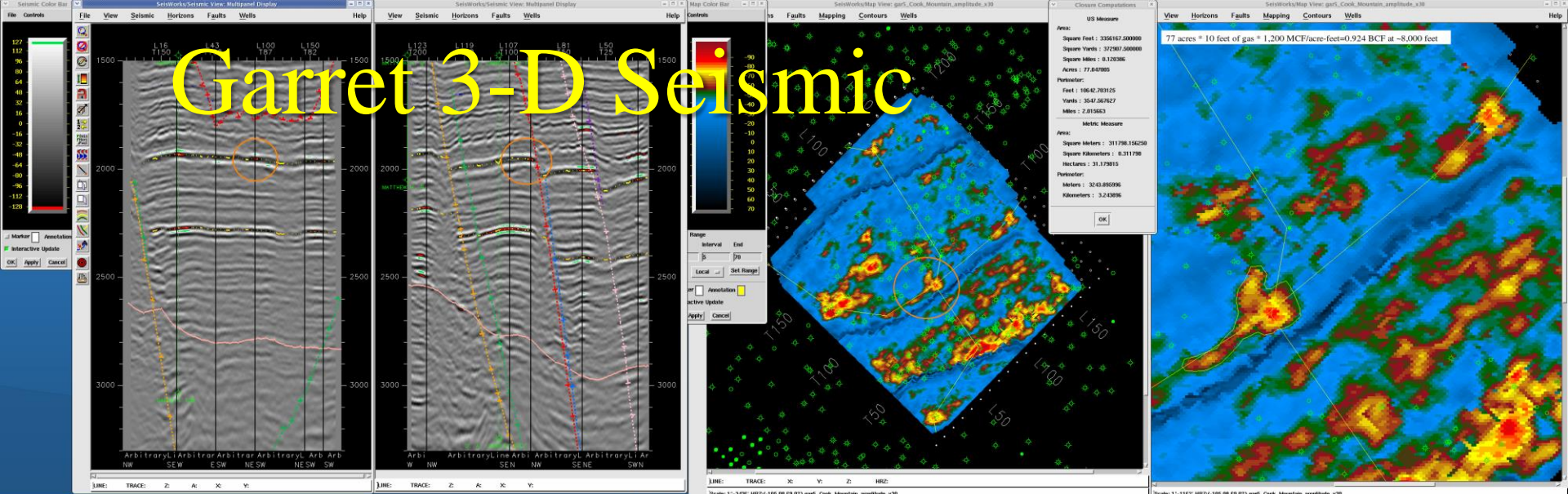




Depth	Formation	Acreage	Formation Acreage	Reserves in BCF (acres*20 ft gas * 1.2 MCF/acre ft / 1000 MCF/BCF)				
1	100-500ms Miocene	5		0.12	20	1.2	\$3	
2	500-1s Miocene	39		0.936				
3	1s-Base Miocene	32.7		0.7848				
3	1s-Base Miocene	140		3.36				
3	1s-Base Miocene	152		3.648				
3	1s-Base Miocene	158		3.792				
3	1s-Base Miocene	177		4.248				
3	1s-Base Miocene	229		5.496				
3	1s-Base Miocene	235		5.64				
3	1s-Base Miocene	342		8.208				
3	1s-Base Miocene	375		9				
3	1s-Base Miocene	479	2363.7	11.496	56.7288	\$170,186,400		
4	Base Miocene +-20	46		1.104				
4	Base Miocene +-20	79.8		1.9152				
4	Base Miocene +-20	94		2.256				
4	Base Miocene +-20	207		4.968				
4	Base Miocene +-20	1663	2089.8	39.912	50.1552	\$150,465,600	\$119,736,000	
5	Middle Frio +-100	27		0.648				
6	Middle Frio-Lower Frio	29	56	0.696	1.344	\$4,032,000		
7	Lower Frio	59	59	1.416	1.416	\$4,248,000		
8	Hackberry+-100	5	5	0.12	0.12	\$360,000		
9	Hackberry-Lower Yegua	24.9		0.5976				
9	Hackberry-Lower Yegua	25		0.6				
9	Hackberry-Lower Yegua	25.2		0.6048				
9	Hackberry-Lower Yegua	28		0.672				
9	Hackberry-Lower Yegua	28.2		0.6768				
9	Hackberry-Lower Yegua	31		0.744				
9	Hackberry-Lower Yegua	50	212.3	1.2	5.0952	\$15,285,600		
10	Lower Yegua +-100	39		0.936				
10	Lower Yegua +-100	43	82	1.032	1.968	\$5,904,000		
11	Lower Yegua-5000	24.2		0.5808				
11	Lower Yegua-5000	34	58.2	0.816	1.3968	\$4,190,400		
		4926	4926	118.224	118.224	\$354,672,000		SC8 - 130

Potential Value Undrilled Anomalies

Garret 3-D Seismic



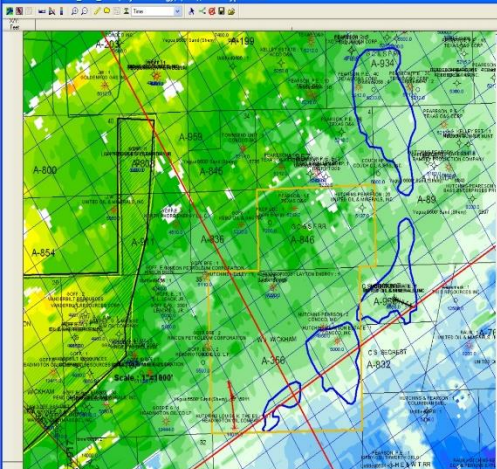
Prospect	Time	Depth	CFGE
gar-m98	488	1850	1176000
gar-m66	498	1900	792000
gar-fv46	941	3450	552000
gar-fv163	989	3650	1956000
gar-y26	1406	5350	312000
gar-y16	1406	5350	192000
gar-y90	1440	5500	1080000
gar-y161	1454	5550	1932000
gar-y245	1437	5500	2940000
gar-by133	1634	7100	1596000
gar-cm77		8000	924000
gar-cm54		7800	660000
gar-cm61		8200	732000
gar-cm35		7800	420000
gar-cm307		7800	3684000
gar-lcm279		9750	3348000
gar-lcm138		10200	1656000
gar-lcm40		10900	480000
gar-lcm30		10900	360000
			24792000

XY:
Feet

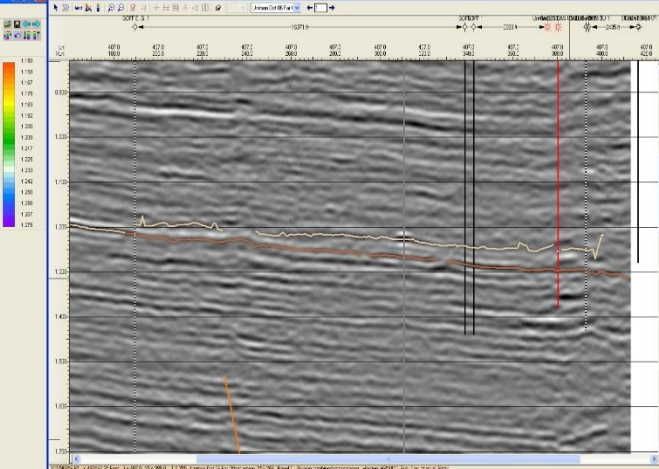


6825.086
6231.982
5638.875

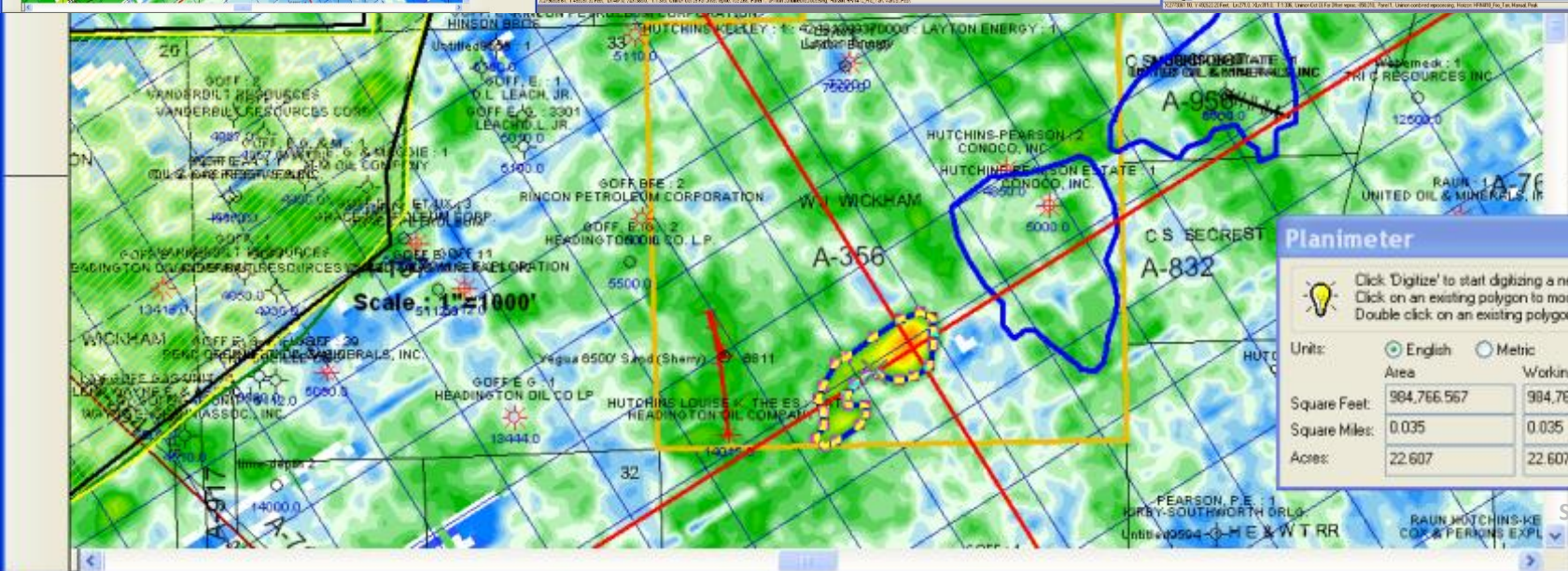
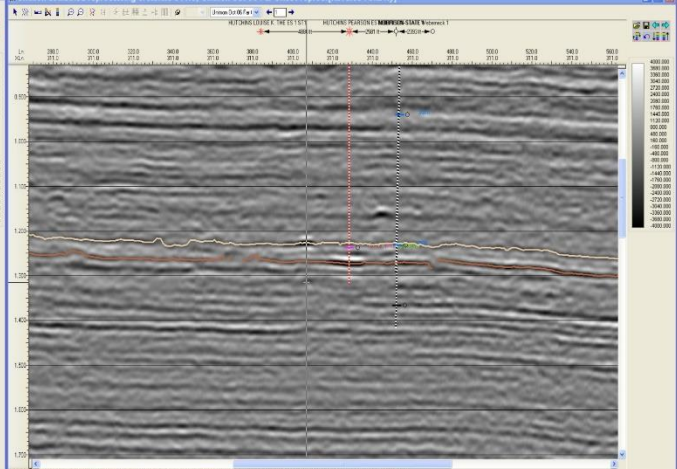
Horizon: HRN#10_Frio_Tan (Layton Energy) (Tan), Data Type: Time



Unimon combined reprocessing Line 407.0, Unimon Oct 06 Far Offset reproc. [Reverse Polarity]



Unimon combined reprocessing Crossline 311.0, Unimon Oct 06 Far Offset reproc. [Reverse Polarity]



Planimeter



Click 'Digitize' to start digitizing a new polygon. - or -
Click on an existing polygon to modify its shape. - or -
Double click on an existing polygon to change its properties.

Units:

☒ English ☐ Metric

Area

Working Interest

Square Feet:

984,766.567

984,766.567

Digitize

Square Miles:

0.035

0.035

Close

Acres:

22.607

22.607

Help

SC8 - 132

Frio Point Bars



Time_0814



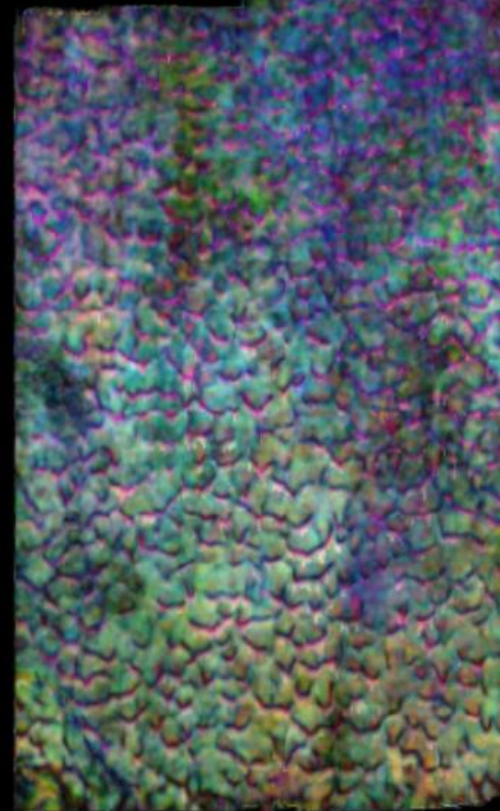
Time_0824



Time_0834

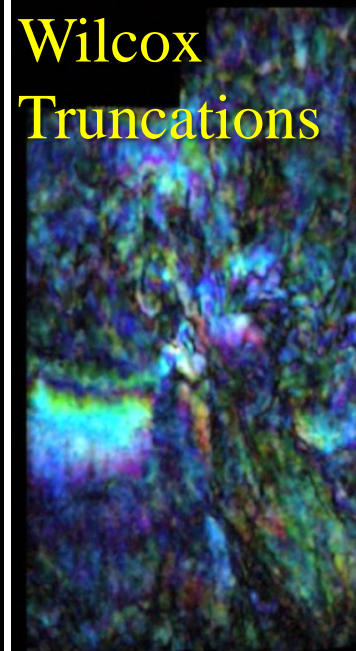
Tracy Stark Processing

Clinoforms along
Age Surface



RGT_1150

Wilcox
Truncations

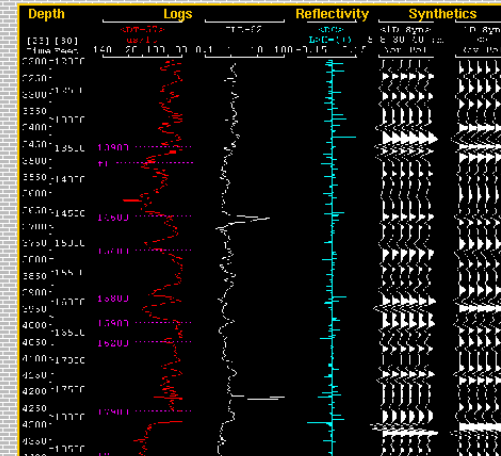
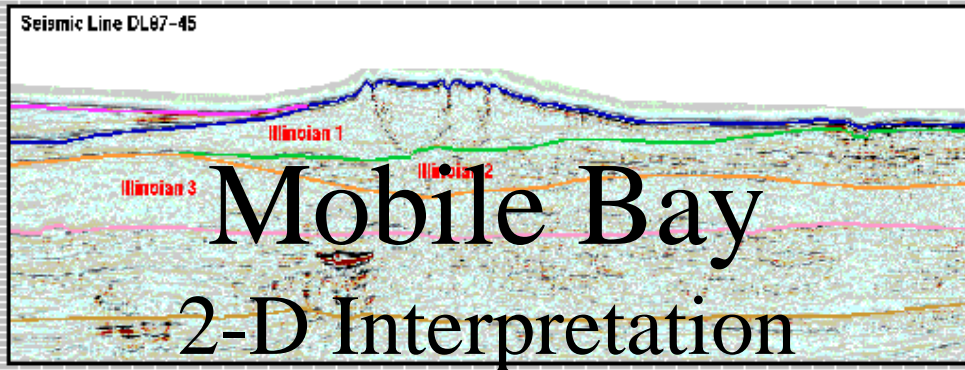


Time_2400

Data are instances of specific meanings occurring in the real-world.

Knowledge is the progressive gathering of bits of experience, along with the links which associate these disparate parts into a unified whole.

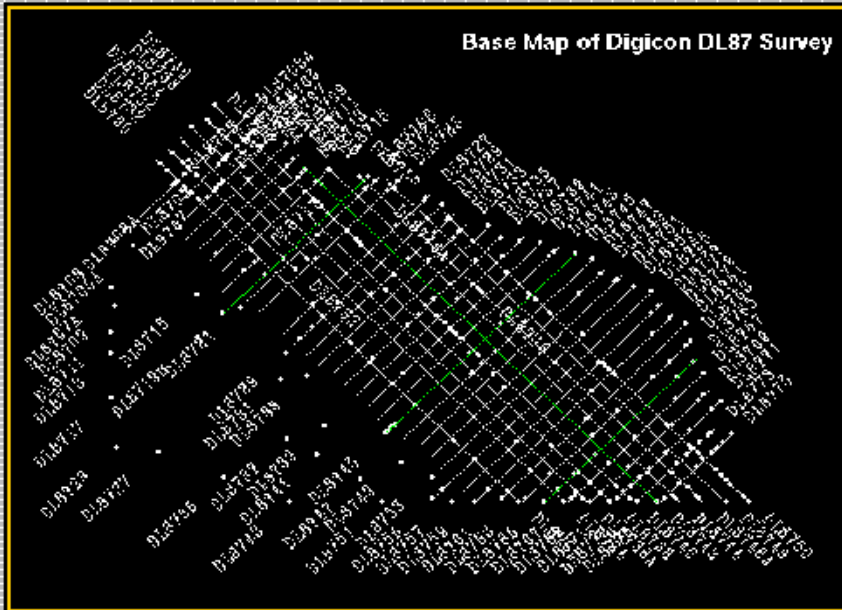
Seismic Line DL87-45



Information is data in context, related to a specific purpose.

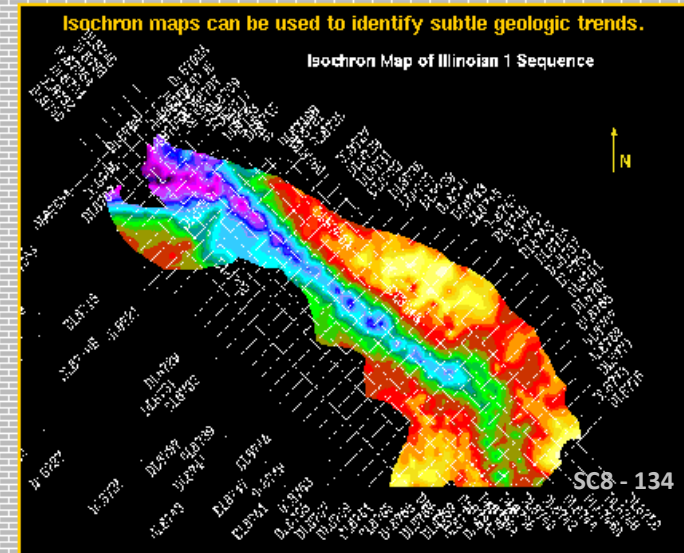
Wisdom is knowledge of what is true or right coupled with good judgement, and is embodied in those who remember the recipe and can tell the stories.

Base Map of Digicon DL87 Survey

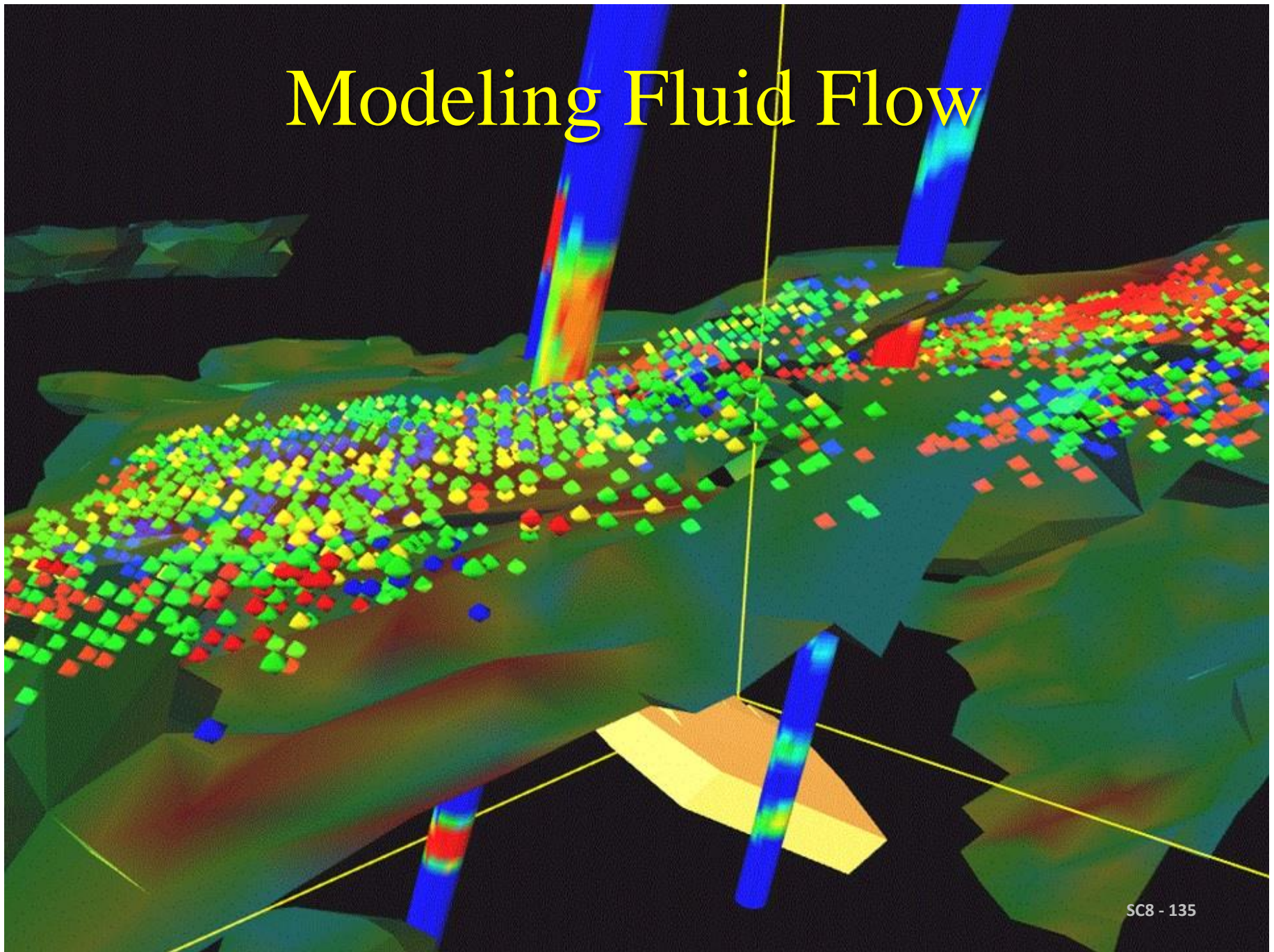


Isochron maps can be used to identify subtle geologic trends.

Isochron Map of Illinoian 1 Sequence



Modeling Fluid Flow



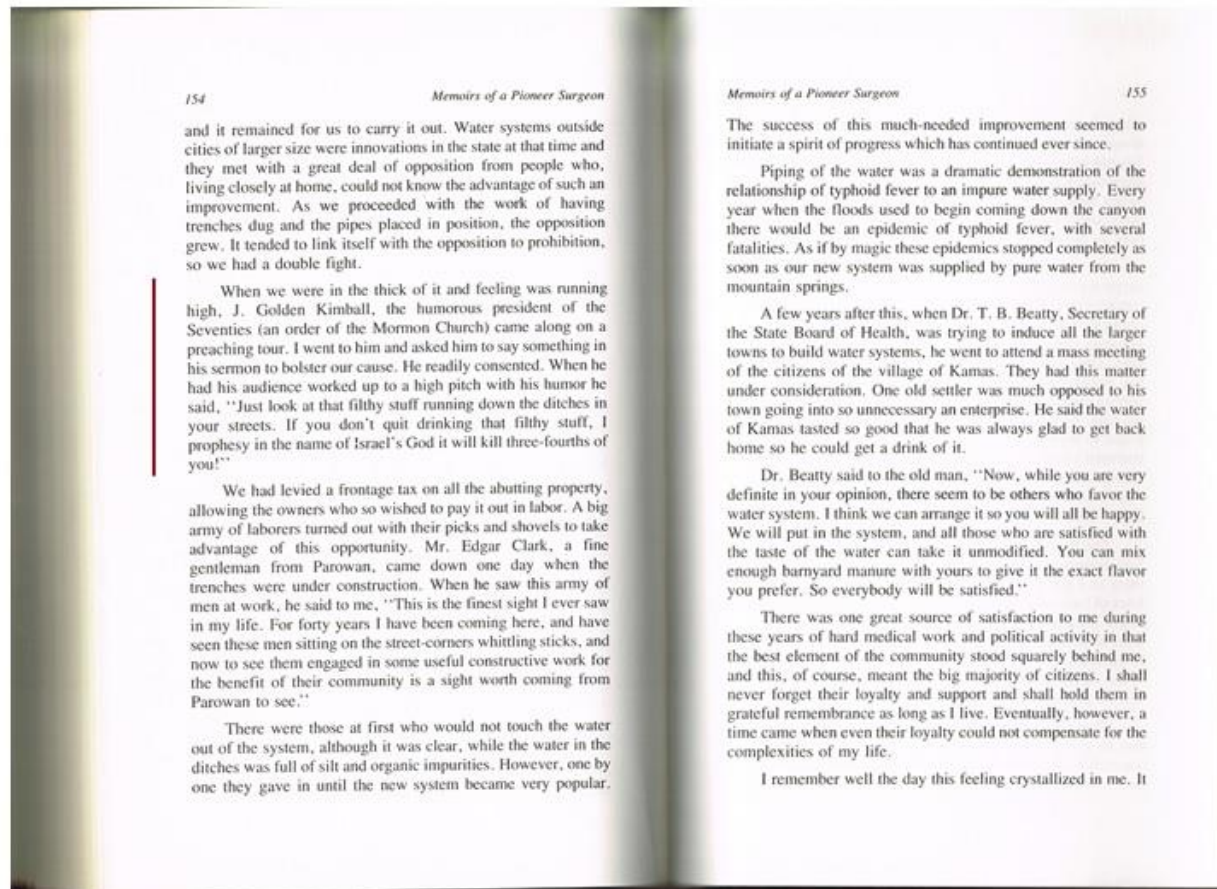
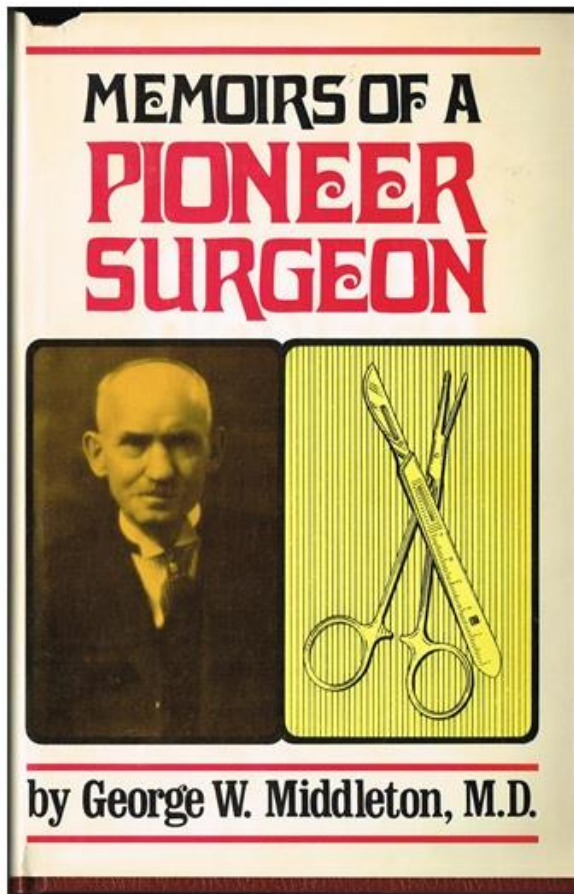
Notes

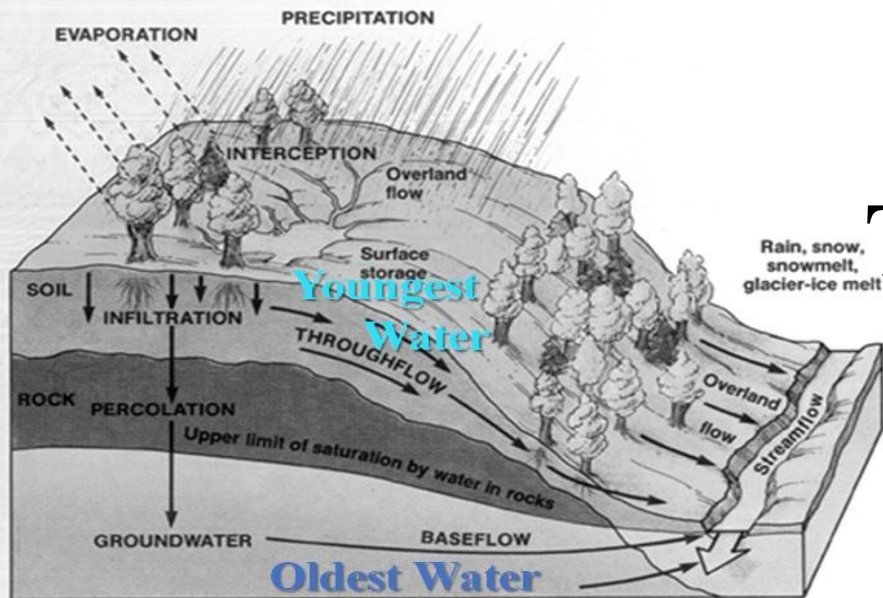
This image shows a single sheet of white paper with horizontal blue ruling lines. The lines are evenly spaced and run across the width of the page. There are no margins, text, or other markings on the paper.



Water is a Critical Natural Resource

Historical Water Issue in Cedar City

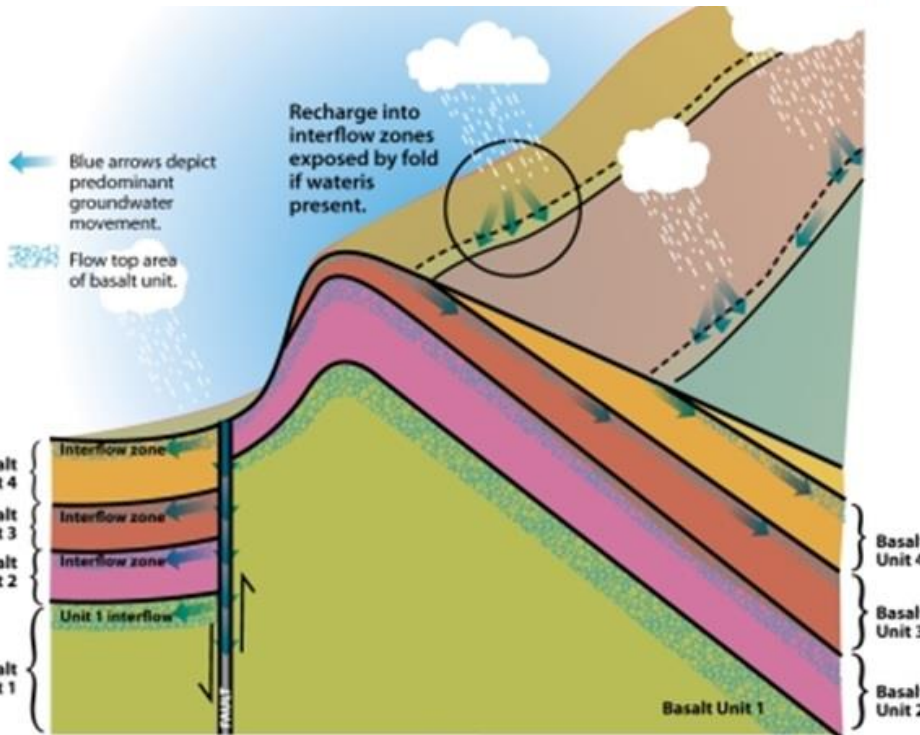




http://snobear.colorado.edu/Markw/geog5321_webpage_04.html

Applying Experience Today to Cedar Valley Water Problems

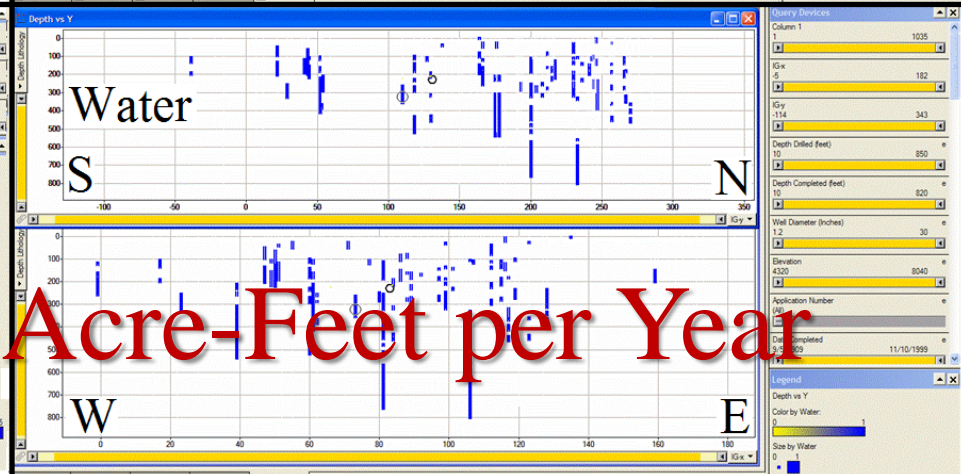
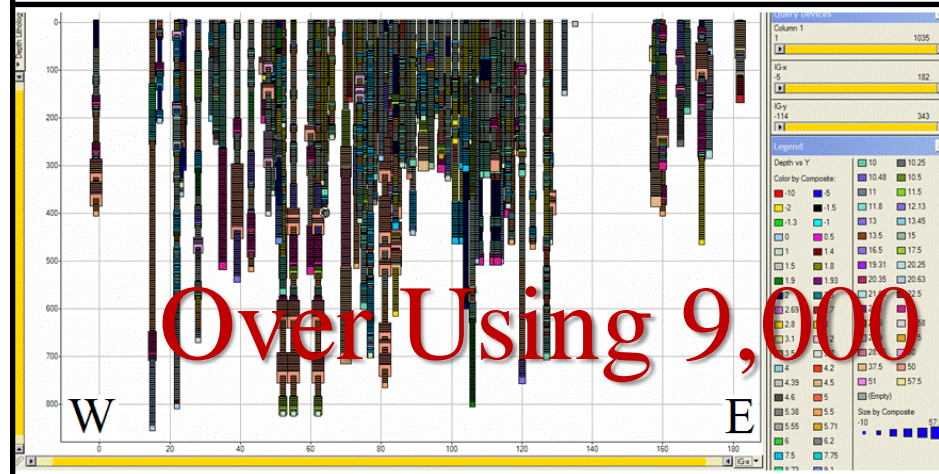
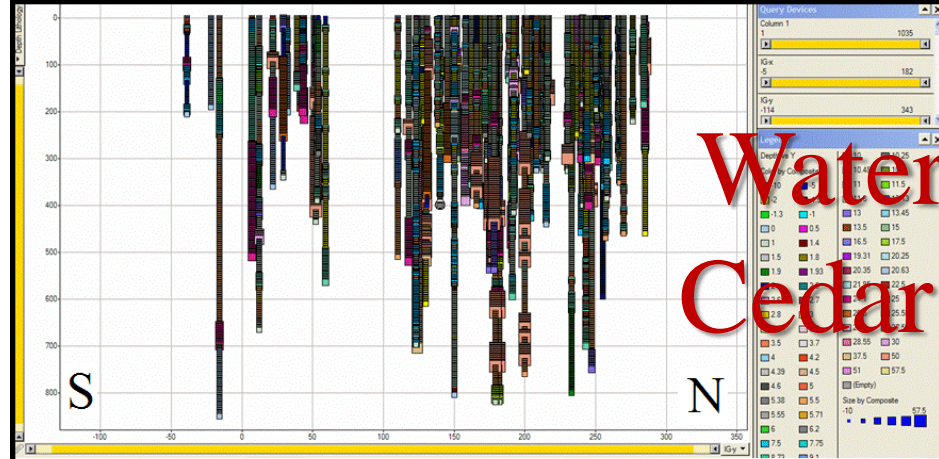
- Bedrock dips to the east;



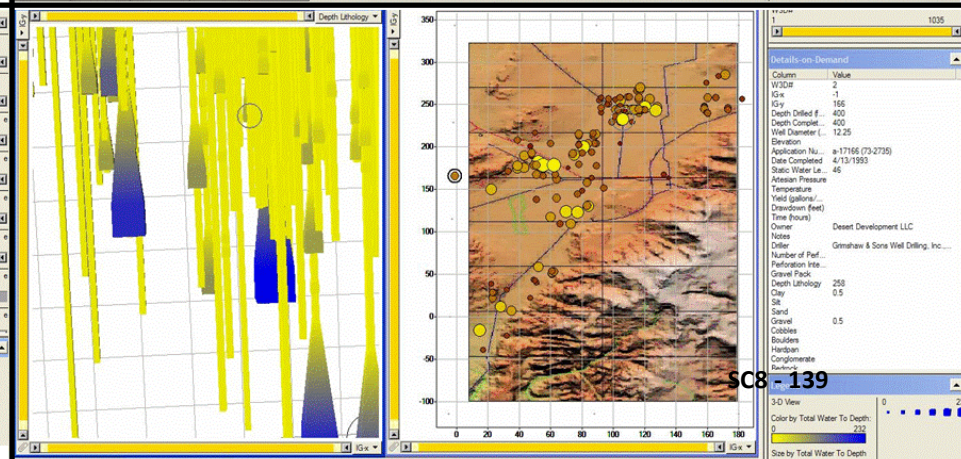
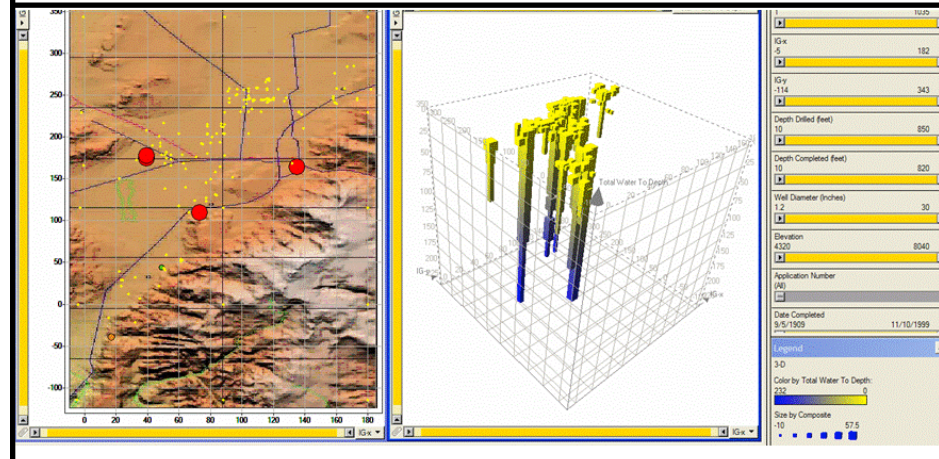
http://cbgwma.org/index.php?option=com_content&task=view&id=60&Itemid=115

- Faults bounding the valley disrupt baseflow, especially into the Cedar Valley basin fill aquifer, which is isolated by clays and is very shallow.

Water Wells Cedar Valley



Over Using 9,000 Acre-Feet per Year



Geology & Geophysics Are Key

Geology of Cedar Valley, Iron County, Utah

How do Geoscientists see under the ground?

- Line 711 was my first assignment in Mobil Field Operations in February 1978 (it was cold, saw bear tracks).
- When I learned of Bengt Nelson's first winter (1856-1857) at Iron Springs.
- Figures to right from Line 704.

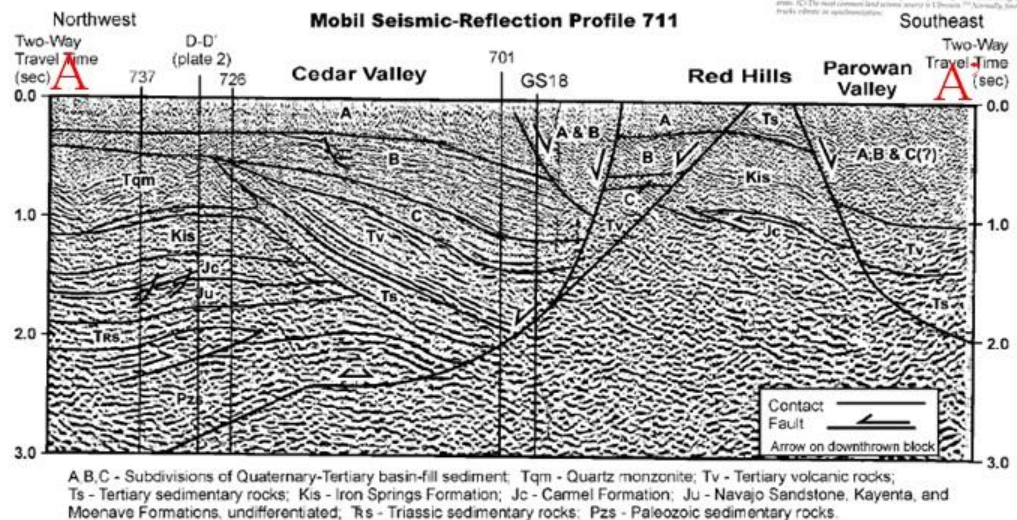
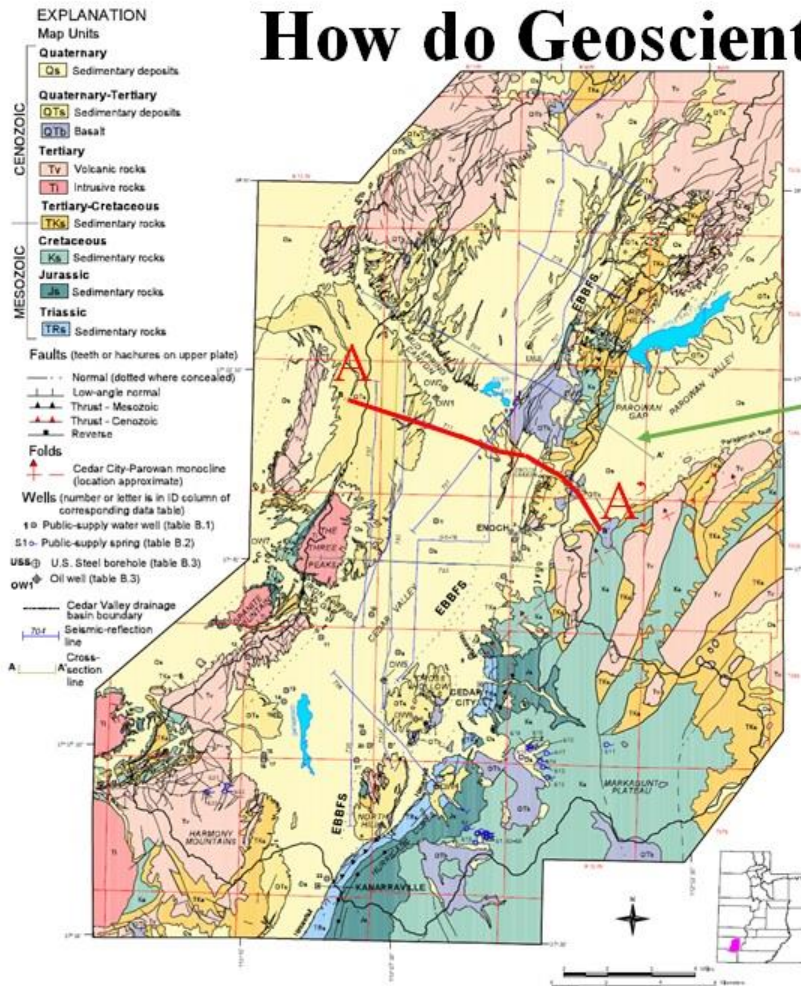
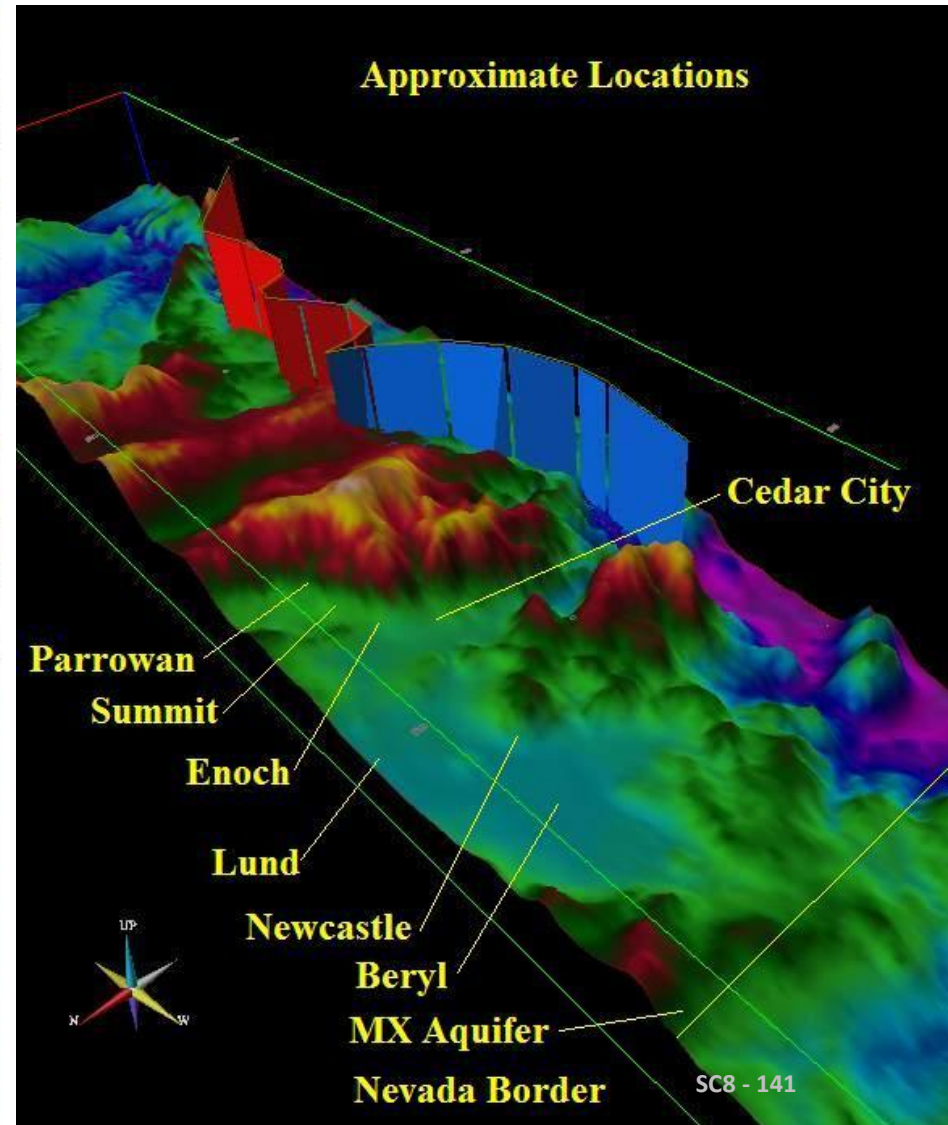


Figure 3-5. Typical land entry operations in southwestern Utah. (A) Surface shooting using 500 lb. of explosives over a prime land area. The environmental damage is temporary, but considerable, the equipment, also, causes long-term problems. (B) Shallow hole shooting of only 50 lb. of dynamite per shotpoint is better in agricultural areas. (C) The most common land entry method is U.S. Dept. of the Interior, Bureau of Land Management, aerial photography.

Figure 6. Simplified geologic map of Cedar Valley drainage basin and adjacent areas. EBBFS is eastern basin-bounding fault system. See figure 5 for stratigraphic column, and appendix A for correlation of map units with those on plates 1 and 2.

Mobil Line 711 cross-section



Water at Iron Springs

Where Bengt & Ellen Nelson Lived



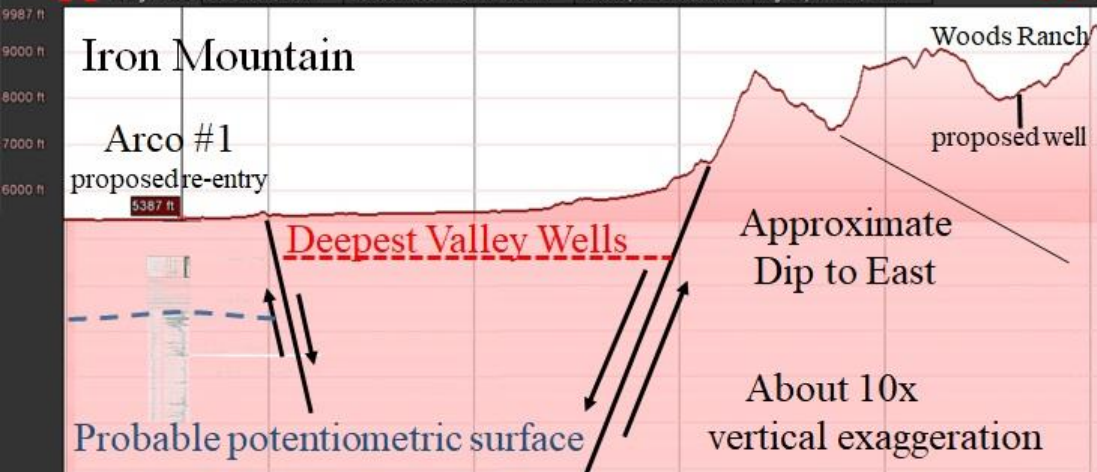
Arco #1 – Woods Ranch cross-section

- An opportunity to test the Fractured Quartz Monzonite Aquifer is to reopen this well.

Top Qm = 2,322'
Fractured: 2,500'-2,615'

Fractured: 2,960'-3,050'

- The proposed test in the Cretaceous rocks is at Woods Ranch or Shepherd's Cabin.



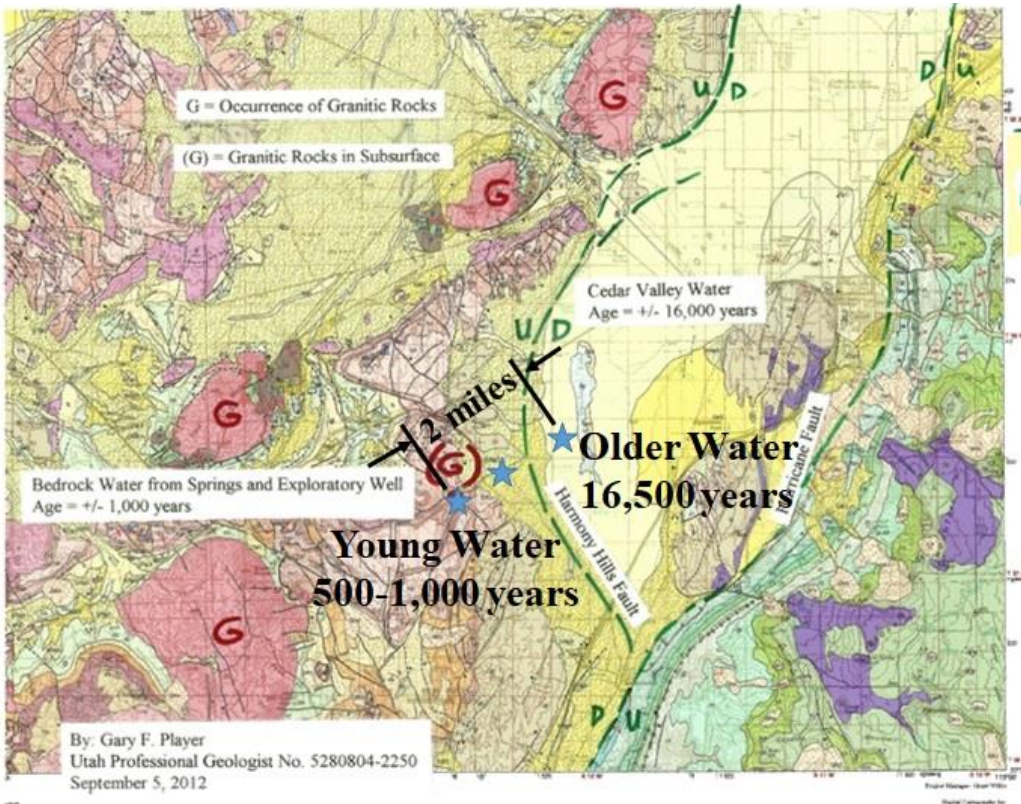
Untapped Fractured Quartz Monzonite Aquifer

Photograph of water in Blowout Pit at Iron Mountain

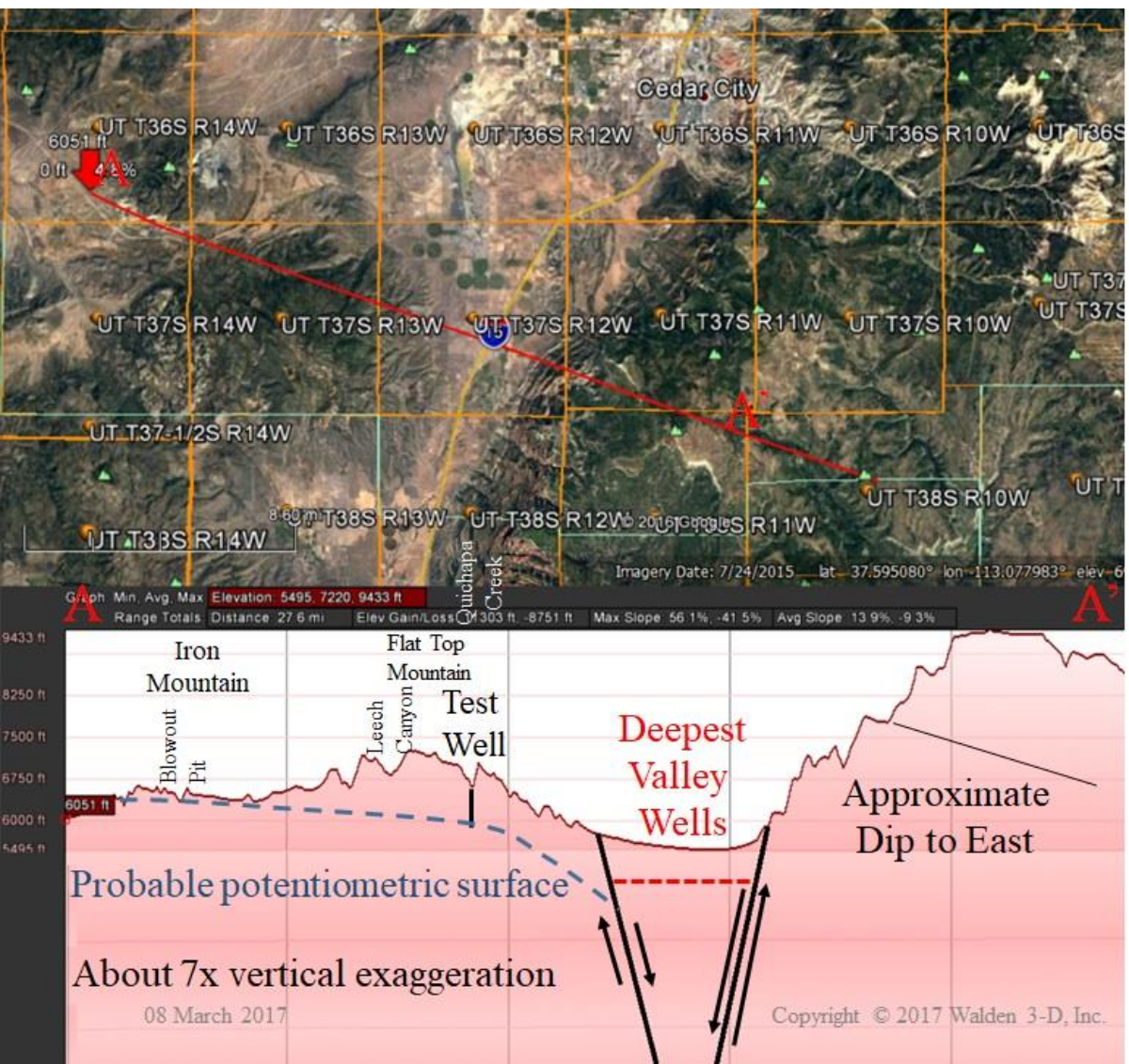


Photograph by Gary Player

Water from
Fractured
Quartz
Monzonite
Fills Blowout
Pit and Other
Iron Mine Pits



Fractured Quartz Monzonite Wells Will Hopefully Be “New Water”

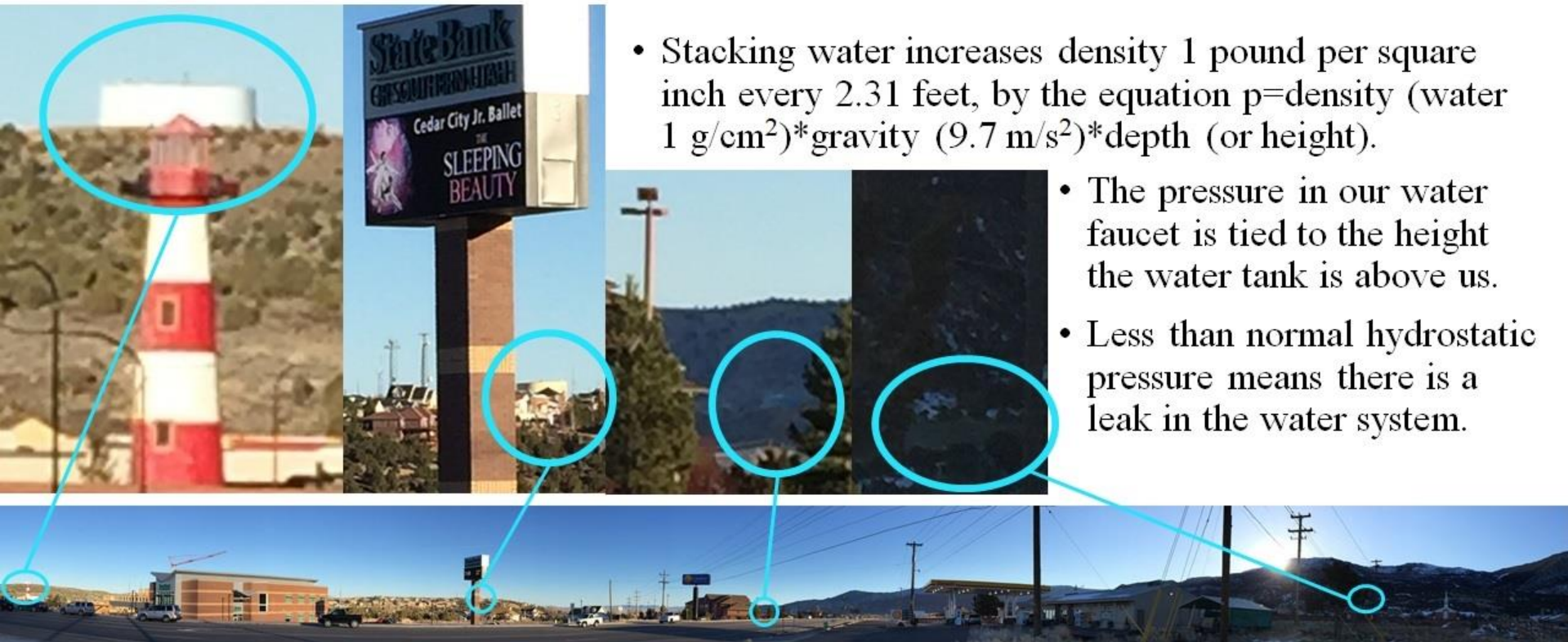


Blowout Pit Cross-Section

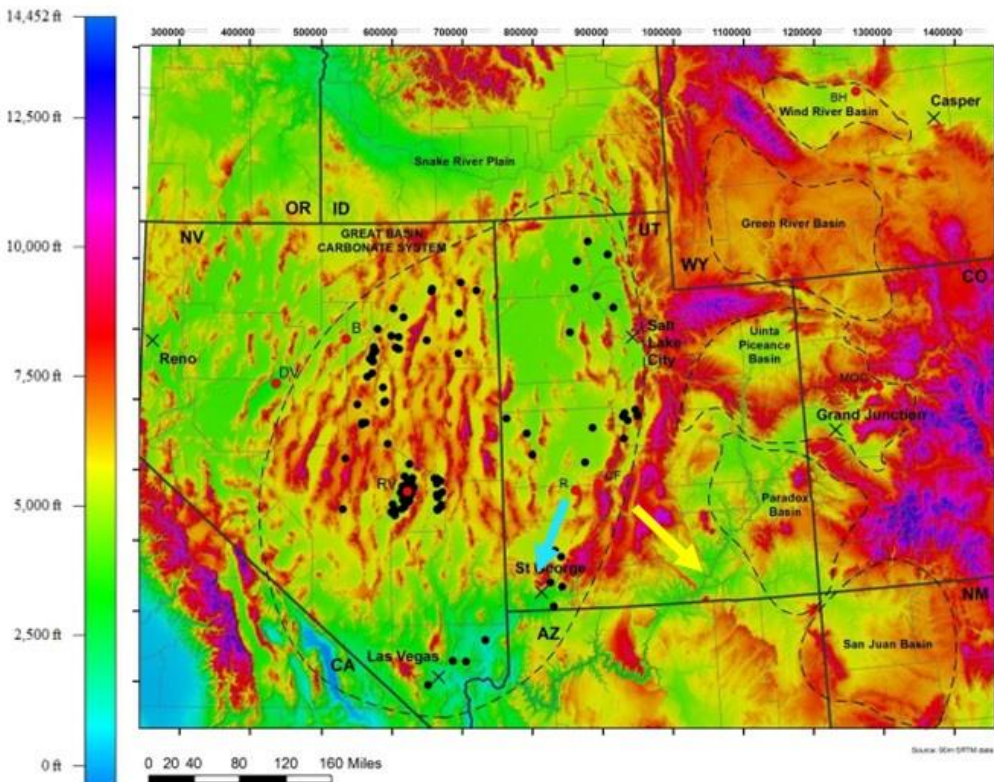
- Dip on bedrock to east drives water falling on Cedar Mountain east.
- Throw of Hurricane Fault allows water to drop down 5,000 feet to the porous Jurassic Sandstone.
- Water filling Blowout Pit tested in Quichapa Creek test well.

Hydrostatic Pressure Is Key

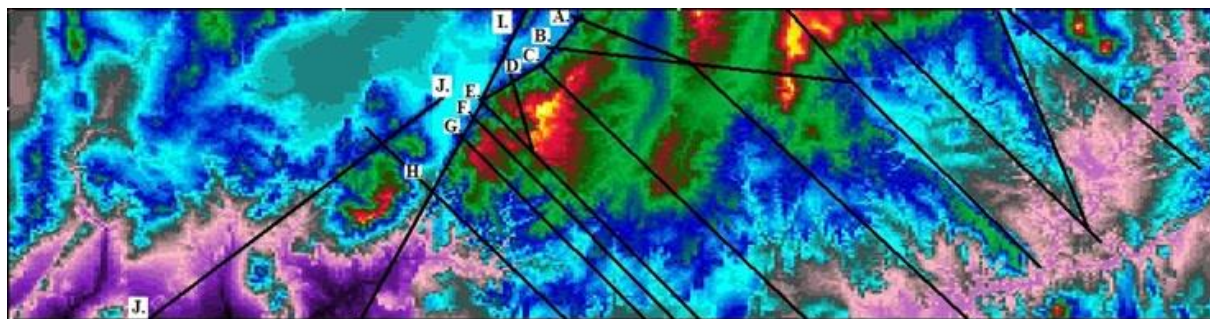
Water Tanks in Cedar City demonstrate hydrostatic pressure



Looking at the Bigger Picture



- There is significant baseflow discharge from The Great Basin (e.g. Cedar City at 5,000 feet) to the south (e.g. St. George at 3,000 feet).
- There is equal or larger baseflow discharge from The Great Basin (e.g. Cedar Valley) to the southeast (e.g. The Grand Canyon).
- This discharge is much deeper than 800 feet, with water running below the isolated Cedar Valley Fill Aquifer.



Possible Fault Geopressure Leak Pathways from Cedar Valley to the Colorado River

Less Than
Normal
Hydrostatic
Pressure

Untapped Cretaceous Aquifer
above the repeated road repairs in Cedar Canyon
(note most significant flow is on east facing outcrops, because beds dip east)



Water
Flowing East
Is Within
Drainage
Basin

What is the cost to repair the road?

Compared to the cost of drilling a deviated hole
and draining the water out of the cliffs to prevent landslides?



Deviated Hole Requires No Pumps and Turbines in the Well Generate Power

Cretaceous Aquifer east of Cedar City

Straight Cliffs Formation over Dakota Formation, north of Highway 14 at Mile 8, east of Cedar City.

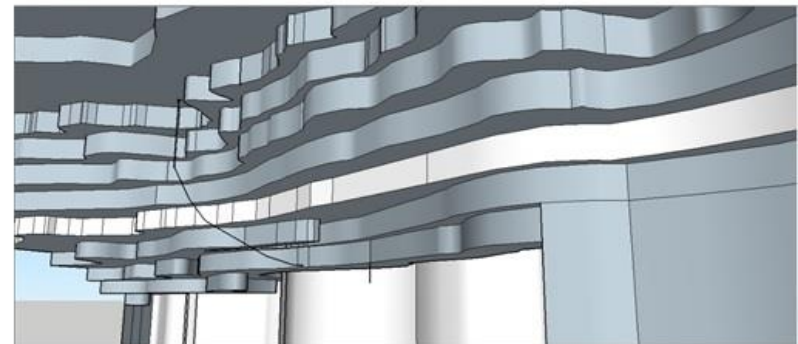
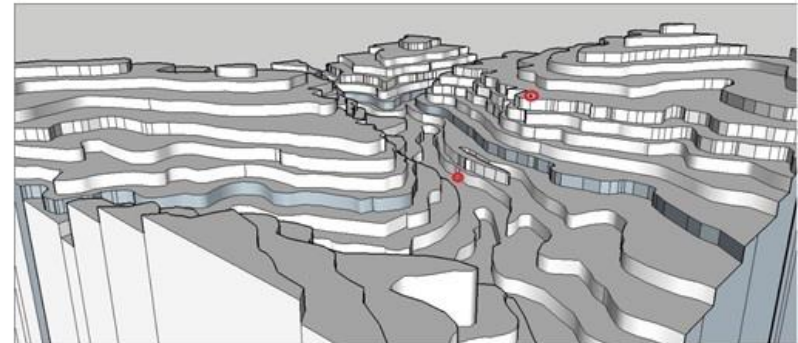
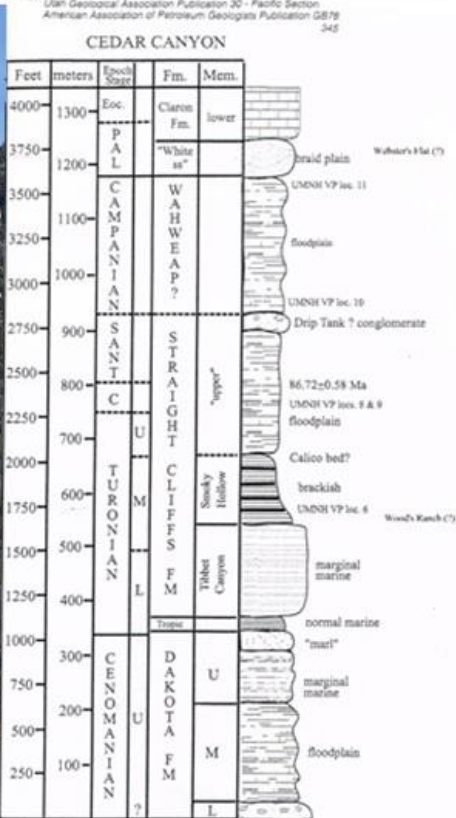


Figure 5. Comparison of Upper Cretaceous and lower Tertiary stratigraphy in Cedar and Parowan Canyons. The Parowan section is hung on the contact between the Claron and Grand Castle Formations. UGA Pub. 30

Photo by Gary F. Player, Utah Professional Geologist 5280804-2250, March 14, 2015

Notes

This image shows a single sheet of white paper with horizontal blue ruling lines. The lines are evenly spaced and run across the width of the page. There are no margins, text, or other markings on the paper.



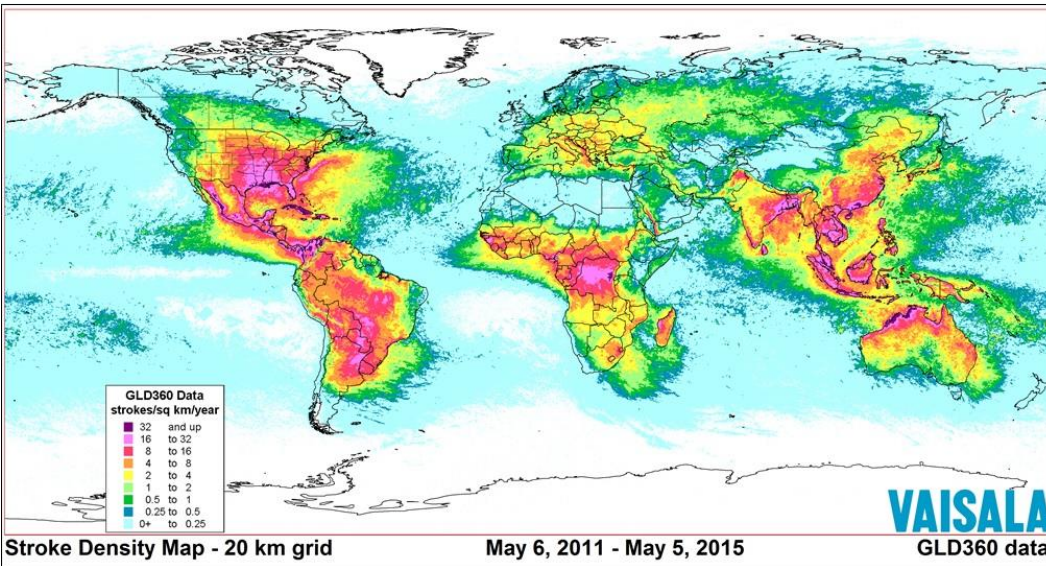
How can we find
and optimize
natural resources?



SC8 - 150

Lightning Occurs Everywhere

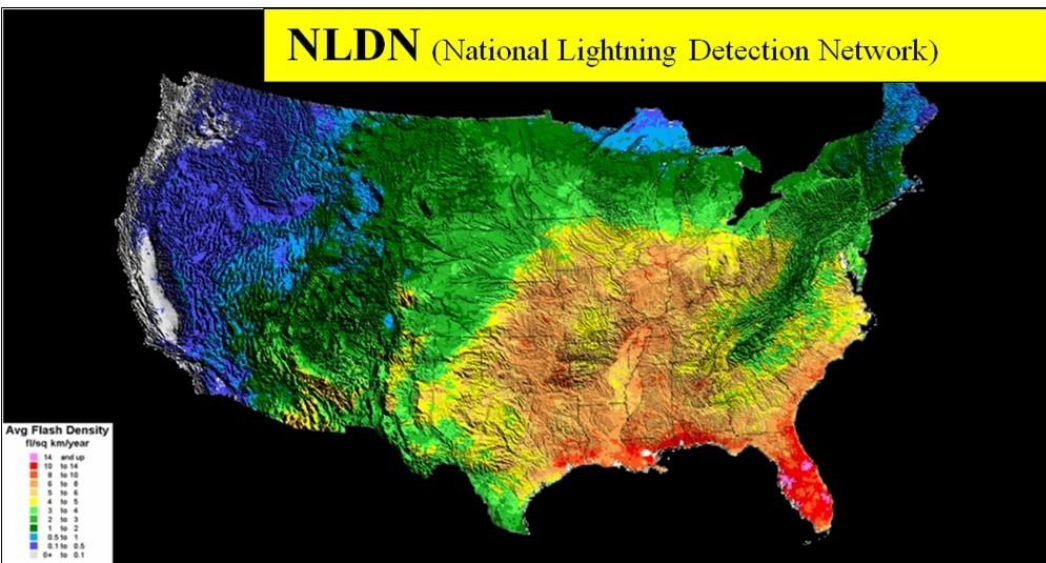
5+ Years of Data in GLD-360 Data Base



Lightning Data Was Only Used For Insurance, Safety, & Meteorological Purposes

The U.S. has the most complete database

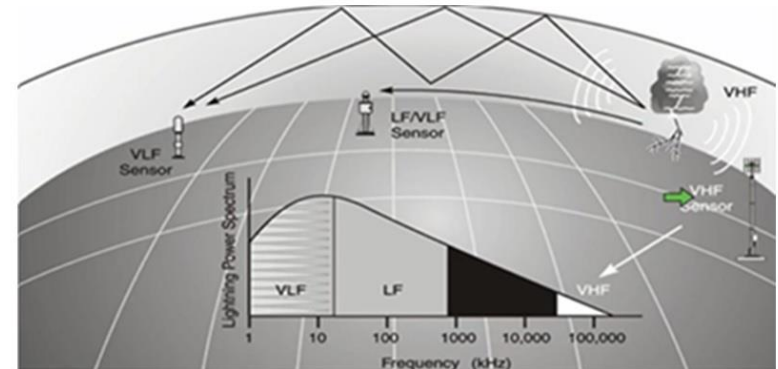
18+ Years of Data in the NLDN Data Base



Originally Collected for Insurance, Meteorology, and Safety Reasons

Sensors measure Direction to strike & Lightning Attributes

Strike Triangulated &
Measurements Reconciled



Vaisala: Martin Murphy
2016 Webinar used with permission

SC8 - 151

We Discovered Strike Locations Are Controlled by Telluric Currents



US009523785B2

(12) **United States Patent**
Denham et al.

(10) **Patent No.:** **US 9,523,785 B2**
(45) **Date of Patent:** **Dec. 20, 2016**

(54) **METHOD FOR DETERMINING
GEOLOGICAL SURFACE AND SUBSURFACE
RESISTIVITY**

(71) Applicant: **Dynamic Measurement, LLC**, Cedar
City, UT (US)

(72) Inventors: **L. R. Denham**, Houston, TX (US); **H.
Roice Nelson, Jr.**, Cedar City, UT
(US); **D. James Siebert**, Katy, TX (US)

(73) Assignee: **Dynamic Measurement, LLC**

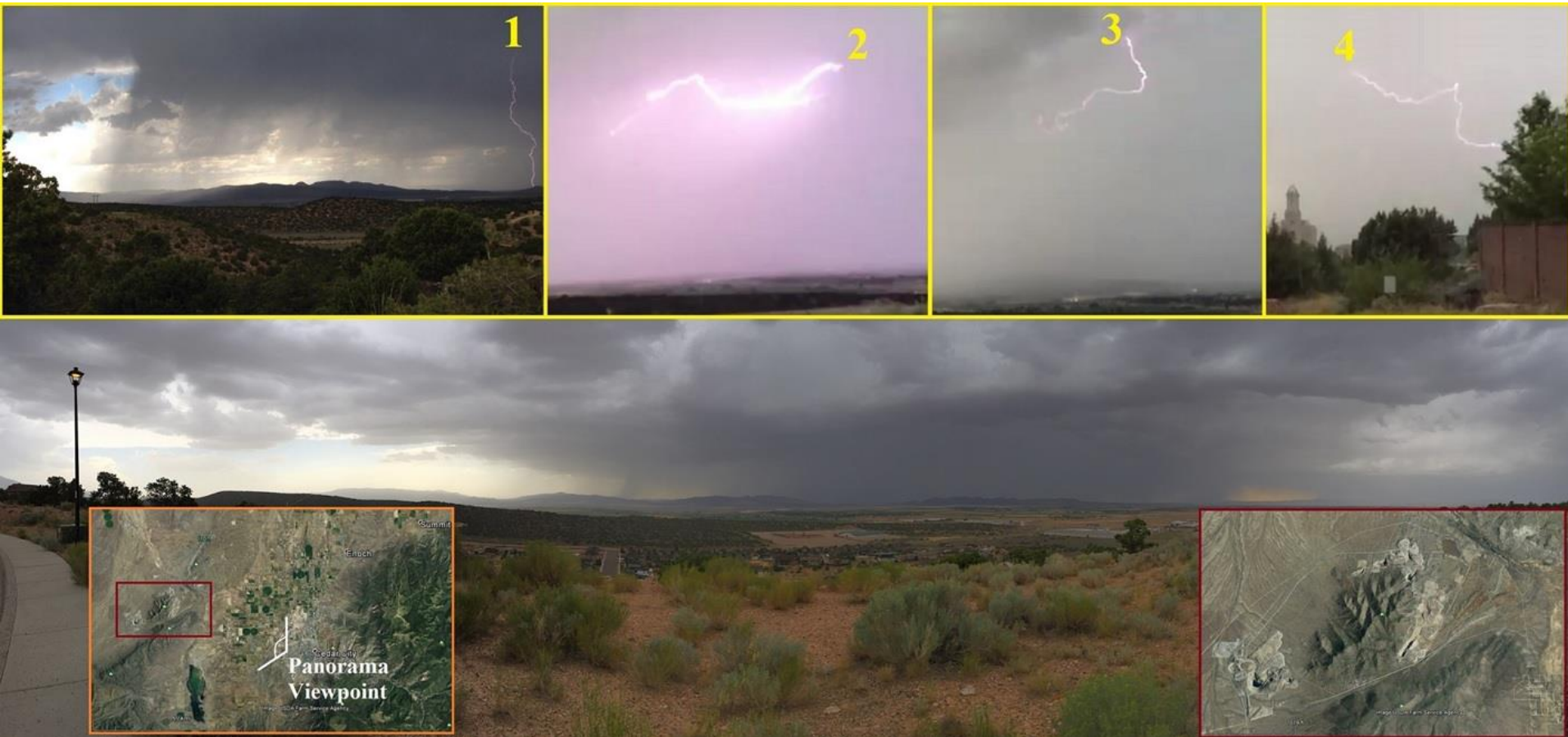
(57) **ABSTRACT**

A method for determining geological subsurface resistivity. The method includes obtaining a set of lightning parameters associated with a lightning strike received by a geological volume of material, the set of lightning parameters including an indicium of the current of the lightning strike at a first initial time and an indicium of the current of the lightning strike at a first decay time subsequent to the first initial time, and inferring the resistance of the volume of geological material, at least in part, from the set of lightning parameters.

SC8 - 152

6 Claims, 2 Drawing Sheets

The Magnetite at Iron Mountain Attracts Lightning Strikes



What is a Lodestone?

Lodestones are rocks that are magnetized. They are made of Magnetite , a type of iron ore. Magnetite itself is not necessarily magnetic. A piece of magnetite that is magnetic qualifies as a lodestone.

What makes a Lodestone magnetic?



For a piece of magnetite to become magnetized it must be exposed to a magnetic field. The weak magnetic field of the earth is not strong enough so another source must be looked to. One way it may occur is by lightning strikes on magnetite causing the magnetite particles to align in the right way to produce a magnetic field.

The first compasses were made over 2000 years ago using lodestones. If a long piece of lodestone is freely suspended it will rotate until it lings up with the Earth's poles. Early navigators were able to use lodestones to help them find their way.

Lightning
Strikes
Encourage
Rock
Hounding

Lodestone Examples



Fulgurites are fused sand from lightning strikes



Sand fulgurites found on the top of Mount Raymond. U.S. quarter for scale.

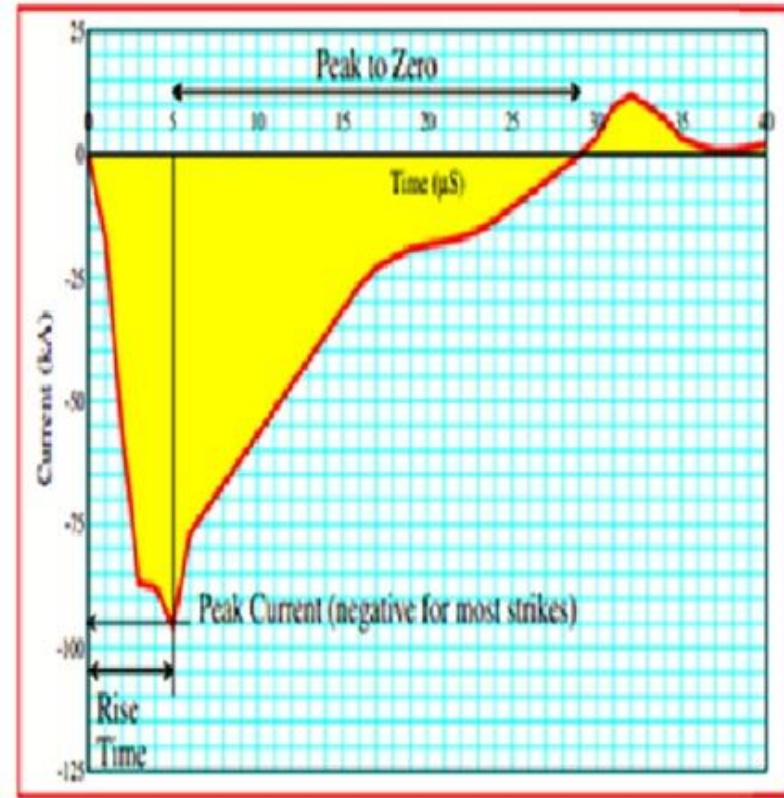
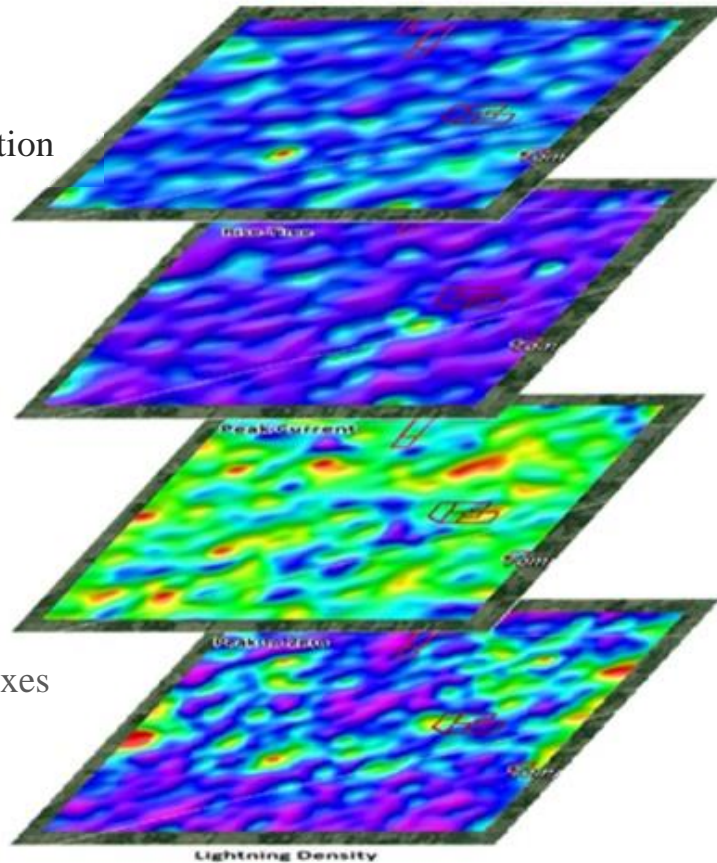


Rock fulgurite (circled in white) found on quartzite at the summit of Mount Raymond in the Wasatch Range, Salt Lake County, Utah. Hammer for scale.

Utah is a major source of iron ore and in particular, natural magnetic ore called lodestone or magnetite. These particular specimens both very rich in iron, making them magnetic.

Lightning Measurements

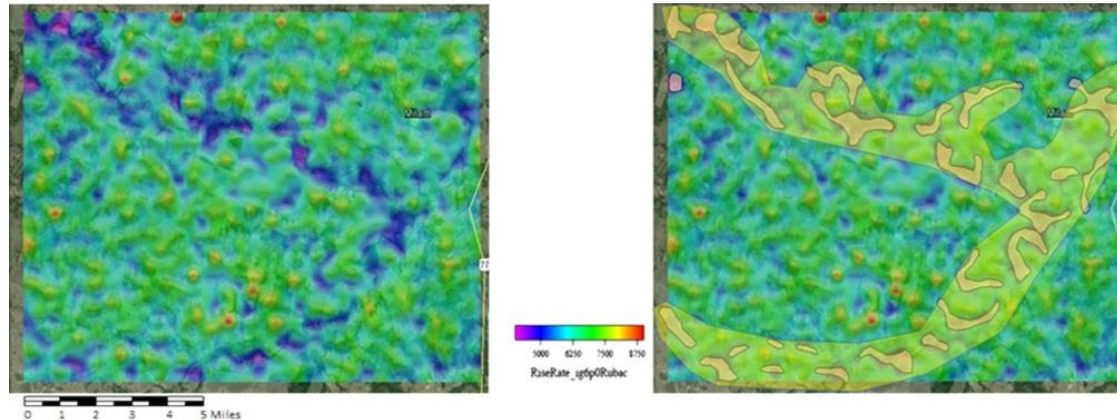
- Location
- Time and Duration
- Rise Time
- Peak Current
- Polarity
- Peak-to-Zero
- Density
- Major/Minor Axes
- Chi-Squared



- Other attributes calculated from these measurements.
- The time of the lightning strike is correlated with solar and lunar tides.
- Measurements separated by time.

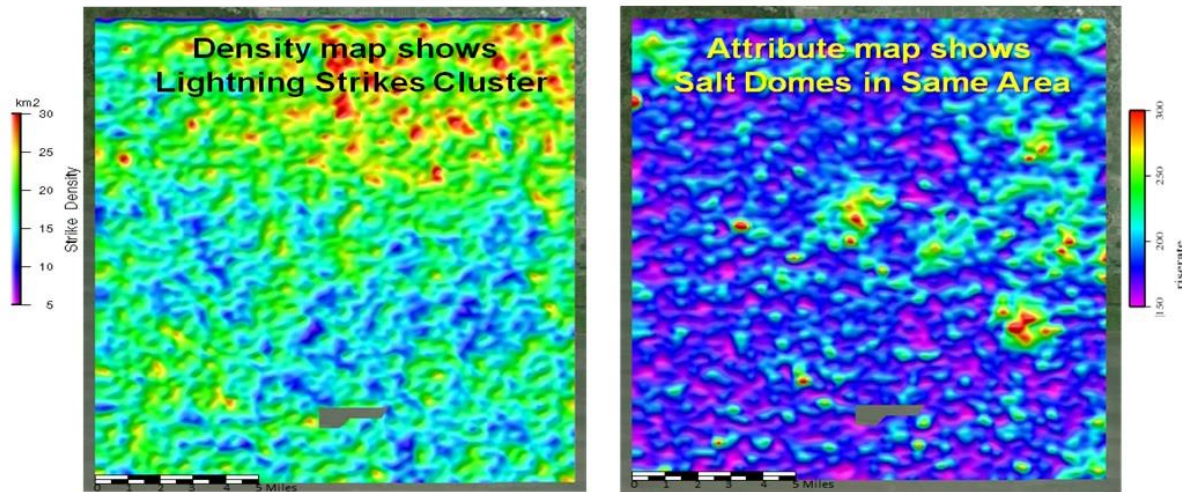
Lightning Analysis & Attributes

1. Analysis area selected.
2. Patented and Patent-Pending Processes produce maps and volumes of derived rock properties and lightning attributes.
3. Existing geology and geophysics integrated with new data.



Lightning Attribute: Rate of Rise-Time – Milam County, Texas

Louisiana Example



Density Map

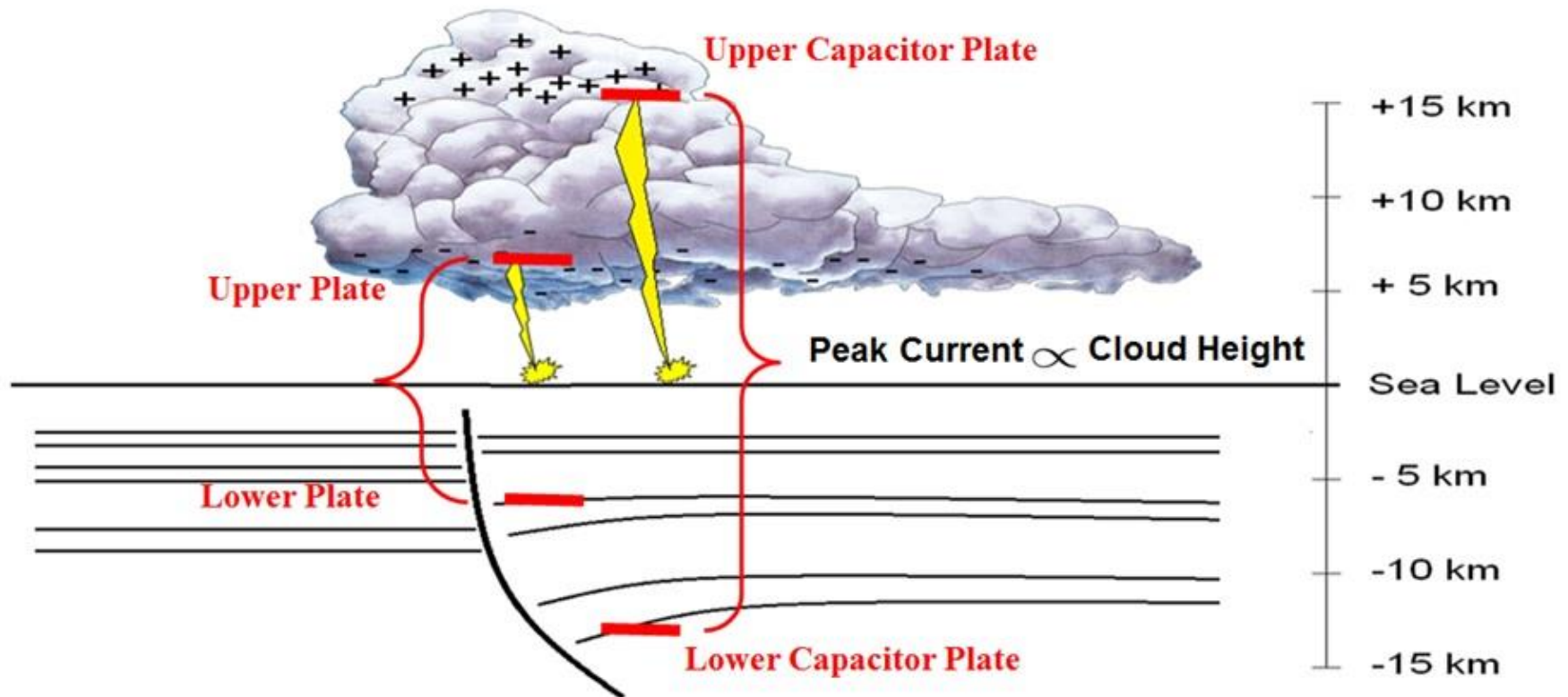
&

Rate-of-Rise-Time Map

Rock Property & Attribute Maps & Volumes

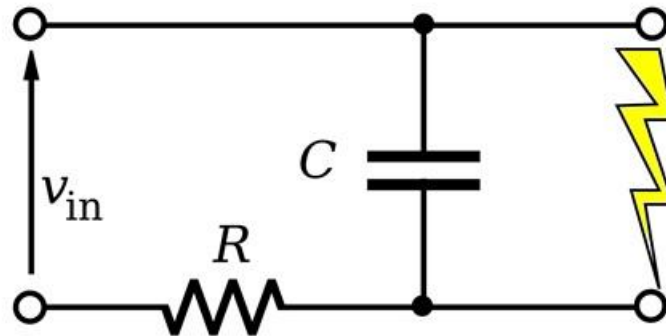
Key Assumptions:

1. Lightning occurs when there is sufficient charge to bridge the capacitor.
2. Lightning is affected by geology to a depth proportional to cloud height, as derived from Peak Current



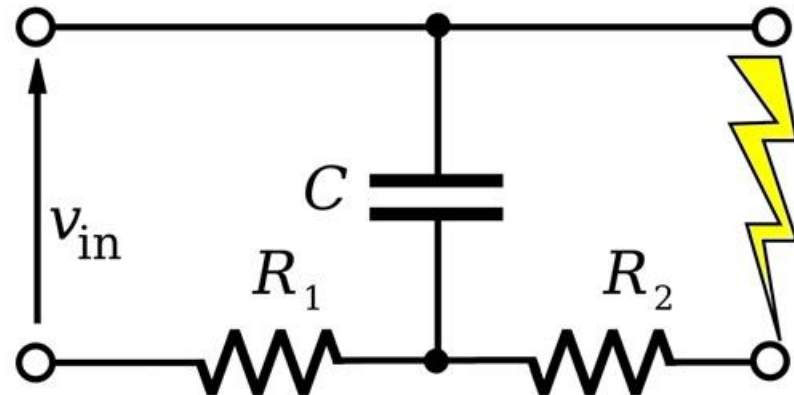


Relaxation Oscillator Physics and Lightning (a giant neon tube)

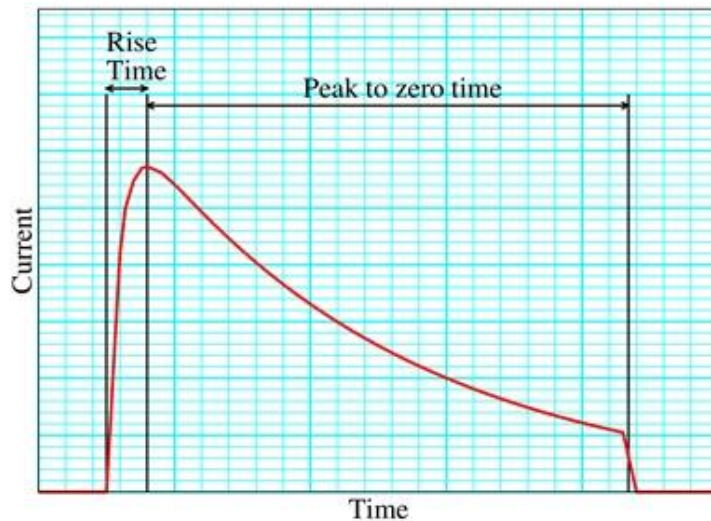


- The atmospheric capacitor is like a relaxation oscillator
- Just an additional resistance (R_2) limiting the current

- R_2 is the resistance between the lightning strike point and the bottom plate of the capacitor

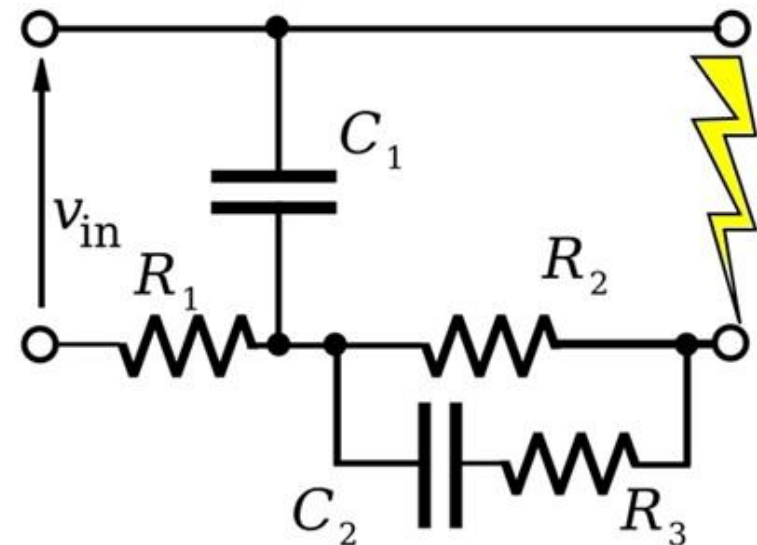


Lightning and the Induced Polarization Effect



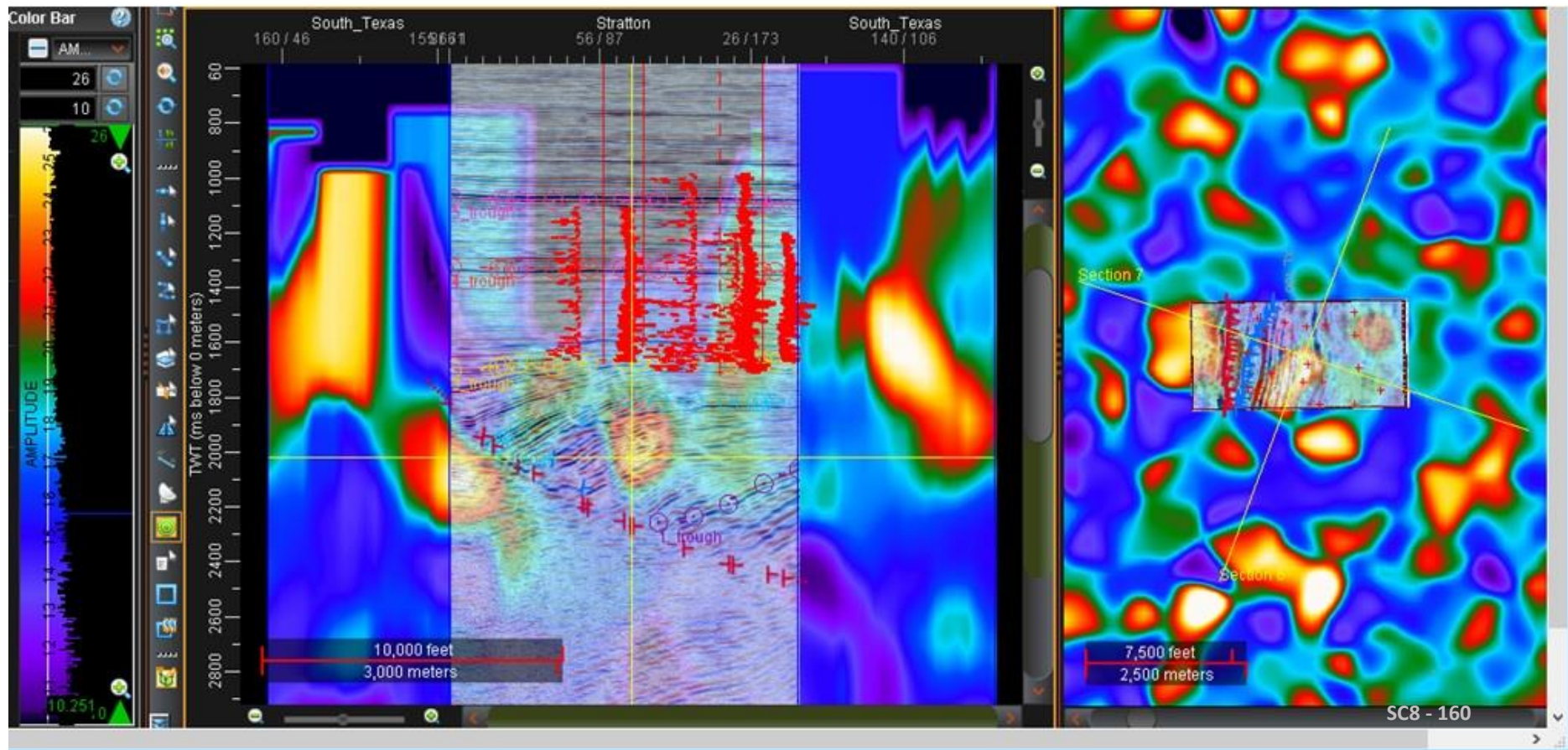
- By treating this steep onset as charging a capacitor (C_2) through a resistor (R_3), an apparent capacitance can be calculated.
- From the apparent capacitance a value for average permittivity can be calculated

- Lightning does not have a square waveform
- But it does have a very steep onset
- Variations in the onset as measured (rise-time) show the IP Effect



Dynamic Uses Seismic Techniques

Stratton Apparent Resistivity Sections

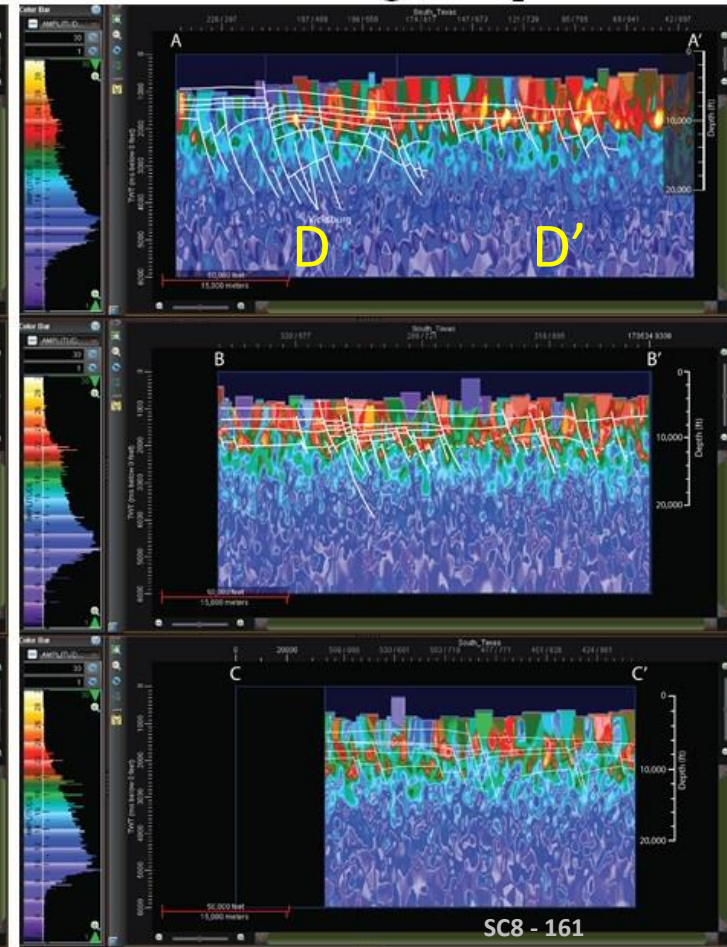
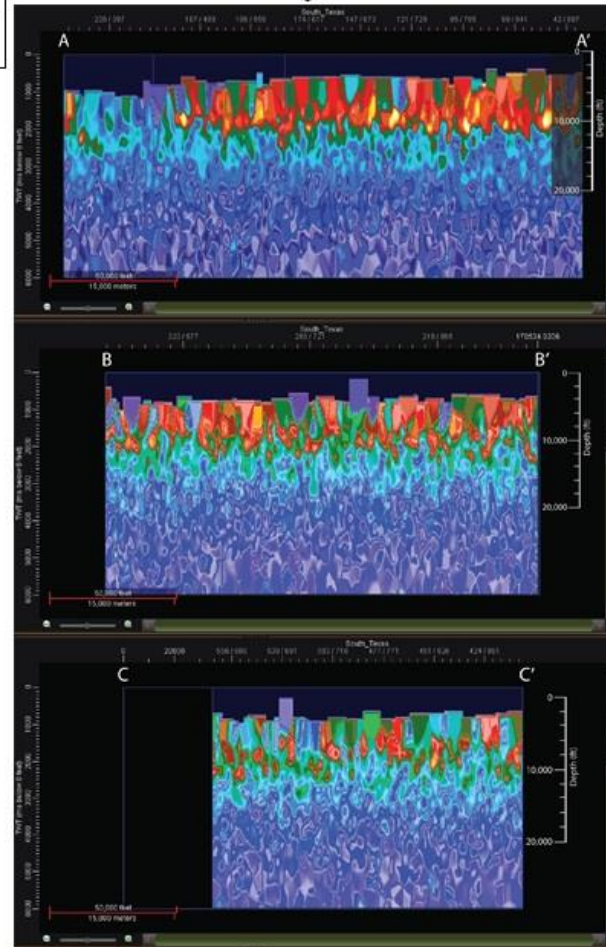
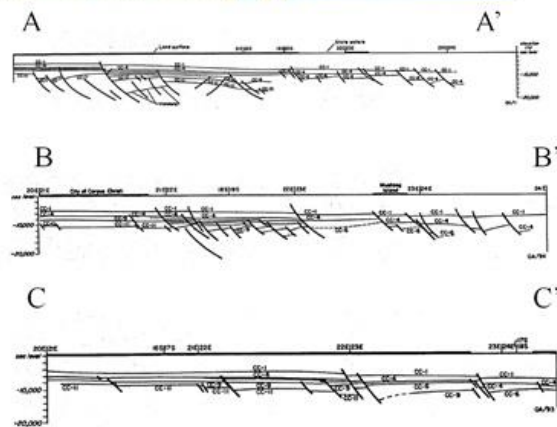


South Texas Example



Resistivity Sections

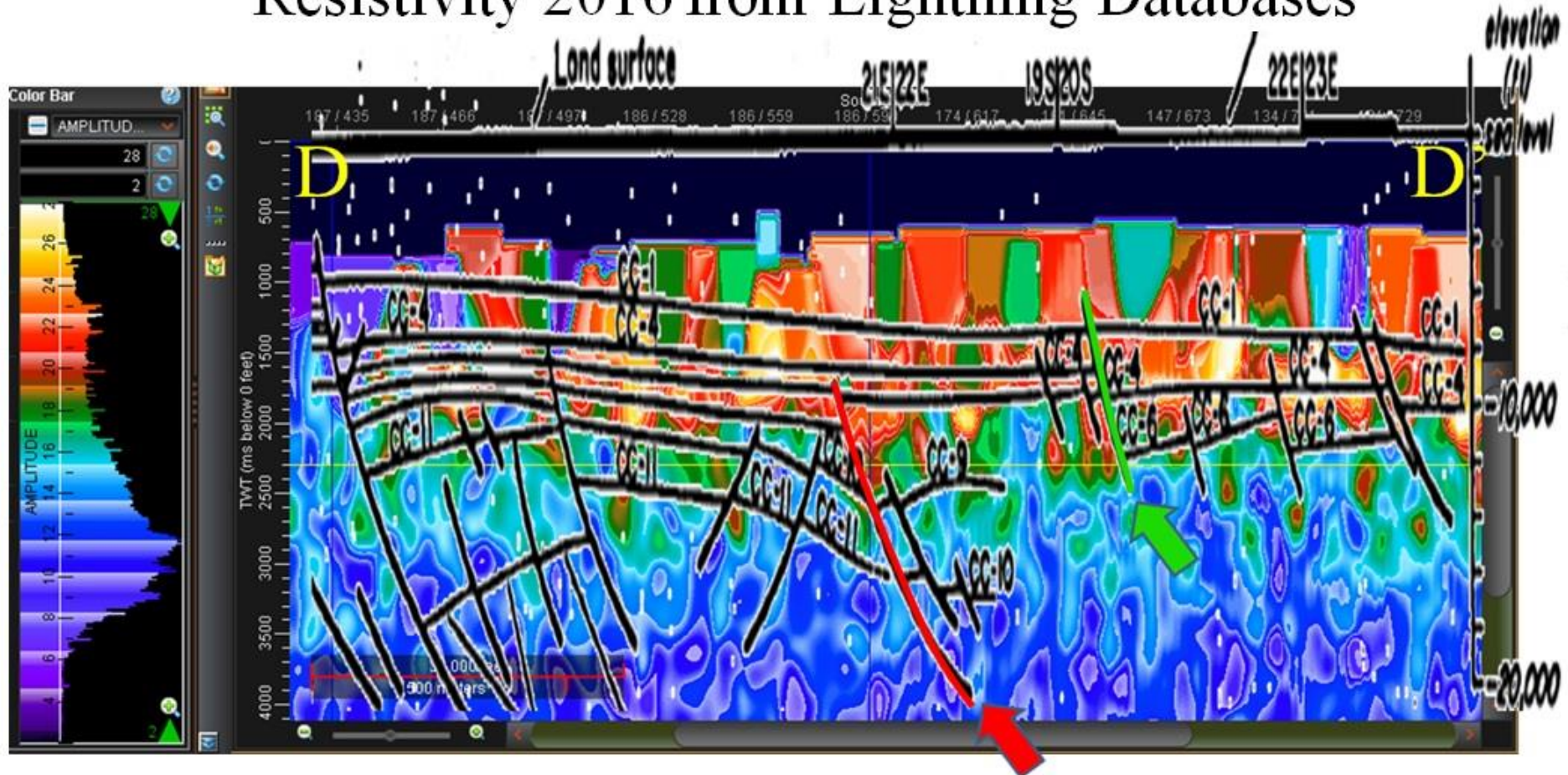
with Ewing interpretation



Ewing, T.E., 1986, Structural Styles of the Wilcox and Frio Growth-Fault Trends in Texas: Constraints on Geopressed Reservoirs: BEG, Report of Investigations, 154, 27-56.

D-D' Close-Up on Graben to the west

Interpretation 1986 by Tom Ewing, Apparent Resistivity 2016 from Lightning Databases

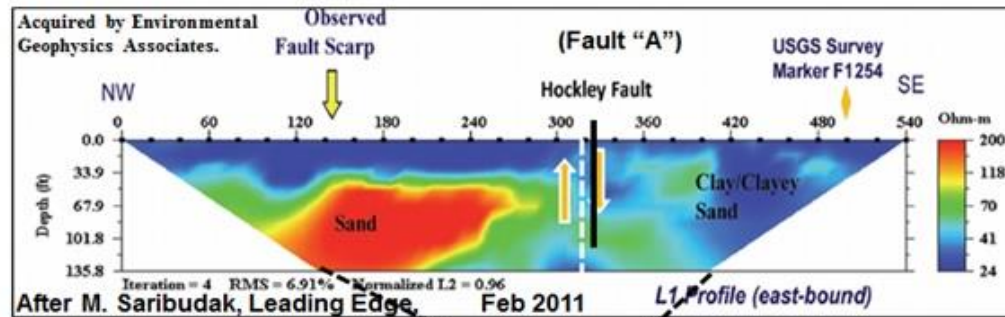


Note: interpretation by Tom Ewing in 1986. The resistivity section calculated from lightning in 2016. Co-located sections show breaks where faults were interpreted. There are resistivity plumes tied to faults.

Hockley, Texas

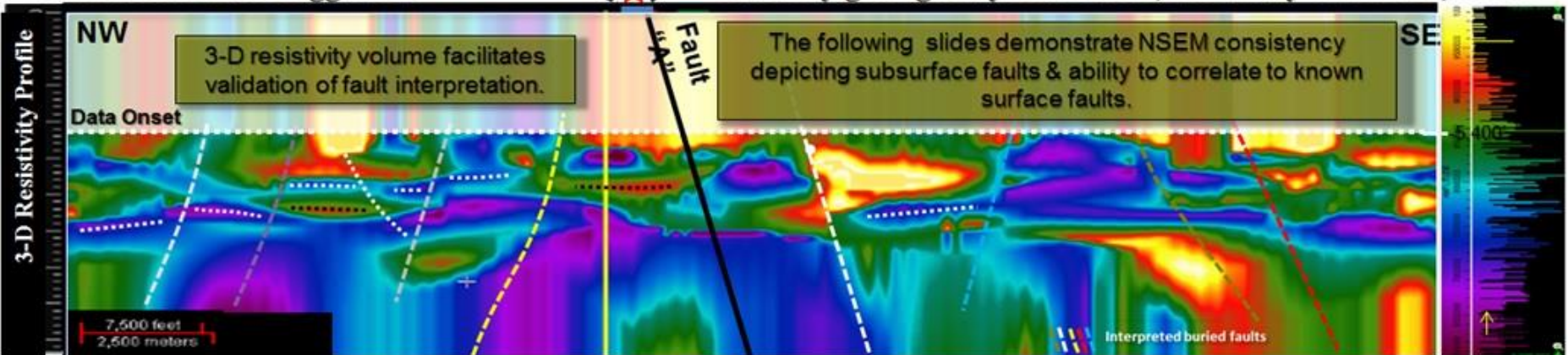
(where it all started)

Texas Example



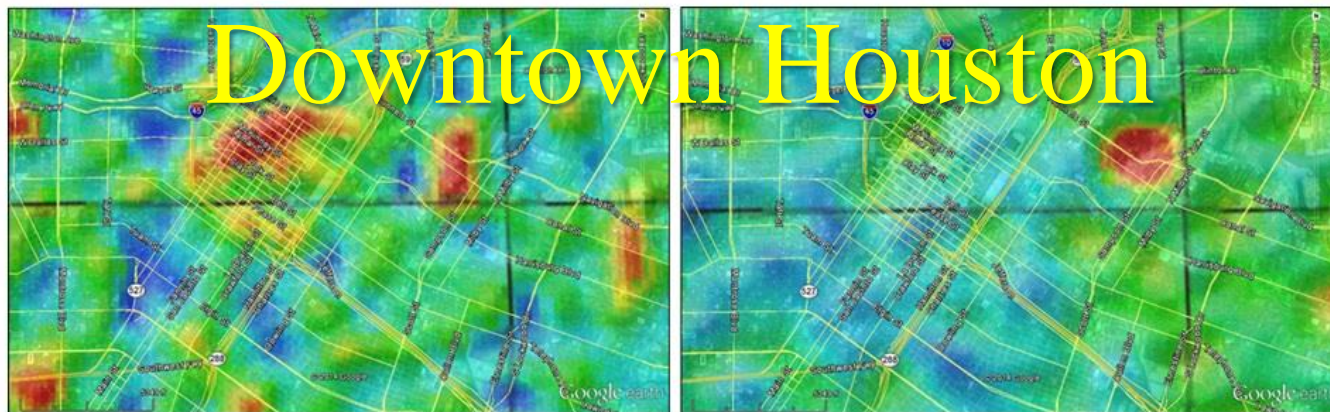
Additional faults suggested.

Are they geologically reasonable, internally consistent, valid?

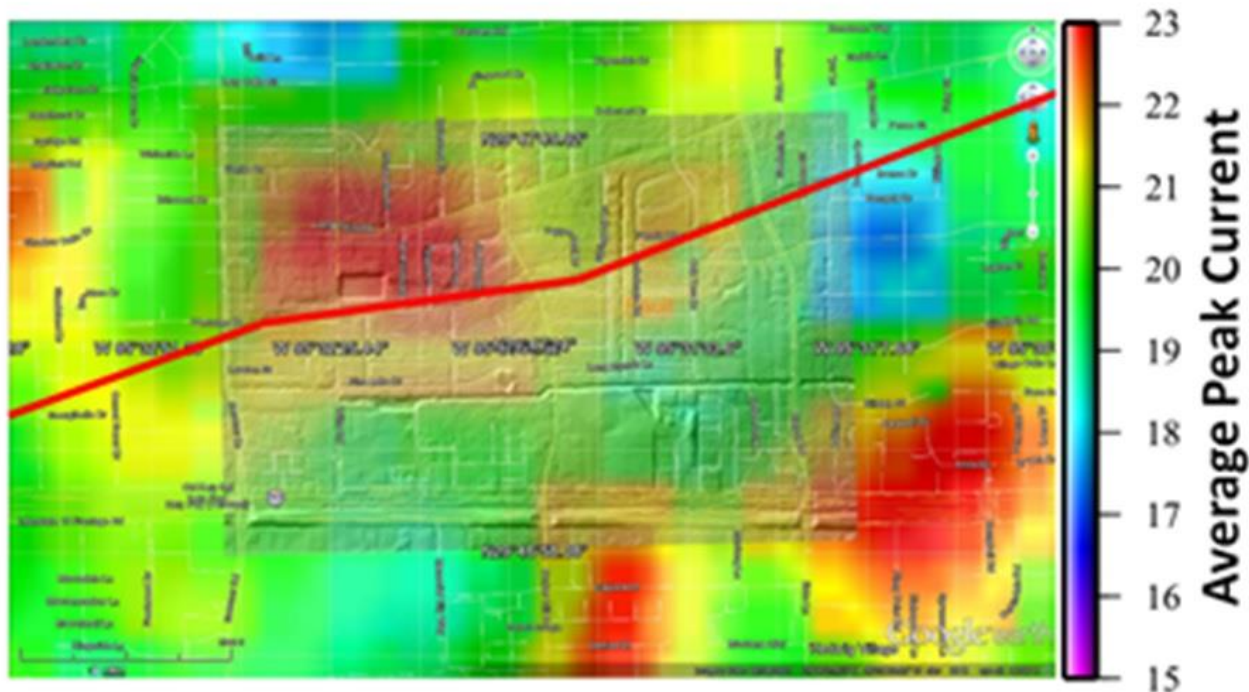


2-D Resistivity Survey ties Lightning Derived Resistivity Cross-Section

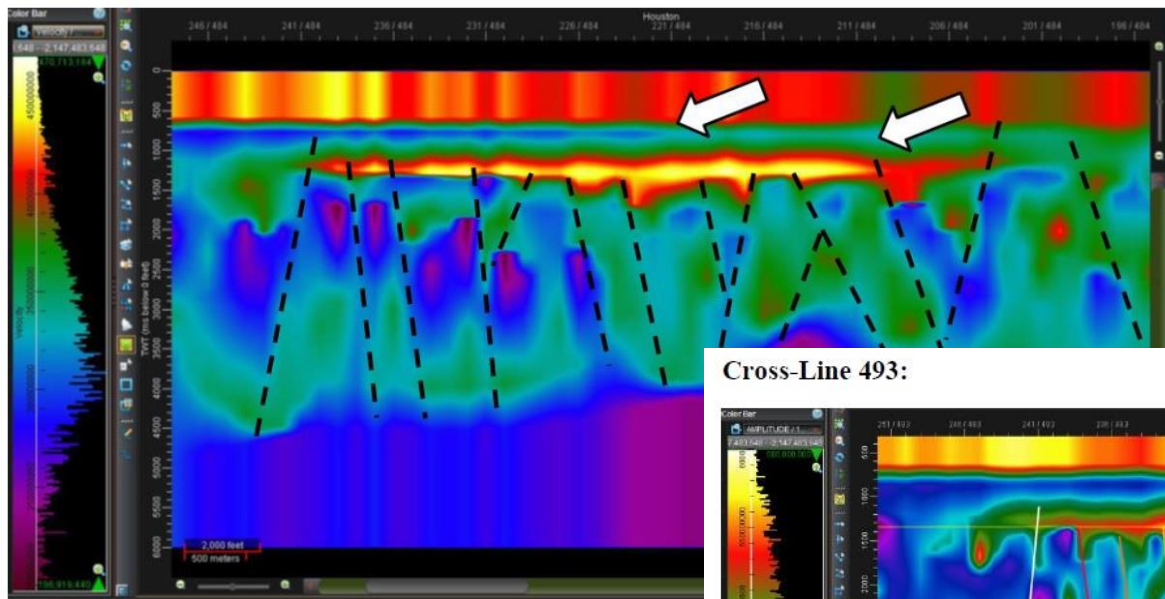
Average Negative Peak Current vs. Density



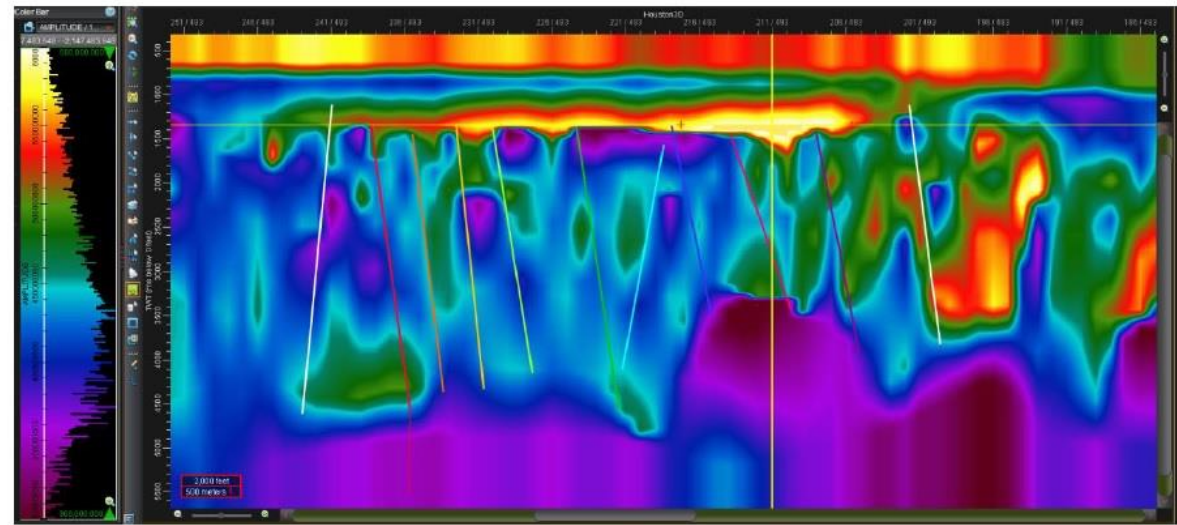
Peak Current Zoom with LIDAR & Long Point Fault



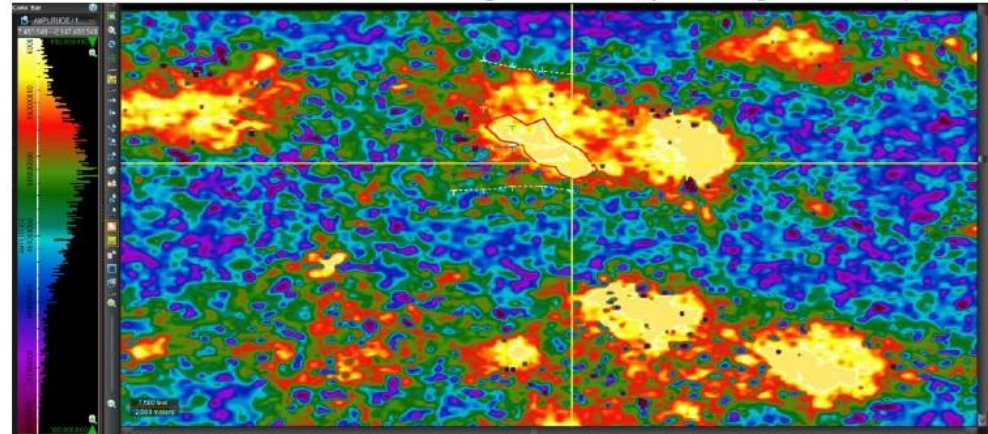
Possible Gas Field in Northwest Houston



Cross-Line 493:

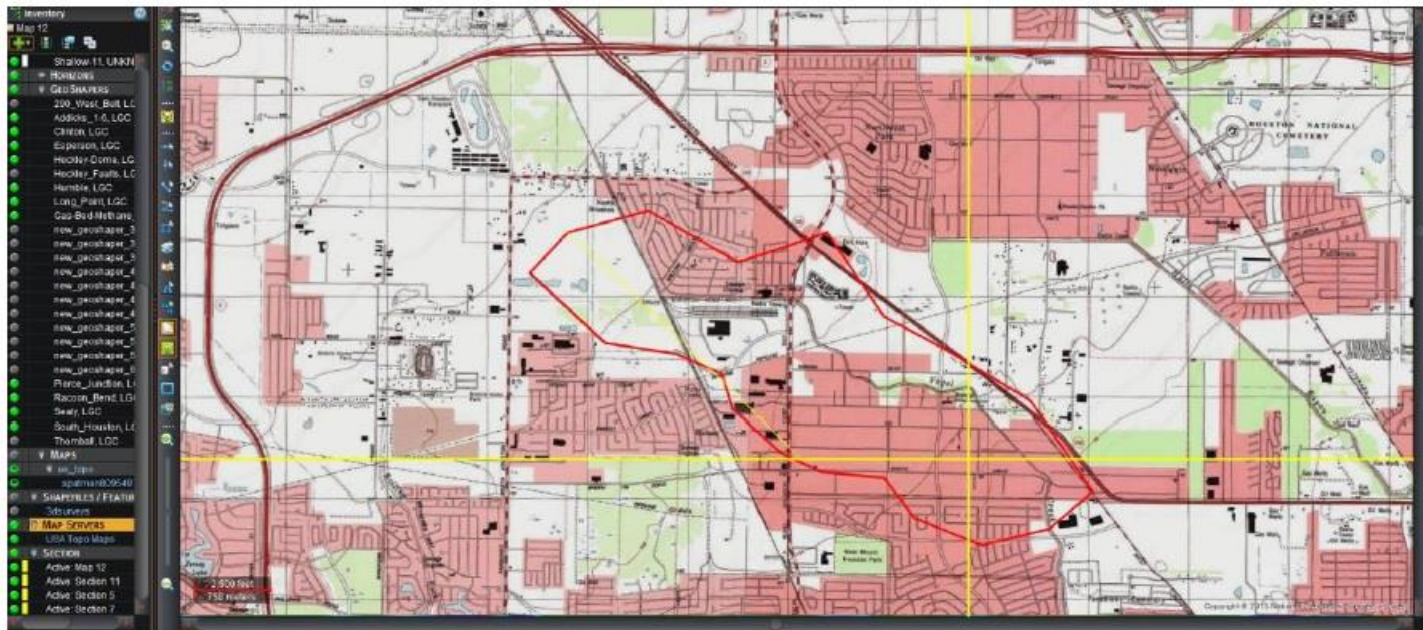


Time-Slice 1345 ms and red outline of highest resistivity in interpreted area (note other anomalies):



Location & Economics

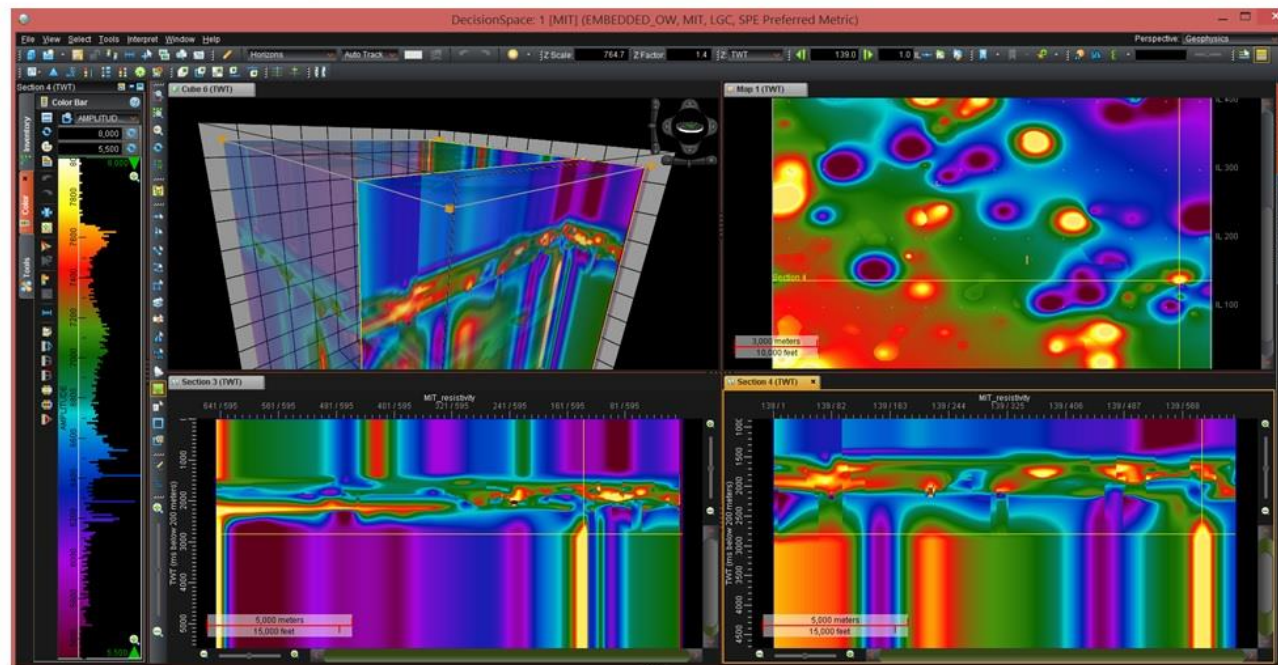
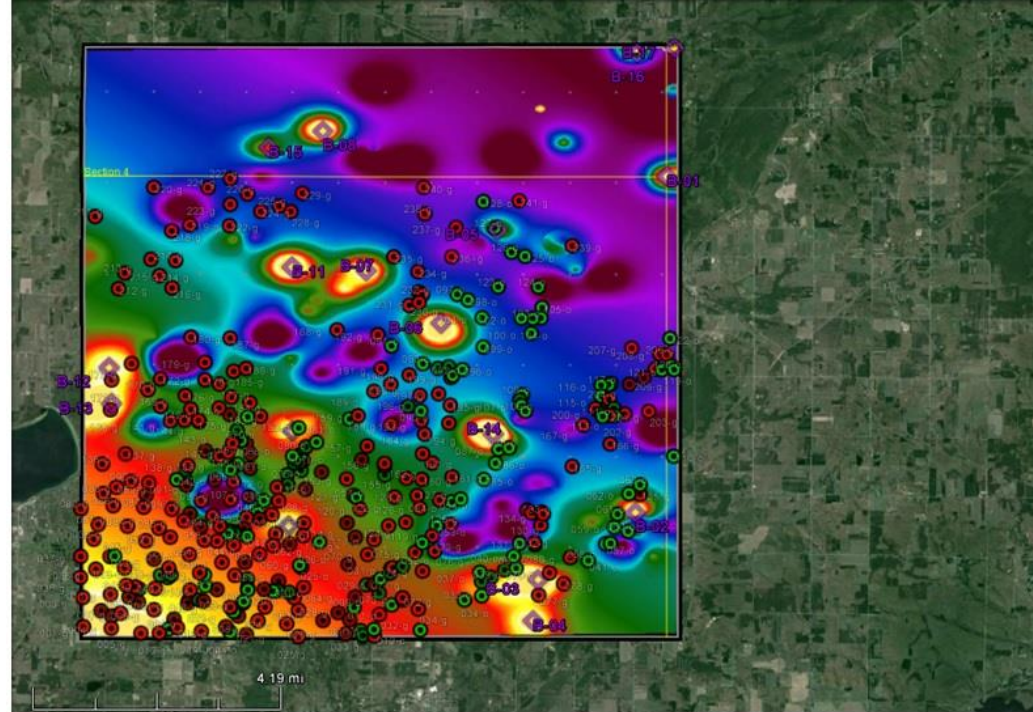
Zoom on Houston Infrastructure for this area:



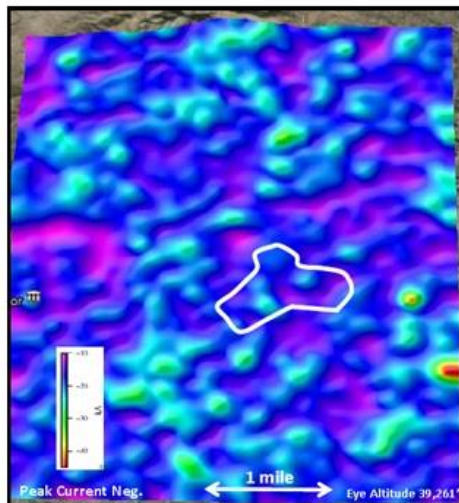
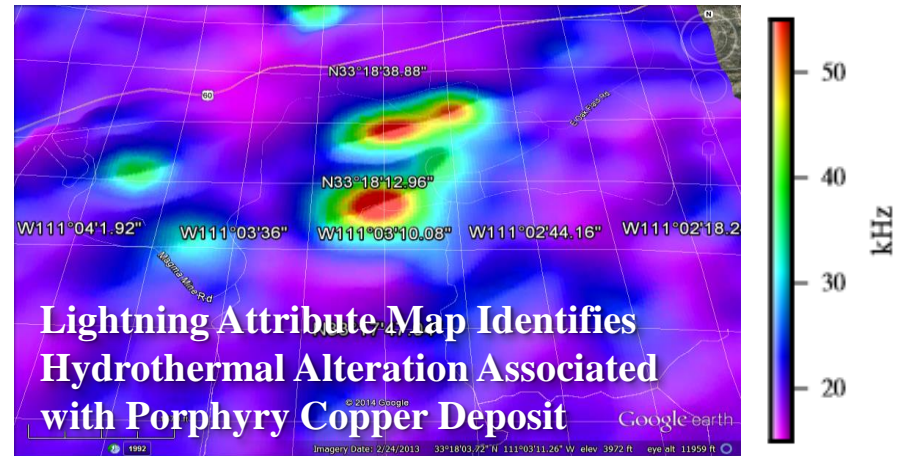
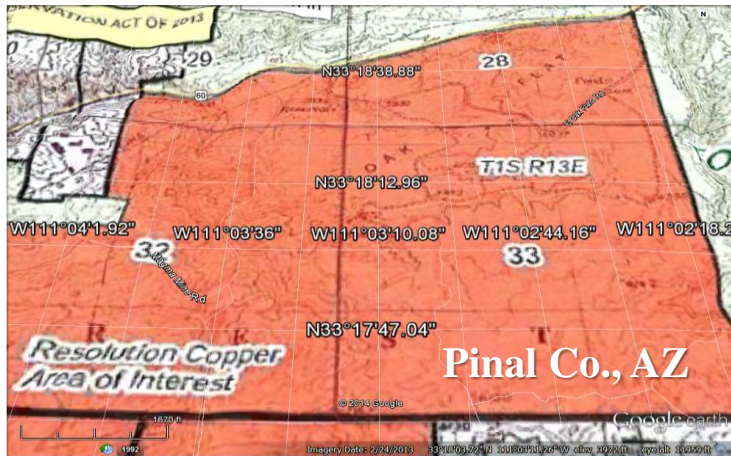
Quick Overview Economics for a 3 square mile area:

	Area	acre-feet	barrels	MCF @ 15 cf/b	MCF @ 23 cf/b	MCF @ 100 cf/b
Square Miles	3					
Acres	1920					
10 foot sand		19200	148,960,655	2,234,410	3,426,095	14,896,066
50 foot sand		96000	744,803,273	11,172,049	17,130,475	74,480,327
100 foot sand		192000	1,489,606,546	22,344,098	34,260,951	148,960,655
Value 10 foot sand at \$2/MCF				\$ 4,468,820	\$ 6,852,190	\$ 29,792,131
Value 50 foot sand at \$2/MCF				\$ 22,344,098	\$ 34,260,951	\$ 148,960,655
Value 100 foot sand at \$2/MCF				\$ 44,688,196	\$ 68,521,901	\$ 297,921,309

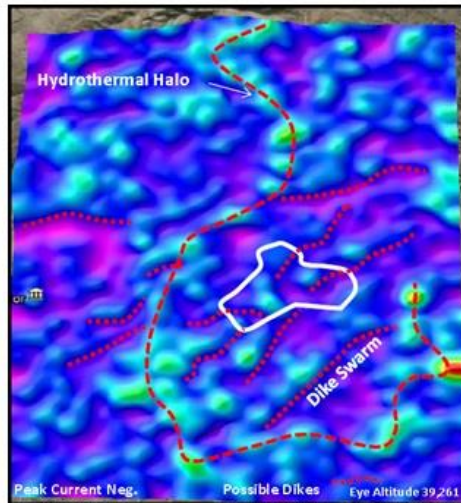
Reefs in Michigan



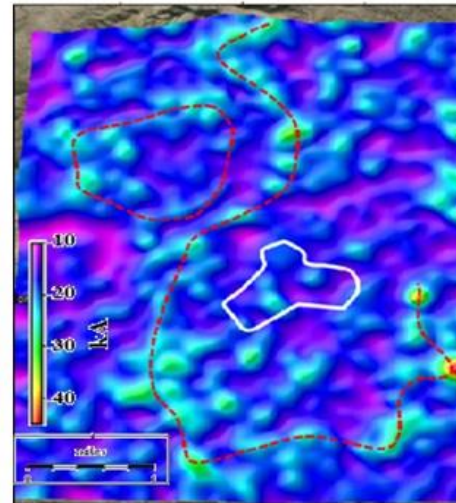
\$6 Billion Resolution Copper Mine Superior, Arizona



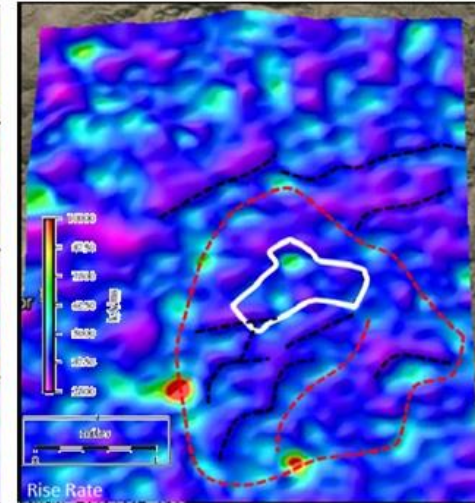
Negative Peak Current



Negative Peak Current



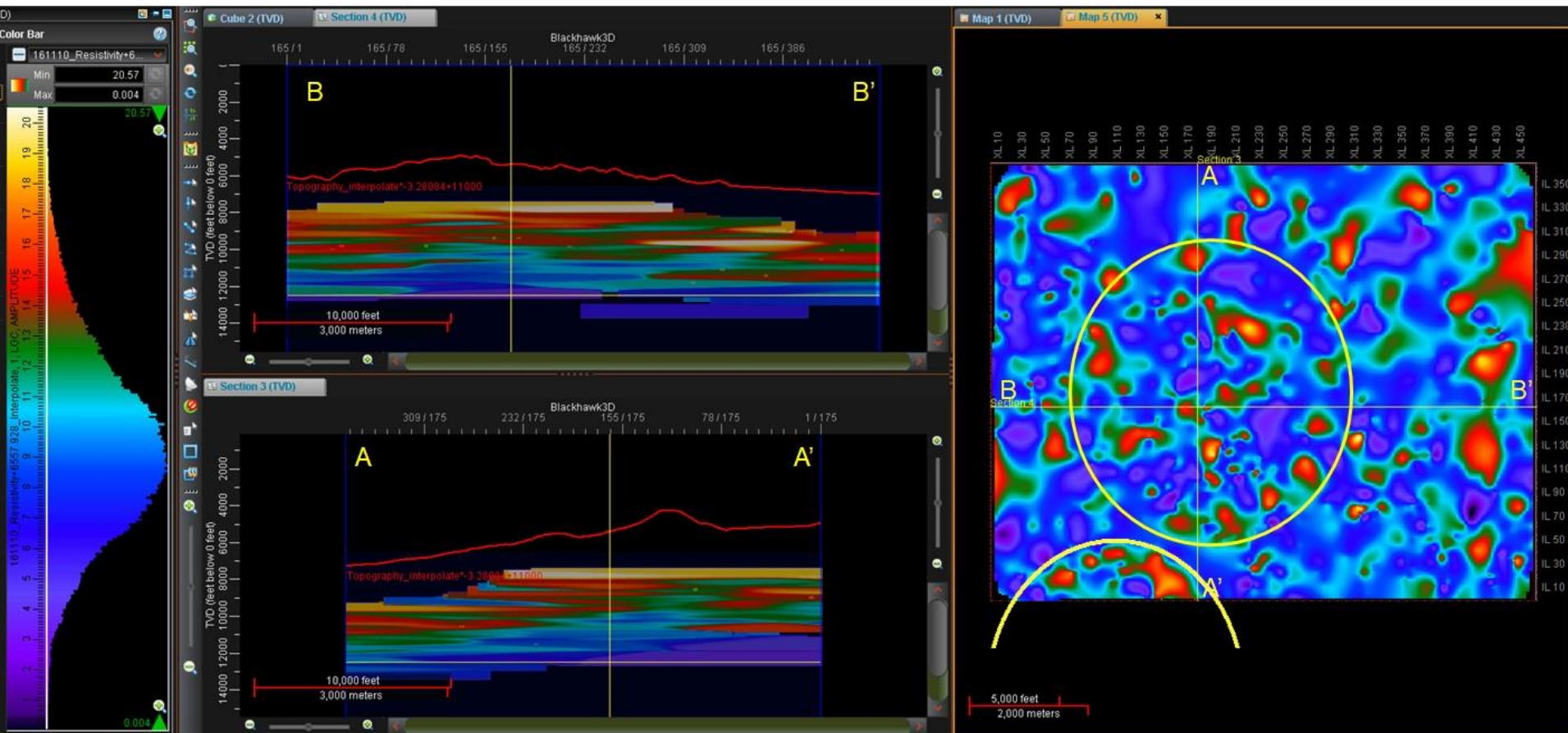
Peak Current



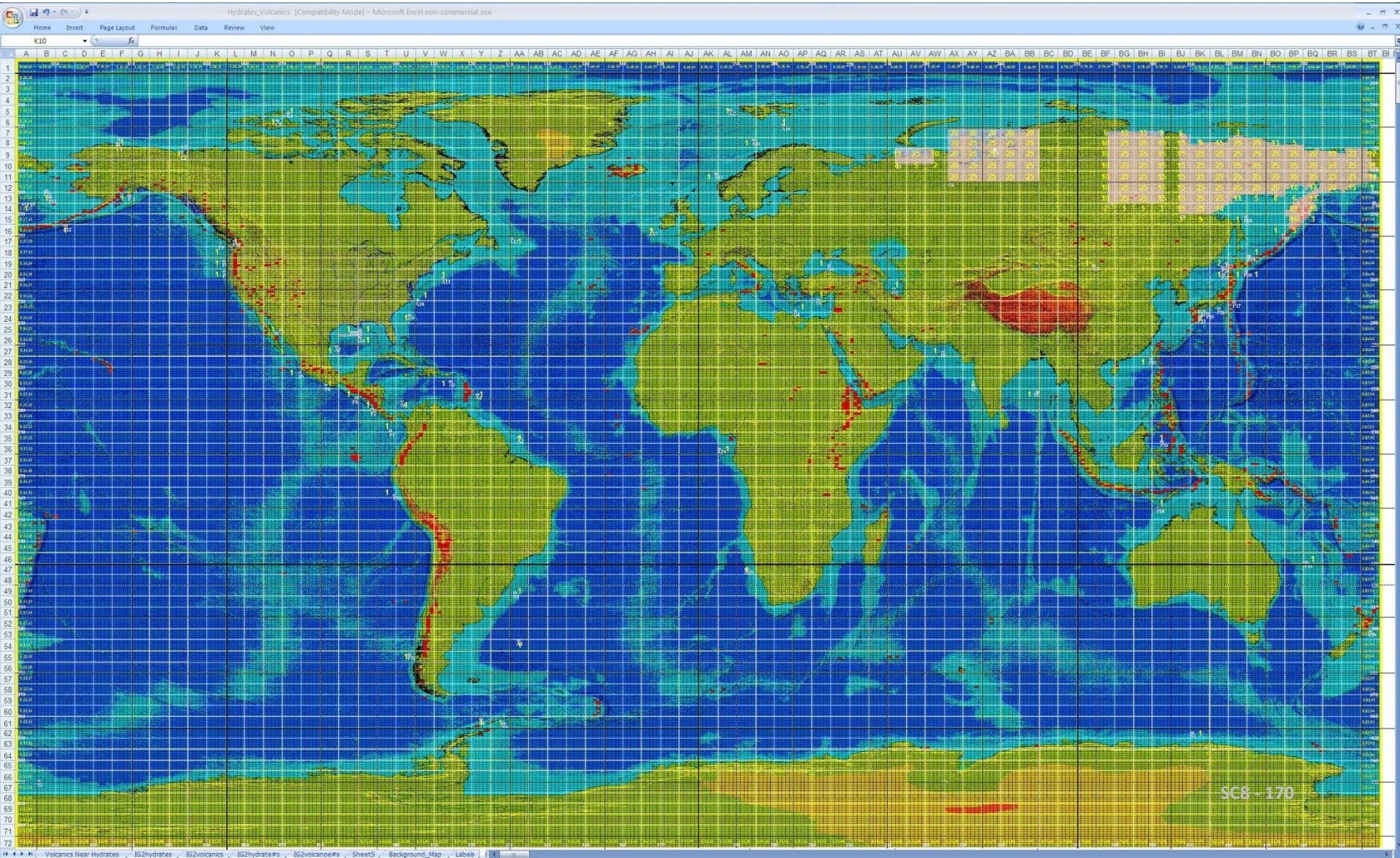
Rise-Rate

Gold Mine, San Bernardino County, CA

Interpretation of Anomaly on Surface Resistivity Map



A Future Project: Gas Hydrates



Notes

This image shows a single sheet of white paper with horizontal blue ruling lines. The lines are evenly spaced and run across the width of the page. There are no margins, text, or other markings on the paper.

2017 Science Camp

- What was best about 2017 Science Camp?

- _____
- _____
- _____

- What would be your ideal 2018 Science Camp Theme?

- _____
- _____
- _____